

APPROVAL SHEET

Title of Dissertation: Developing stealth nanomaterials for intravenous
administration to overcome complement-mediated
hypersensitivity reactions

Name of Candidate: Nuzhat Maisha
Doctor of Philosophy, 2021

Dissertation and Abstract Approved: _____

Erin Lavik, Ph.D.

Associate Dean for Research and Faculty
Development COEIT

Professor

Department of Chemical, Biochemical, and
Environmental Engineering

Date Approved: _____

NOTE: *The Approval Sheet with the original signature must accompany the thesis or
dissertation. No terminal punctuation is to be used.

CURRICULUM VITAE

Name: Nuzhat Maisha

Degree and date to be conferred: Ph.D., 2021

Collegiate institutions attended: Bangladesh University of Engineering and Technology,
Bachelor of Science
(Chemical Engineering), 2015

University of Maryland Baltimore County,
Doctor of Philosophy
(Chemical and Biochemical Engineering), 2021

Major: Chemical and Biochemical Engineering

Professional Publications: Kulkarni, C., **Maisha, N.**, Schaub, L. J., Glaser, J., Lavik, E., & Janeja, V. P. (2021). Computational Design Map for Heterogeneous Experimental Studies. bioRxiv.

Kulkarni, C., **Maisha, N.**, Schaub, L. J., Glaser, J., Lavik, E., & Janeja, V. (2021). Temporal Progression: A case study in Porcine Survivability through Hemostatic Nanoparticles. bioRxiv.

Maisha, N., Coombs, T, and Lavik. E. (2020). Development of a Sensitive Assay to Screen Nanoparticles in vitro for Complement Activation. ACS Biomaterials Science & Engineering.

Onwukwe, C., **Maisha, N.**, Holland, M., Varley, M., Groynom, R., Hickman, D., Uppal, N., Shoffstall, A., Ustin, J., & Lavik, E. (2018). Engineering intravenously administered nanoparticles to reduce infusion reaction and stop bleeding in a large animal model of trauma. *Bioconjugate chemistry*, 29(7), 2436-2447.

Fernandez-Moure, J., **Maisha, N.**, Lavik, E. B., & Cannon, J. W. (2018). The chemistry of lyophilized blood products. *Bioconjugate chemistry*, 29(7), 2150-2160.

Syeda, S. R., **Maisha, N.**, & Ferdous, A. (2017). Risk map for facility siting of an ammonia-Urea Complex. *Journal of Chemical Engineering*, 29(1), 56-60.

Professional positions held: Prospective position (August 2021 –)
Scientist 1, Formulation
Bluebird Bio
60 Binney St.
Cambridge, MA 02142

Graduate Research Assistant
(August 2016 – July 2021)
University of Maryland, Baltimore County
1000 Hilltop Circle
Baltimore, MD 21250

Graduate Teaching Assistant
(August 2017 – December 2017)
University of Maryland, Baltimore County
1000 Hilltop Circle
Baltimore, MD 21250

ABSTRACT

Title of Document: DEVELOPING STEALTH
NANOMATERIALS FOR INTRAVENOUS
ADMINISTRATION TO OVERCOME
COMPLEMENT-MEDIATED
HYPERSENSITIVITY REACTIONS

Nuzhat Maisha, Doctor of Philosophy, 2021

Directed By: Erin Lavik, Ph.D.
Associate Dean for Research and Faculty
Development COEIT
Professor, Department of Chemical,
Biochemical, and
Environmental Engineering

A significant hurdle in clinical translation of intravenously infused nanoparticles is that it may lead to complement-mediated infusion reactions. The complement pathway is a part of the innate immune system, always active in eliminating threats to the immune system. However, complement activation can lead to the unwanted clearance of therapeutic nanomaterials. This can result in complement-mediated hypersensitivity reactions and cause anaphylaxis, which can even be fatal. Moreover,

the bioavailability of the therapeutic is impacted as well. As 7-10% of the human population are prone to complement activation, this is a significant safety challenge while designing nanomaterials meant to be delivered intravenously. Materials properties and surface architecture of nanoparticles are significant contributors to the complement response. These dictate the interaction with plasma and complement proteins when the nanoparticles are in the bloodstream. We hypothesized that tuning materials properties would generate stealth nanoparticles that do not activate the complement pathways. To test our hypothesis, we also required a sensitive screening tool, as current methods of quantifying complement are qualitative or semiquantitative and often overlook the interference introduced due to the presence of nanomaterials. Hence, our research objectives were to:

1. Develop a sensitive assay for tracking changes in complement proteins
2. Determine impact of surface and material properties by using the developed assay
3. Design stealth nanomaterials by applying the gathered input

To achieve our research objective, we first determined the optimum assay conditions to assess the complement-mediated response *in vitro*, mimicking the *in vivo* response. Using the screening tool, we tracked how surface properties like zeta-potential and PEGylation impact the complement pathways. Based on the outcomes, we worked on developing stealth polyurethane-based nanomaterials that did not lead to complement activation. Overall, the knowledge gathered from this dissertation will be critical in designing stealth nanomaterials that would not lead to complement-mediated infusion reactions.

DEVELOPING STEALTH NANOMATERIALS FOR INTRAVENOUS
ADMINISTRATION TO OVERCOME COMPLEMENT-MEDIATED
HYPERSENSITIVITY REACTIONS

By

Nuzhat Maisha

Dissertation submitted to the Faculty of the Graduate School of the
University of Maryland, Baltimore County, in partial fulfillment
of the requirements for the degree of
Doctor of Philosophy

2021

© Copyright by

Nuzhat Maisha

2021

Acknowledgements

I would first acknowledge the support and guidance of my advisor Dr. Erin Lavik through this journey. I am thankful she gave me the chance to explore the field of biomaterials and build my skills at my own pace while challenging me to reach my highest potential. Throughout my time as a graduate student, she has patiently motivated me in my research and been an invaluable guide by sharing her depth of knowledge whenever I had hit a rough patch. I hope I can do justice to her mentoring by being as passionate and meticulous a scientist as she is.

I would like to thank Dr. Douglas Frey, Dr. Zeev Rosenzweig, Dr. Govind Rao, Dr. Dipanjan Pan and Dr. Greg Szeto for their guidance and valuable insights. I would also extend my acknowledgments to Dr. Jacob J. Glaser and Leasha Schwab at the Naval Medical Research Unit San Antonio, Dr. Pam VandeVord, Dr. Vandana Janeja, Dr. Sarah Stabenfeldt, Dr. Zin Khaing, Dr. Rosemary Kozar, and Dr. Wei Cao for giving me the chance of experiencing the extended applications of our developed biomaterials through collaborative research.

I would like to thank the Lavik Lab members for being there as friends, as compassionate listeners, and as critiques to bring out the best in my research. Sydney Menikheim, Adam Day, Narendra Pandala, Devorah Cahn, Mark Holland, Rakan El Mayta, Chimdiya Onwukye, Josh Leckron, Michael Lascola, and Chris Williams have unwearingly supported me through this process. Tobias Coombs, Nidhi Naik, and Mawuyon Okesola have worked tirelessly along with me in our quest to learn

more about biomaterials. Several undergraduate and graduate students have been a part of the lab and our research and contributed to making this work possible. I would like to thank Michael Rubenstein and Chhaya Kulkarni for their assistance in this research by offering their expertise.

I would extend my gratitude to the CBEE graduate students. Lunches and coffee hours with these amazing people I have met as fellow graduate students have eased my life as an international graduate student over the last few years. I would also thank Victor Fulda, Andrea Miller and Fabiola Attime for their support regarding research logistics as well as technical assistance.

I wish to thank the friends who made Maryland a home away from home for me, by keeping me fed, letting me vent about the world, and through board games while tolerating my penchant for food videos and choice of music. Thank you for letting me recharge whenever I was running out of energy. To the friends who believed in my ability more than I did, thank you.

Lastly, I would like to thank my friends and family back home in Bangladesh, for still bearing with me even though I prioritized my work over them. To my sister and brother-in-law, Jumana Asrar and Razib Mahmud, thanks for being there for our parents, so that I could peacefully be invested in my research. I do not have enough words to express my gratitude toward my parents, Munira Rahman and Abdul Matin, for letting me pursue my dreams. This work could not have been possible without their support and encouragement.

Thank you.

Table of Contents

Acknowledgements	ii
Table of Contents	iv
List of Figures.....	xi
Chapter 1: Introduction	1
Acknowledgements.....	8
References.....	9
Chapter 2: Complement-mediated initial infusion reactions for intravenously administered nanoparticles: a hindrance to clinical translation	14
Infusion reactions from nanoparticle-based therapeutics	15
Intravenous infusion of nanoparticles and complement activation.....	17
The complement pathways and their role in innate immune response	17
Nano-bio interaction and complement activation: The mechanism of activation	19
Role of species on complement activation.....	21
Existing approaches for quantifying changes in complement proteins	22
Hemolysis assays: CH50 and AH50	23
Quantifying eluted complement proteins from nanoparticle corona	23
Enzyme-linked immunoassays.....	23
Critical factors in optimizing complement protein assays	24
Anticoagulant used for collecting blood	24

Impact of incubation time	25
Differences in response for whole blood, plasma, and serum	25
The impact of surface architecture and material properties on the complement interaction	26
PEGylation.....	27
Zwitterionic coatings	29
Surface functional groups	30
Surface decoration with complement inhibitors	30
The impact of the core of nanoparticles on complement activation	30
Conclusions.....	31
References.....	33

Chapter 3: Developing a sensitive Assay to Screen Nanoparticles in vitro for

Complement Activation.....	46
Abstract.....	46
Introduction.....	47
Experimental Section	51
Materials	51
Methods.....	52
Developing complement assay conditions.....	52
Validating assay's sensitivity to mimic in vivo response in vitro	53
Nanoparticles used for validating the assays	54
Statistical Analysis.....	55

Results.....	56
Comparing complement response observed in citrated and heparinized human blood plasma	56
Impact of incubation time in generating complement response in human blood matrices	57
Differences in complement response generated in human blood, plasma, and serum.....	58
Validating impact of zeta-potential of nanoparticles observed in vivo through developed in vitro assay.....	63
Discussion	74
Conclusions.....	82
Acknowledgements.....	83
References.....	84
 Chapter 4: Engineering PEGylated polyester nanoparticles to reduce complement-mediated infusion reaction.....	 99
Abstract	99
Introduction.....	100
Materials and Methods.....	103
Materials	103
Synthesis and characterization of nanoparticles	104
Generating complement response in vitro and quantification through complement assay	106

Generating immune response in vitro and quantification through cytokine array	106
Detecting the levels of IL-6 generated from rat endothelial cells exposed to PLA and PLA-PEG nanoparticles	107
Statistical Analysis.....	108
Results.....	108
Characterization of nanoparticles with changing amount of surface PEGylation and combination of different PEG lengths.....	108
Change in complement protein C5a in vitro for different PEG corona structures	111
Change in complement response in vitro for changing ratio of PEGs with different lengths	114
Change in cytokine response for PEGylated nanoparticles	116
Change in IL-6 for nanoparticles incubated with rat endothelial cells	120
Discussion	121
Conclusion	126
Acknowledgements.....	126
References.....	128
Chapter 5: Designing polyurethane-based hemostatic nanocapsules to evade complement-mediated initial infusion reactions	137
Abstract.....	137
Introduction.....	138

Materials and methods	142
Materials	142
Methods.....	142
Developing PEGylated polyurethane nanocapsules	142
Characterization of the nanocapsules.....	143
Determining amount of PEG in the nanocapsules	143
Conjugating with GRGDS peptide motif to develop hemostatic nanocapsules	144
Quantifying amount of peptide through ortho-phthalaldehyde assay.....	144
Generating complement response in vitro and quantification through complement assay	144
Generating immune response in vitro and quantification through cytokine array	145
Evaluating coagulation in vitro using whole blood through rotational thromboelastometry	146
Statistical analysis.....	146
Results.....	147
Synthesis and characterization of PEGylated polyurethane nanocapsules	147
Evaluating changes in complement protein C5a in vitro	150
Identifying the changes in cytokines in vitro upon incubation with polyurethane nanocapsules	151
Validating the hemostatic activity through in vitro coagulation assay	154
Discussion	155

Conclusion	160
Acknowledgements.....	161
References.....	162
Chapter 6: Conclusions	170
Summary of findings.....	170
Validation of the stealth activity of hemostatic nanoparticles in vivo.....	172
Future Directions	176
Broader impact.....	178
References.....	179
Appendices.....	182
Supplementary materials for chapter 3	182
Impact of anticoagulant in blood and plasma on complement response	182
Impact of species of blood donor on quantifying complement response.....	183
Generating response with lower dosages of zymosan	183
Synthesis of Polymers.....	184
Fabrication of nanoparticles with different zeta-potentials	187
Fabrication and characterization of aggregated nanoparticles.....	188
Impact of the dosage of PLA-PEG nanoparticles on the complement response in porcine and human whole blood.....	188
References.....	190
Supplementary materials for chapter 4	191
Calculating extent of PEGylation	191

Change in complement protein C5a for medium and high-density PEG brush in complement protected human serum	194
Impact of PEG length in dense PEG corona structures: Change in complement protein C5a in complement protected human serum	195
Supplementary materials for chapter 5	196
Calculating amount of PEG present.....	196
References.....	203
Supplementary Materials: Injury model used for the porcine trauma	204
Ethical Approval and Accreditation.....	204
Injury model and in vivo study	204
References.....	206

List of Figures

Figure 1. Determining the optimum assay conditions for sensitive screening of complement response in vitro. ¹⁹	3
Figure 2. Evaluating extents of PEGylation and impact of PEG chain lengths to avoid complement-mediated infusion reactions	5
Figure 3. Developing stealth polyurethane based hemostatic nanocapsules to evade complement-mediated infusion reactions	7
Figure 4. Change in cardiopulmonary vitals with changing zeta potential for a naive administration model in porcine animals ¹⁶	17
Figure 5. Complement activation occurs through three distinct pathways. The precursors for the activation routes are different, but each pathway results in generating C3a and C5a. Anaphylatoxins C3a and C5a cause allergic reaction, and the pathway goes forward generating terminal complex SC5b-9.....	19
Figure 6. Complement protein C3b binds to a different surface through a covalent thioester bonding, and in the presence of properdin and magnesium ion, it forms the C3 convertase that further breaks down C3 into C3a and C3b. More C3b then amplifies the alternative complement pathway.....	21
Figure 7. Validation of incubation time at 45 minutes. Statistical analysis using one-way ANOVA shows the fold-change at 5mg/ml dosage for 45 minutes incubation is significantly different from the fold-change for the same time-point at 1mg/ml dosage.	58

Figure 8. Comparing complement response among single donor and pooled plasma and serum. A. Incubation of blood plasma and serum with zymosan at a dosage of 0.25mg/ml and quantifying complement protein C5a. The C5a levels in the samples are quantified through enzyme immunoassay, and the fold change is determined with respect to the amount of C5a determined in the serum or plasma incubated with PBS. B. The change in complement protein C5a in single donor heparinized plasma resulted in a fold change of 20 ± 4 fold. C. The change in complement protein C5a in single donor serum resulted in 12 ± 2 fold. D. The complement protein C5a changed by 5 ± 0.4 fold in pooled heparinized plasma. E. The complement protein C5a changed by 14 ± 1 fold in pooled serum. Using t-test, the means observed for PBS and zymosan were compared for each sample and the means were significantly different.

..... 60

Figure 9. Complement response in heparinized whole blood. A. Schematic of process. B. Fold change and complement level in donor 3. C. Fold change and complement level in donor 4. D. Fold change and complement level in donor 5. The changes due to a dosage of 0.25 mg/ml were 14 ± 6 folds, 31 ± 1.7 and 20 ± 1.9 , respectively. Using t-test, the means observed for PBS and zymosan were compared for each donor and the means were significantly different. 62

Figure 10. Method for generating complement response *in vitro*. Heparinized whole blood is incubated with nanoparticles suspended in PBS at dosages of 0.25mg/ml for 45 minutes at 37°C in a rotating shaker. The samples are centrifuged to separate the

nanoparticles and the supernatant serum is used to quantify the complement activation biomarker C5a through immunoassay. 64

Figure 11. Change in cardiopulmonary vitals upon infusion of PLGA-PLL-PEG nanoparticles in swine. Infusion of the nanoformulation PLGA-PLL-PEG-cRGD-1 resulted in increased rate of blood loss and fluctuations in the vitals with exsanguination at 10 minutes post-infusion. A. Change in heart rate, B. Change in end-tidal CO₂, C. Change in blood pressure, D. Change in rate of blood loss due to PLGA-PLL-PEG-cRGD-1 infusion. Infusion of the nanoformulation PLGA-PLL-PEG 1 increased rate of blood loss and led to exsanguination at 5 minutes post infusion. E. Change in heart rate, F. Change in end-tidal CO₂, G. Change in blood pressure, H. Change in rate of blood loss due to PLGA-PLL-PEG-1 infusion; Infusion of the nanoformulation PLGA-PLL-PEG-cRGD-2 increased rate of blood loss slightly without causing exsanguination, however, fluctuations were exhibited in the vitals. I. Change in heart rate, J. Change in end-tidal CO₂, K. Change in blood pressure, L. Change in rate of blood loss due to PLGA-PLL-PEG-cRGD-2 infusion. These data are from a previous study looking at the impact of modulating zeta potential on the complement response to hemostatic nanoparticles in a porcine model of trauma.³¹ 67

Figure 12. Fold change in complement protein C5a due to incubation of whole blood with PLGA-PLL-PEG nanoparticles. One-way ANOVA followed by Tukey analysis shows that while the means of fold changes are significantly different for the nanoformulations compared to Zymosan, the difference is not statistically significant

for the changes within the three groups PLGA-PLL-PEG-cRGD-1, PLGA-PLL-PEG-1 and the PLGA-PLL-PEG-cRGD-2.	68
Figure 13. Characterization of nanoparticles with varied zeta-potential. A. Nanoparticles with poly(lactic acid) core and poly(ethylene glycol) corona. B. Varying amino and carboxyl groups to vary zeta-potential. C. Hydrodynamic diameter of nanoparticles. D. Zeta-potential of nanoparticles. 3400PEG indicates PEG with a molecular weight of 3400Da while 5000PEG indicates a molecular weight of 5000Da for the PEG units, respectively.....	
	70
Figure 14. Impact of zeta potential of nanoparticles on complement response. Neutral nanoparticles lead to decreased complement activation <i>in vitro</i> leading to lower fold change in complement protein C5a. However, aggregation of particles with a low zeta potential led to an increase in complement protein C5a.	
	72
Figure 15. Impact of aggregation of particles. The complement activation as marked by C5a is increased with aggregated particles at levels similar to unaggregated particles with a high zeta potential relative to the whole blood with PBS control.	
	74
Figure 16: Summary of characterization data for nanoparticles with varying amounts of surface PEG	
	109
Figure 17: Summary of DLS data for nanoparticles with a combination of PEG lengths in the corona	
	110
Figure 18: Change in complement protein C5a upon incubation of heparinized whole blood with PLA nanoparticles. Using Chi-square analysis, p-value obtained was less	

p<<0.05 when compared against an expected value of 1 for the level in sample incubated with PBS..... 112

Figure 19: Impact of the extent of PEGylation on the normalized change in complement protein C5a in vitro upon incubation of heparinized human blood with nanoparticles at a concentration of 0.25mg/ml. As a positive control, Zymosan was used. The normalized change was calculated in comparison to the sample incubated with PBS. Using Chi-square analysis, p-value obtained was less p<0.05 when compared against an expected value of 1 for the level in sample incubated with PBS for the 24 and 51% PEGylation but not for the other groups. 113

Figure 20: Impact of PEG chain length on normalized change of complement protein C5a in vitro upon incubation of heparinized human blood with highly PEGylated nanoparticles at a concentration of 0.25mg/ml. As a positive control, Zymosan was used. The normalized change was calculated in comparison to the sample incubated with PBS. A. The normalized change in C5a observed for PEG lengths of 3400Da and 5000Da. B. The normalized change in C5a observed for mixing different PEG lengths. Using the Chi-square analysis, the p-value>0.05 was obtained, indicating the C5a levels observed are similar to the levels observed in samples incubated with PBS. 115

Figure 21: Impact of extent of PEGylation of nanoparticles on the cytokine levels in heparinized human whole blood. 120

Figure 22: Change in IL-6 due to encounter of nanoparticles with rat endothelial cells.

The change in IL-6 was significantly higher for the positive control Zymosan but remained downregulated for the PLA and PLA-PEG nanoparticles. 121

Figure 23: Synthesizing PEGylated polyurethane nanocapsules and consequent bioconjugation to prepare hemostatic nanocapsules. In the first step, polyurethane nanocapsules are synthesized through interfacial condensation polymerization between Isophorone diisocyanate (IPDI) in the oil phase and 1,6 hexanediol (1,6 HDOH) in the aqueous phase. Immediately adding poly(ethylene glycol) with hydroxyl end group allows conjugation of PEG chain to the surface. In the second step, hemostatic nanocapsules are prepared by utilizing NHS/EDC zero-length linkers; peptide motif GRGDS is conjugated to the carboxyl end groups present in the PEG chains. 148

Figure 24: Characterization of PEGylated polyurethane nanocapsules. A. Schematic representation of polyurethane nanocapsules with and without PEGylation. B. A summary of the size and surface charge of the PEGylated and non-PEGylated nanocapsules. The presence of PEG was confirmed through ¹H-NMR in deuterated water. C. TEM images of the nanocapsules confirm the size observed through DLS. 149

Figure 25: Quantifying complement protein in vitro for polyurethane nanocapsules. Polyurethane nanocapsules lead to low levels of complement protein C5a in vitro. Nanocapsules were incubated with complement protected human serum and

incubated for 45 minutes at 37°C. The complement protein C5a was least for the non-PEGylated nanocapsules and the highly PEGylated nanocapsules.	151
Figure 26: Normalized changes in the integrated pixel densities for the detected cytokines in vitro in heparinized human whole blood.	154
Figure 27: Evaluating the impact on coagulation in vitro. A. A schematic representation of the control and hemostatic nanocapsules. B. The clotting time was lower for the hemostatic nanocapsules at 2.5mg/ml concentration but not significantly different. C. The clotting time was the least for the hemostatic nanocapsules at 5mg/ml concentration and significantly different as evaluated using t-test.	155
Figure 28: Changes in cardiopulmonary vitals in large animals receiving PLA-PEG nanoparticles	174
Figure 29: Changes in prothrombin time after infusion of PLA-PEG based hemostatic and control nanoparticles in the in vivo porcine trauma model	175
Figure 30. Comparison of fold change for complement protein C3 in heparinized and citrated human blood plasma. For similar experimental conditions and a zymosan dosage of 1mg/ml, heparinized human blood plasma showed higher complement response, indicating that anticoagulants like heparin preserved with the complement activity.....	182
Figure 31. Change in complement protein C3 in heparinized porcine plasma. The data in the dashed box is expanded below for clarity	184
Figure 32. Poly(l-lactic acid)-b-poly(ethylene glycol) (PLLA-PEG) with terminal amine and carboxyl groups, and poly(d-lactic acid) (PDLA) were synthesized through	

ring-opening polymerization. The polymer is synthesized through ring-opening polymerization based on Connor et al. ² The gel permeation chromatography peaks were used to determine the molecular weights of the polymer	186
Figure 33. A. Impact of blending PLA-PEG-NH ₂ and PLA-PEG-COOH in zeta-potential of nanoparticles. B. SEM image of synthesized nanoparticles	188
Figure 34. Change in complement protein C5a for different concentrations of PLA-PEG nanoparticles in human heparinized blood.	189
Figure 35. 1-H NMR peak in CDCl ₃ for varying extents of PEGylation.....	191
Figure 36. 1-H NMR peak in CDCl ₃ for varying PEG chain lengths on the surface	192
Figure 37. Change in complement protein C5a for changing amount of surface PEGylation in complement protected human serum	194
Figure 38. Impact of PEG length on change in complement protein C5a for dense PEG corona. A. The normalized change in C5a observed for PEG lengths of 3400Da and 5000Da in complement protected serum. B. The normalized change in C5a observed for mixing different PEG lengths in complement protected serum.	195
Figure 39. 1H-NMR peak for Polyurethane nanocapsules in deuterated water	199
Figure 40. 1H NMR Peak for PEGylated Polyurethane (PEGm) nanocapsules in deuterated water	200
Figure 41. 1H NMR peak for PEGylated Polyurethane (PEG-COOH) nanocapsules in deuterated water	201
Figure 42. 1H NMR peak for NMR Peak for PEGylated Polyurethane nanocapsule in deuterated water	202

Chapter 1: Introduction

Nanoparticles engineered for biomedical applications such as drug delivery can improve conventional pharmaceutical products due to their improved solubility, pharmacokinetics, and biodistribution. While nanoparticles delivered through oral, local, and topical routes have gained acceptance by regulatory institutions, intravenous administration still faces significant challenges based on the biological encounter within the bloodstream.¹⁻² Once the nanoparticles are delivered systemically, plasma proteins and immune cells in the bloodstream immediately bind to them.³ This leads to reduced bioavailability³ as the macrophages clear up the nanoparticles, which decrease their therapeutic efficiency. Moreover, in the case of complement-mediated uptake and clearance, as the pathways get activated trying to clear the nanoparticles out of the bloodstream, hypersensitivity reactions as severe as anaphylaxis can occur. This complement-mediated response, often termed an infusion reaction,⁴⁻⁵ is of concern for several organic and inorganic nanoparticles.^{4, 6-12} Hence it is critical that in designing nanomaterials delivered intravenously, their impact on the complement system be evaluated. This is essential to ensure the safety of the nanomaterials *in vivo*. As 7-10%¹³ of the human population is prone to complement activation, this is a significant safety concern when developing nanoformulations. Yet, for an emerging field such as nanomedicine, there are no existing guidelines. Moreover, depending on the heterogeneity within different species, the clinical translation is further challenged when moving from a preclinical to a clinical phase.

Materials properties and surface architecture¹⁴⁻¹⁵ of nanoparticles are major contributors to the complement response, as they influence the interactions of nanoparticles with proteins. Therefore, tuning materials and surface properties could lead to desirable stealth properties. However, currently, processes of quantifying complement-mediated response *in vitro* are limited for several reasons, which include differences observed between *in vitro* and *in vivo* responses for the same precursors, differences in the complement systems in different species, and lack of highly sensitive tools for quantifying the changes.

This dissertation aimed to understand the impact of surface architecture and materials properties of nanoparticles on complement activation. The first step in achieving that was developing sensitive screening tools and assay conditions for investigating complement-mediated hypersensitivity reactions *in vitro*. The overall goal is to develop nanomaterials with stealth properties to overcome complement-mediated infusion reactions *in vivo* utilizing the developed screening tool and the insights gathered from our *in vitro* experiments.

One of the first steps in achieving our research goal was identifying and quantifying the biomarkers associated with the infusion reaction. Currently, existing methods of quantifying complement *in vitro* are either qualitative or semi-quantitative.¹⁶⁻¹⁸ Moreover, the interference due to the addition of nanoparticles needs to be considered in the development of quantitative assays for biomarkers associated with the infusion reaction. To realize our first research objective, we have worked on developing complement assay conditions and sample preparation techniques that can

be highly sensitive in assessing the complement-mediated response *in vitro*, mimicking the *in vivo* activity. We determined the impact of incubation time, nanoparticle dosage, anticoagulants, and donor species (i.e., human vs porcine blood, plasma, or serum) in both blood and blood components (Figure 1). We investigated the role of donor species as different species show different sensitivity levels with regard to complement activation. We have validated the optimal assay conditions by replicating the impact of zeta potential seen *in vivo* on complement activation *in vitro*. We have validated the developed assays by comparing them to previous *in vivo* studies. These assay conditions would play a vital role in assessing the safety of intravenously administered nanomedicines.

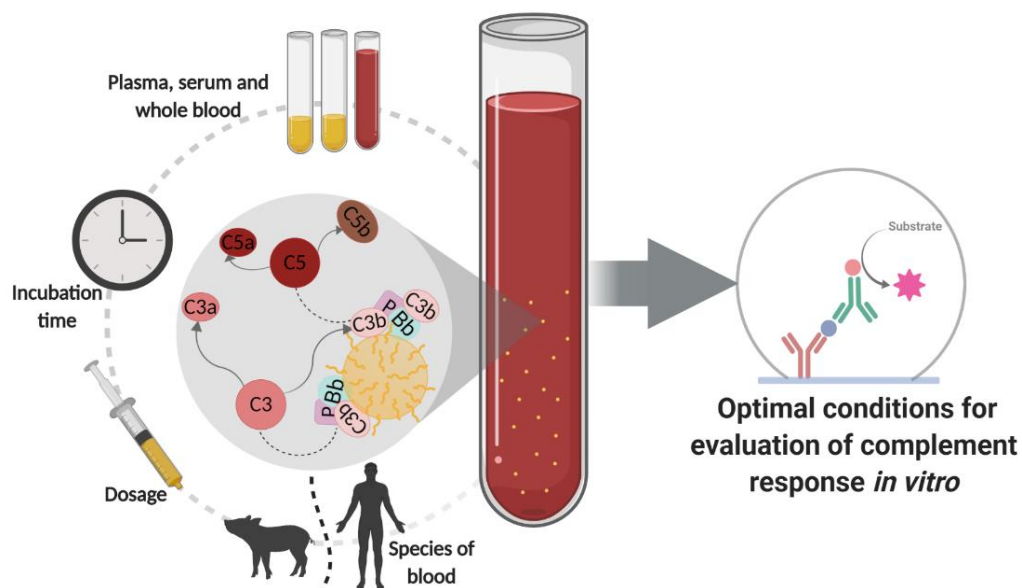


Figure 1. Determining the optimum assay conditions for sensitive screening of complement response *in vitro*.¹⁹

Utilizing the developed sensitive assay, we investigated how surface properties impact the complement activation in vitro. Nanoparticle surface properties are a relevant design feature, as they are critical in controlling the interaction with blood proteins. PEGylation of nano-surfaces is a surface modification technique that can improve the blood circulation of nanoparticles and reduce opsonization.²⁰⁻²² In our experiments we sought to understand whether modifying the surface architecture by varying the PEG density impact the complement response in vitro (Figure 2). For that, we have utilized block-copolymers of poly(lactic acid)-b-poly(ethylene glycol) prepared with poly(ethylene glycol) macroinitiators of different molecular weights (3400Da and 5000Da). As a point of comparison, we used PLA nanoparticles without any PEGylation on the surface. We tracked the complement biomarker C5a using the developed sensitive assay to understand changes in complement proteins based on PEGylation. We also investigated the impact of incorporating PEG chains of two different lengths to further strengthen stealth properties. Lastly, we tracked whether proinflammatory cytokines are generated upon blood incubation with nanoparticles in vitro to understand the extent to which inflammation may occur and the crosstalk between the complement and immune responses. The overall purpose was to determine the parameters crucial to develop stealth nanoparticles that do not lead to infusion reactions upon intravenous administration utilizing the highly sensitive screening tools.

90% PDLA
10% PLLA-*b*-PEG5000

50% PDLA
50% PLLA-*b*-PEG5000

25% PDLA
75% PLLA-*b*-PEG5000

25% PDLA-*b*-PEG3400
75% PLLA-*b*-PEG5000

HOOC-(O-CH₂-CH(CH₃))_n-OH $M_n=3400\text{Da}$

HO-(CH₂-CH₂-O)_m-H $M_n=5000\text{Da}$

Figure 1 illustrates the four different copolymers used in the study. The top row shows schematic representations of the copolymers, each consisting of a central orange circle with radiating lines representing the polymer chains. The bottom row shows the chemical structures of the copolymers, including the PEG chain and the carboxylic acid end group, with the molecular weight (M_n) indicated.

- PLLA-*b*-PEG3400
- 75% PLLA-*b*-PEG3400 / 25% PDLA-*b*-PEG5000
- 25% PLLA-*b*-PEG3400 / 75% PDLA-*b*-PEG5000
- PLLA-*b*-PEG5000

Chemical structures shown below the schematics:

- Structure 1 (Left): PLLA-*b*-PEG3400. The structure shows a blue wavy line representing the PLLA chain and a PEG chain with a carboxylic acid end group. The molecular weight is $M_n = 3400\text{Da}$.
- Structure 2 (Right): PLLA-*b*-PEG5000. The structure shows a green wavy line representing the PLLA chain and a PEG chain with a carboxylic acid end group. The molecular weight is $M_n = 5000\text{Da}$.

Lastly, we applied the developed screening tools and the knowledge gained from evaluating surface and material properties' impact to develop a nanomaterial system that would not lead to complement-mediated infusion reaction. In our studies, we investigated changes in the complement activation for commonly used polyester nanomaterials, and found out that even with stealth coatings, it is not entirely possible to eliminate complement activation for such nanomaterials. Hence, we synthesized nanoparticle core materials that display hemocompatibility and do not lead to complement-mediated hypersensitivity reactions in vitro (Figure 3). We then utilized these nanomaterials system to develop hemostatic nanomaterials with stealth

properties. Trauma is a leading cause of death for people under 46.²³ Hemostatic nanomaterials with polyester cores have the potential of increasing survivability after traumatic injuries.²⁴⁻²⁶ However, hemostatic nanomaterials can also lead to complement-mediated infusion reactions, especially in large animals.¹² The response itself can lead to significant morbidity and increased healthcare costs. It may require discontinuation of the therapeutic in the long run to avoid adverse reactions despite its better therapeutic effects in complement-sensitive patients.²⁷⁻²⁸ In our quest to understand the molecular features that dictate the interaction between the blood proteins and the nanoparticles, we have synthesized a polyurethane-based nanocapsule system that could be designed as a hemostatic nanomaterial. The objective was to eliminate complement-mediated initial infusion reaction *in vivo*. As a first step in assessing the system's safety, we have utilized *in vitro* screening tools to validate that the polyurethane nanocapsules with and without PEGylation do not activate the complement pathways. While non-PEGylated polyurethane nanocapsules do not lead to complement activation, we have considered the impact of PEGylation as well, as PEGylation can later be used to further decorate the nanoparticles with targeting moieties. We have also evaluated the hemostatic activity of these nanocapsules *in vitro* using ROTEM-based coagulation assays. This study is critical in developing hemostatic polyurethane nanocapsules for traumatic injuries, especially before preclinical studies with relevant animal trauma models.

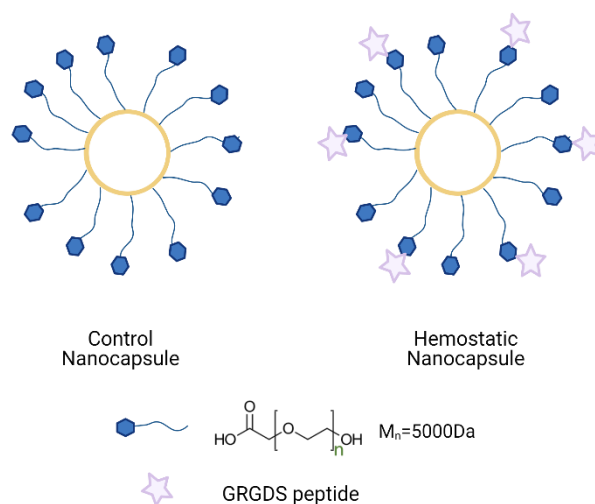


Figure 3. Developing stealth polyurethane based hemostatic nanocapsules to evade complement-mediated infusion reactions

As previously mentioned, the overall goal of this work is to contribute to developing clinically translatable nanomedicines for intravenous administration. The outcome of this study not only supports the development of stealth hemostatic nanoparticles but also ensures that safety can be assessed for a wide array of nanoparticles developed for systemic delivery. The highly sensitive optimum assay conditions and sample preparation methods to generate *in vitro* complement response like *in vivo* are critical in ensuring safety from the earliest stages of developing a nanoparticle. Moreover, we have developed materials utilizing the screening tools from the earliest stages of development that impart the stealth property and can be utilized as hemostatic nanomaterials. The knowledge gathered regarding the impact of surface architecture and materials properties is critical for designing stealth

nanomaterials for therapeutic applications to overcome initial infusion reactions.

Knowing how complement activation due to nanomaterials could be tuned would be beneficial in several ways as many nanomaterials for chemotherapeutic applications (such as Doxil) or those delivered in bolus could be administered safely at higher dosages without leading to unwanted adverse reactions that may lead to medical complications.

Acknowledgements

Some of the figures were created with Biorender.com.

References

1. Anselmo, A. C.; Mitragotri, S., Nanoparticles in the clinic. *Bioengineering & translational medicine* **2016**, *1* (1), 10-29 DOI: 10.1002/btm2.10003.
2. Anselmo, A. C.; Mitragotri, S., Nanoparticles in the clinic: An update. *Bioengineering & Translational Medicine* **2019**, e10143 DOI: 10.1002/btm2.10143.
3. Dobrovolskaia, M. A.; Aggarwal, P.; Hall, J. B.; McNeil, S. E., Preclinical studies to understand nanoparticle interaction with the immune system and its potential effects on nanoparticle biodistribution. *Mol Pharm* **2008**, *5* (4), 487-95 DOI: 10.1021/mp800032f.
4. Wibroe, P. P.; Anselmo, A. C.; Nilsson, P. H.; Sarode, A.; Gupta, V.; Urbanics, R.; Szebeni, J.; Hunter, A. C.; Mitragotri, S.; Mollnes, T. E.; Moghimi, S. M., Bypassing adverse injection reactions to nanoparticles through shape modification and attachment to erythrocytes. *Nat Nanotechnol* **2017**, *12* (6), 589-594 DOI: 10.1038/nnano.2017.47.
5. Szebeni, J.; Bedőcs, P.; Csukás, D.; Rosivall, L.; Bünger, R.; Urbanics, R., A porcine model of complement-mediated infusion reactions to drug carrier nanosystems and other medicines. *Advanced Drug Delivery Reviews* **2012**, *64* (15), 1706-1716 DOI: 10.1016/j.addr.2012.07.005.
6. Szebeni, J.; Bedőcs, P.; Rozsnyay, Z.; Weiszhár, Z.; Urbanics, R.; Rosivall, L.; Cohen, R.; Garbuzenko, O.; Báthori, G.; Tóth, M., Liposome-induced complement activation and related cardiopulmonary distress in pigs: factors

- promoting reactogenicity of Doxil and AmBisome. *Nanomedicine: Nanotechnology, Biology and Medicine* **2012**, 8 (2), 176-184 DOI: 10.1016/j.nano.2011.06.003.
7. Chanan-Khan, A.; Szebeni, J.; Savay, S.; Liebes, L.; Rafique, N. M.; Alving, C. R.; Muggia, F. M., Complement activation following first exposure to pegylated liposomal doxorubicin (Doxil): possible role in hypersensitivity reactions. *Ann Oncol* **2003**, 14 (9), 1430-7 DOI: 10.1093/annonc/mdg374.
 8. Wang, G.; Chen, F.; Banda, N. K.; Holers, V. M.; Wu, L.; Moghimi, S. M.; Simberg, D., Activation of Human Complement System by Dextran-Coated Iron Oxide Nanoparticles Is Not Affected by Dextran/Fe Ratio, Hydroxyl Modifications, and Crosslinking. *Front Immunol* **2016**, 7, 418 DOI: 10.3389/fimmu.2016.00418.
 9. Banda, N. K.; Mehta, G.; Chao, Y.; Wang, G.; Inturi, S.; Fossati-Jimack, L.; Botto, M.; Wu, L.; Moghimi, S. M.; Simberg, D., Mechanisms of complement activation by dextran-coated superparamagnetic iron oxide (SPIO) nanoworms in mouse versus human serum. *Particle and fibre toxicology* **2014**, 11 (1), 64 DOI: 10.1186/s12989-014-0064-2.
 10. De Sousa Delgado, A.; Léonard, M.; Dellacherie, E., Surface Properties of Polystyrene Nanoparticles Coated with Dextrans and Dextran-PEO Copolymers. Effect of Polymer Architecture on Protein Adsorption. *Langmuir* **2001**, 17 (14), 4386-4391 DOI: 10.1021/la001701c.
 11. Fornaguera, C.; Caldero, G.; Mitjans, M.; Vinardell, M. P.; Solans, C.; Vauthier, C., Interactions of PLGA nanoparticles with blood components: protein

adsorption, coagulation, activation of the complement system and hemolysis studies.

Nanoscale **2015**, 7 (14), 6045-58 DOI: 10.1039/c5nr00733j.

12. Onwukwe, C.; Maisha, N.; Holland, M.; Varley, M.; Groynom, R.; Hickman, D.; Uppal, N.; Shoffstall, A.; Ustin, J.; Lavik, E., Engineering Intravenously Administered Nanoparticles to Reduce Infusion Reaction and Stop Bleeding in a Large Animal Model of Trauma. *Bioconjugate chemistry* **2018**, 29 (7), 2436-2447 DOI: 10.1021/acs.bioconjchem.8b00335.

13. Szebeni, J., Hemocompatibility testing for nanomedicines and biologicals: predictive assays for complement mediated infusion reactions. *European Journal of Nanomedicine* **2012**, 4 (1), DOI: 10.1515/ejnm-2012-0002.

14. Hamad, I.; Al-Hanbali, O.; Hunter, A. C.; Rutt, K. J.; Andresen, T. L.; Moghimi, S. M., Distinct polymer architecture mediates switching of complement activation pathways at the nanosphere– serum interface: implications for stealth nanoparticle engineering. *ACS nano* **2010**, 4 (11), 6629-6638.

15. Coty, J. B.; Eleamen Oliveira, E.; Vauthier, C., Tuning complement activation and pathway through controlled molecular architecture of dextran chains in nanoparticle corona. *Int J Pharm* **2017**, 532 (2), 769-778 DOI: 10.1016/j.ijpharm.2017.04.048.

16. Costabile, M., Measuring the 50% haemolytic complement (CH50) activity of serum. *J Vis Exp* **2010**, (37), DOI: 10.3791/1923.

17. Ekdahl, K. N.; Persson, B.; Mohlin, C.; Sandholm, K.; Skattum, L.; Nilsson, B., Interpretation of Serological Complement Biomarkers in Disease. *Front Immunol* **2018**, *9*, 2237 DOI: 10.3389/fimmu.2018.02237.
18. Pham, C. T.; Thomas, D. G.; Beiser, J.; Mitchell, L. M.; Huang, J. L.; Senpan, A.; Hu, G.; Gordon, M.; Baker, N. A.; Pan, D.; Lanza, G. M.; Hourcade, D. E., Application of a hemolysis assay for analysis of complement activation by perfluorocarbon nanoparticles. *Nanomedicine* **2014**, *10* (3), 651-60 DOI: 10.1016/j.nano.2013.10.012.
19. Maisha, N.; Coombs, T.; Lavik, E., Development of a Sensitive Assay to Screen Nanoparticles in Vitro for Complement Activation. *ACS Biomaterials Science & Engineering* **2020**, *6* (9), 4903-4915 DOI: 10.1021/acsbiomaterials.0c00722.
20. Torchilin, V.; Papisov, M., Why do polyethylene glycol-coated liposomes circulate so long?: Molecular mechanism of liposome steric protection with polyethylene glycol: Role of polymer chain flexibility. *Journal of liposome research* **1994**, *4* (1), 725-739.
21. Harris, J. M.; Chess, R. B., Effect of pegylation on pharmaceuticals. *Nat Rev Drug Discov* **2003**, *2* (3), 214-21 DOI: 10.1038/nrd1033.
22. Gabizon, A.; Martin, F., Polyethylene glycol-coated (pegylated) liposomal doxorubicin. *Drugs* **1997**, *54* (4), 15-21.
23. Kauvar, D. S.; Lefering, R.; Wade, C. E., Impact of hemorrhage on trauma outcome: an overview of epidemiology, clinical presentations, and therapeutic considerations. *Journal of Trauma and Acute Care Surgery* **2006**, *60* (6), S3-S11.

24. Bertram, J. P.; Williams, C. A.; Robinson, R.; Segal, S. S.; Flynn, N. T.; Lavik, E. B., Intravenous hemostat: nanotechnology to halt bleeding. *Sci Transl Med* **2009**, *1* (11), 11ra22 DOI: 10.1126/scitranslmed.3000397.
25. Shoffstall, A. J.; Atkins, K. T.; Groynom, R. E.; Varley, M. E.; Everhart, L. M.; Lashof-Sullivan, M. M.; Martyn-Dow, B.; Butler, R. S.; Ustin, J. S.; Lavik, E. B., Intravenous Hemostatic Nanoparticles Increase Survival Following Blunt Trauma Injury. *Biomacromolecules* **2012**, *13* (11), 3850-3857 DOI: 10.1021/bm3013023.
26. Hubbard, W. B.; Lashof-Sullivan, M. M.; Lavik, E. B.; VandeVord, P. J., Steroid-Loaded Hemostatic Nanoparticles Combat Lung Injury after Blast Trauma. *ACS Macro Letters* **2015**, *4* (4), 387-391 DOI: 10.1021/acsmacrolett.5b00061.
27. Benjamini, E., *Immunology: a short course*. Vol. 77.
28. Moghimi, S. M.; Simberg, D., Complement activation turnover on surfaces of nanoparticles. *Nano Today* **2017**, *15*, 8-10 DOI: 10.1016/j.nantod.2017.03.001.

Chapter 2: Complement-mediated initial infusion reactions for intravenously administered nanoparticles: a hindrance to clinical translation

Intravenous administration of nanoparticles is often a favorable mode of delivery in both clinical and preclinical settings, as the therapeutic is systemically delivered to all the targeted organs. However, the challenges are immense, as the biological interaction with the blood proteins can not only limit the bioavailability,¹ It could also elicit a complement response.² These infusion reactions are a significant hurdle to the translation of nanotechnology-based products. Infusion reactions usually set in motion within minutes to hours after the therapeutic is received, and the consequences of such hypersensitivity reactions can be as severe as anaphylaxis, a life-threatening condition.³ Temporary infusion interruption, reduced rate of infusion, and symptom management can help control mild-to-moderate hypersensitivity reactions, while severe reactions may need treatment discontinuation.⁴ Due to such complications for many nanoparticle-based therapeutics, the number of regulatory board-approved nanotherapeutics is small.⁵⁻⁶ The activation of the complement pathways is implicated in such infusion reactions.⁷⁻⁸ The nanomaterials have the potential to trigger the complement pathway, a part of the innate immune system due to particle-host interactions. This eventually leads to the uptake of nanoparticles through various macrophages generated due to the immune reactions.⁹ This phenomenon is of concern for several applications involving the use of organic and

inorganic nanomaterials^{7, 10-16} While rare, and only seen in a particular subset of the human population, the incidence rate of complement-mediated responses is close to 10%, with a 0.3% chance of fatality.¹⁷ The fact that nanomaterials can elicit such innate immune response is not surprising because of the sheer surface area exposed to complement proteins. A 400-nm particle can provide a surface area of $5 \times 10^5 \text{ nm}^2$. This fact raises the question of whether tuning the surface through the presence of different functional groups or differences in material properties can impact complement activation and the infusion reaction. The scope of this chapter will focus on cases of nanoparticle-induced infusion reactions, understand the mechanism of complement activations, and get an overview of the materials' properties that could be critical in developing nanoparticles that do not lead to complement-mediated infusion reactions.

Infusion reactions from nanoparticle-based therapeutics

Doxil, an FDA-approved PEGylated liposomal formulation of Doxorubicin, a chemotherapeutic medication for treating various forms of cancers, was one of the first detected nanomedicine that leads to a complement-mediated response.¹¹ In comparison to Doxorubicin, Doxil has a superior therapeutic impact.¹¹ However, a study shows that when Doxil was administered, after 10 minutes of infusion, 92 percent of patients prone to complement activation have raised levels of complement proteins.¹¹ In contrast half of the non-reactive patients also had a complement-mediated response.¹¹ Slower infusion rates and premedication with antihistamines and

glucocorticoids, as well as repeated delivery, can help to limit but not completely prevent such hypersensitivity reactions.¹¹ The reaction itself causes significant morbidity, higher healthcare expenditures, and the inability to take the nanoparticles to prevent unwanted responses in susceptible patients, even though the nanoparticles offer solid therapeutic results.¹¹

These hypersensitivity responses are also a challenge for organic nanoparticles that have shown complement activation in large animal models, despite showing therapeutic effect in small animal models.¹⁶ One such system is the poly(lactic-co-glycolic acid) based hemostatic nanoparticles. The hemostatic nanoparticles consisting of polyester core, with poly(ethylene glycol) corona, have been designed, with a peptide sequence GRGDS conjugated to the PEG corona. The peptide motif binds with glycoprotein IIb/IIIa in the activated platelets and helps in forming clots faster to reduce bleeding, mimicking the activity of fibrinogen.¹⁸⁻¹⁹ While the nanoparticles can reduce bleeding and improve survival in rodent trauma models, in large animals, it triggers the complement system even at very low dosages¹⁶. In a naïve administration model, the nanoparticles caused drastic changes in cardiopulmonary vitals for highly negative and highly positive nanoparticles, while neutral nanoparticles (1.29 mV) showed no significant change (Figure 4).¹⁶ The rapid cardiopulmonary changes and vasodilation are symptoms of infusion reactions, and the nanoparticles with neutral surface charge were able to overcome this hypersensitivity reaction in the porcine animals.

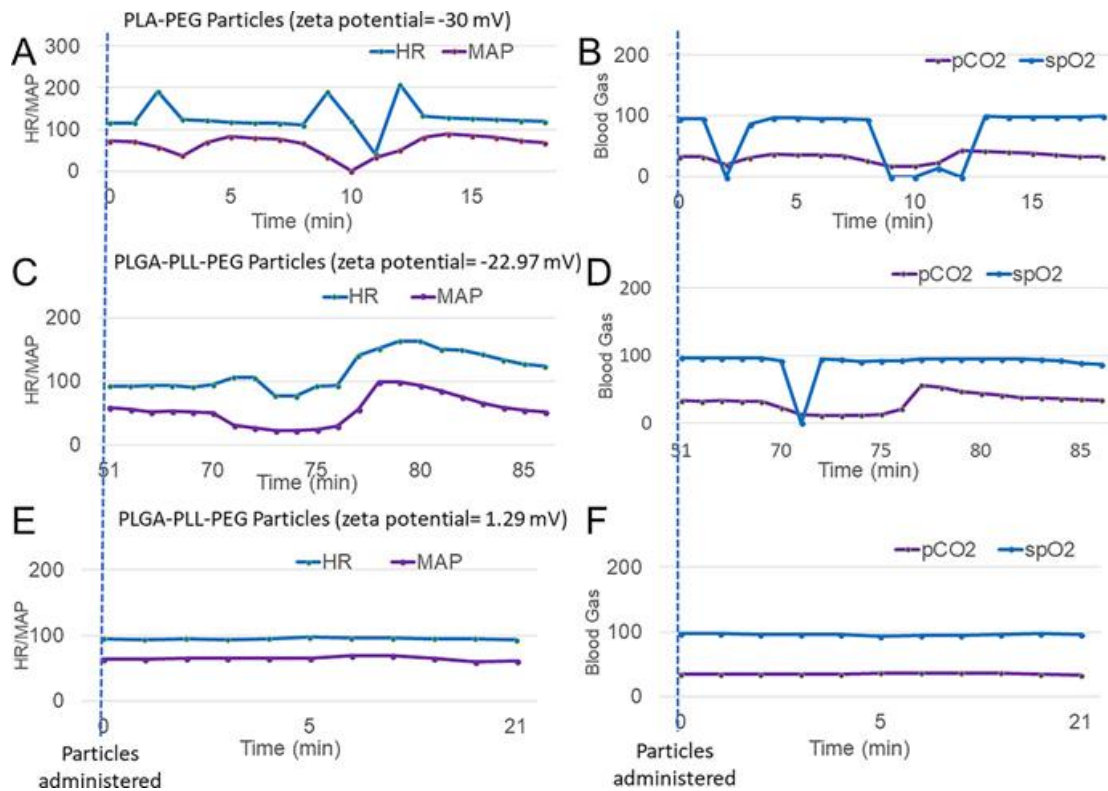


Figure 4. Change in cardiopulmonary vitals with changing zeta potential for a naive administration model in porcine animals¹⁶

Intravenous infusion of nanoparticles and complement activation

The complement pathways and their role in innate immune response

The complement pathways are a part of the innate immune system responsible for primary surveillance against pathogenic entities and are at some level at all times working on the clearance of pathogens and apoptotic cells.²⁰⁻²¹ Their activation can take place through three distinct pathways, each with a separate recognition molecule. These include an antigen-antibody complex dependent classical pathway, pathogen mediated alternative pathway, and the mannose-binding lectin pathway.²⁰⁻²²

Classical Pathway

The classical pathway is activated as the complement protein C1 binds to antigen-antibody complex through recognition of the unit C1q.²³ The attachment leads to subsequent proteolysis and activation of the complement proteins C4 and C2 and formation of initial C3 convertase.²⁴

Alternative Pathway

The second route, alternative pathway, is activated due to the spontaneous hydrolysis of C3 and the activation is further catalyzed by the presence of foreign surfaces.²⁵

Lectin Pathway

The third route of activation is through the lectin pathway. The pathway is activated due to plasma protein mannose-binding lectins attaching to carbohydrate structures.²⁶

In each of the pathway, opsonizing fragments are generated, that further amplifies generation of anaphylatoxins that work towards forming the terminal membrane complex.²¹ (Figure 5) The terminal complex eventually leads to clearance of the foreign agent.²¹ Such immune response leads to vasodilation, increased tissue permeability, edema, and drastic fall in blood pressure leading to shock, with symptoms appearing in minutes after exposure to an allergen and can occur within 30 minutes.^{23, 27} Uninhibited complement activation can eventually lead to inflammatory responses as severe as anaphylaxis, an acute life-threatening respiratory failure due to anaphylatoxin tick-over.²⁸

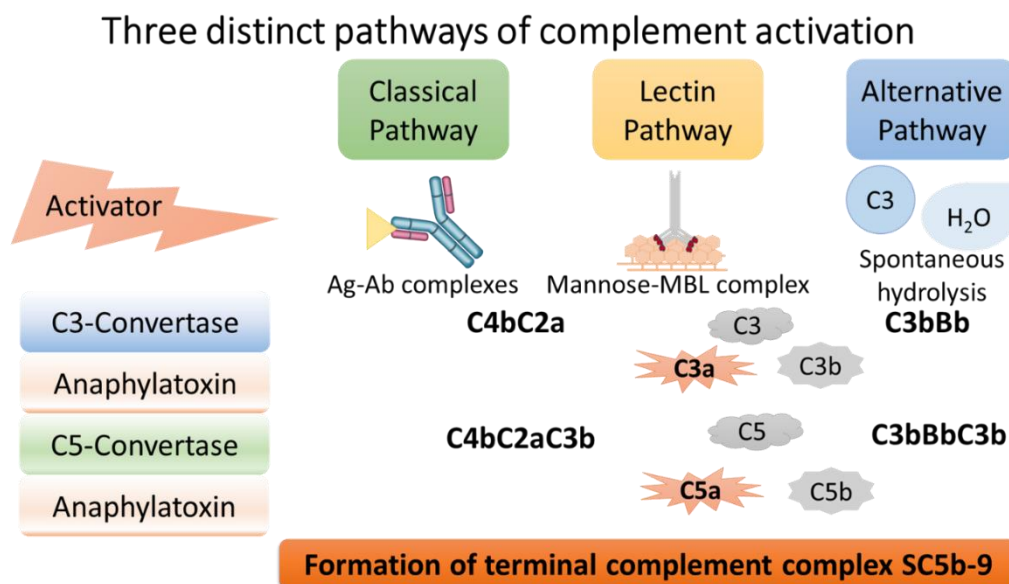


Figure 5. Complement activation occurs through three distinct pathways. The precursors for the activation routes are different, but each pathway results in generating C3a and C5a. Anaphylatoxins C3a and C5a cause allergic reaction, and the pathway goes forward generating terminal complex SC5b-9.

Nano-bio interaction and complement activation: The mechanism of activation

As the complement system is directed towards attacking all components that are not recognized as healthy or familiar, nanomedicines are reported to elicit complement-mediated initial infusion reactions as well. Studies showing the presence of factor B and hydrolyzed C3 on the surface of nanoparticles suggest the alternative pathway being the dominant pathway for complement response.²⁹⁻³⁰ When nanoparticles are administered, upon reaching the blood, they encounter the complement and serum proteins present in blood,¹ where complement proteins either

bind directly to nanoparticle surface or attach to serum proteins adsorbed on the surface of the particles through the covalently binding thioester group in C3b.^{27, 30} C3b deposition on nanoparticles along with factor Bb and properdin, a C3bBb stabilizer in blood serum³⁰, in the presence of Magnesium ions leads to complement activation and further amplification of C3b (Figure 6).^{27, 30} The amplification in this pathway is dependent on the dissociation of the C3bB complex, which is regulated by the amount of properdin. Activation through the alternative pathway, if not inhibited efficiently, leads to prolonged tissue damage and glomerular disease along with the inflammatory responses mentioned above.²⁰ Two components produced along the pathways: C3a and C5a are of relevance because of their biological activity as anaphylatoxins that work in degranulation of mast cells and production of histamines. These lead to local edema further increasing complement protein concentrations. This leads to further amplification of the anaphylatoxins and eventually the pathogens being phagocytized out of the system leading to opsonization.²³ Anaphylaxis, an outcome of activation of the complement pathways, is a type I hypersensitivity reaction. As the anaphylatoxins cause mast cells to release its contents, it leads to vasodilation, increased tissue permeability, edema, and drastic fall in blood pressure leading to shock. Such hypersensitivity reactions start minutes after exposure to allergen and within 30 minutes to an hour.²³

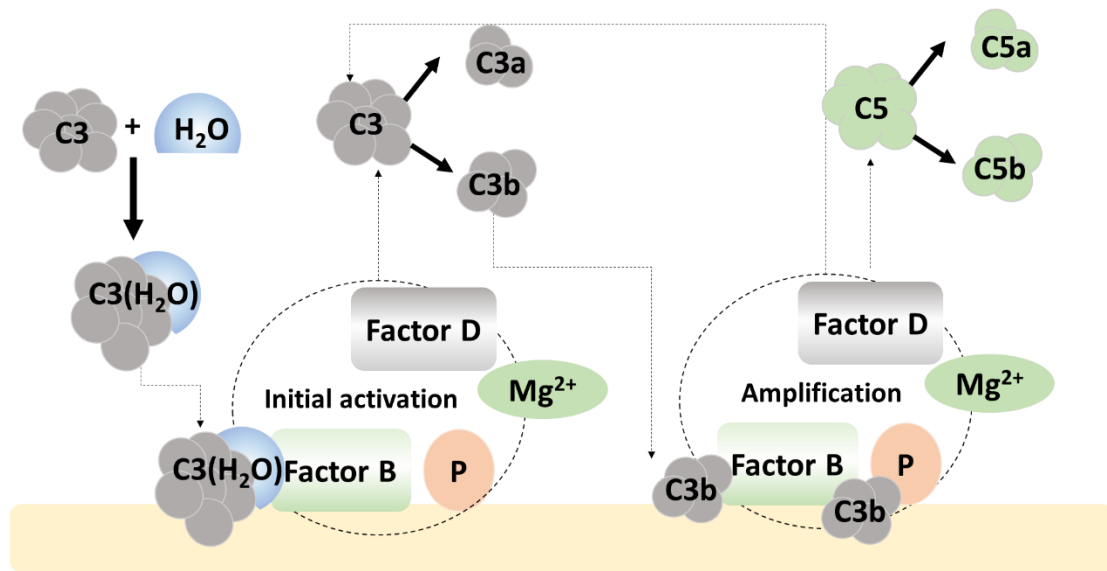


Figure 6. Complement protein C3b binds to a different surface through a covalent thioester bonding, and in the presence of properdin and magnesium ion, it forms the C3 convertase that further breaks down C3 into C3a and C3b. More C3b then amplifies the alternative complement pathway.

Role of species on complement activation

As already discussed, the complement-mediated response is observed in a particular part of the human population. However, it is more reproducibly present in porcine animals. The complement-mediated response is more common in the porcine animals, as the lungs of these animals are lined with pulmonary intravascular macrophages (PIM) that act on clearing these particles.³¹⁻³² While the human lungs are devoid of PIMs, induced PIM can lead to the infusion reaction as well.³¹ Many other species show complement-mediated response, but porcine models are of interest mainly due to showing response to dosages to which reactive humans show the initial

infusion reaction as well. For a liposomal formulation that is known to cause complement activation at a dosage ranging from 0.01-0.3mg/kg in porcine animals, a dosage of 5-25mg/kg is required to get a similar response in rodents and a dose of 0.05-0.1mg/kg in canines. Whereas for reactive human species, which accounts for around 7% of the human population, the required dose is comparable to that observed in porcine animals, i.e., 0.01-0.2mg/kg.^{17, 31} The Kupffer cells³³ in the human liver are responsible for generating multiple complement receptors and clearance of nanoparticles, and these are similar to the PIMs.³⁴ Compared to Kupffer cells, PIMs release significant quantities of vasoconstrictors and complement mediators that are responsible for respiratory distress and inflammation.³² As a result, porcine *in vivo* models are highly sensitive and this naturally raises questions on the relevance of the porcine model. However, since a subset of the human population is also sensitive, the porcine model is a valuable tool to determine whether a nanomaterial leads to unwanted hypersensitivity reaction at a subtherapeutic dosage for confirming the safety of a nanoformulation.³⁵

Existing approaches for quantifying changes in complement proteins

Complement activation is measured through indirect measurements, either through hemolysis assay,³⁶⁻³⁸ or through quantifying the proteins that attach to the nanoparticle surface.^{11-12, 30, 39-40} The other, more direct option is dependent on enzyme-linked immunoassays.^{13, 17} These methods require nanoparticle blood

interaction to generate complement proteins, and then the proteins that attach directly or indirectly on the surface of nanoparticles are quantified.^{12-13, 30}

Hemolysis assays: CH50 and AH50

Hemolysis assays such as CH50 assays and AH50 assays are used to indirectly measure the extent of activation by measuring the amount of serum that causes lysis of 50% of sheep erythrocytes due to serum exposure to complement activator.³⁷ However, the method can include spontaneous hemolysis and variable affinity of the to-be-lysed erythrocytes.³⁶ Thus, methods like hemolysis assays are often semiquantitative.⁴¹

Quantifying eluted complement proteins from nanoparticle corona

Another frequently used technique in several recent complement reaction studies involves incubating blood matrices with nanoparticles and quantifying the attached complement proteins through SDS-PAGE and western blots.^{12, 30, 39} However, as the protein corona is dynamic due to reversible attachment of proteins, this technique can lead to underestimating the overall complement protein levels, mainly quantifying the complement proteins part of the hard corona.⁴²

Enzyme-linked immunoassays

Enzyme-linked immunoassays (ELISAs) for detecting complement proteins have been available for more than two decades, and the assays are more sensitive than the conventional methods,⁴³ but only available for a limited number of complement

proteins. Moreover, the enzyme immunoassays do not account for possible interference in signal outputs due to the presence of nanoparticles in the blood, plasma, or serum. Nanoparticles may lead to adsorption of assay reagents or biomolecules generating outputs with disturbance because of their physiological properties and morphology.⁴⁴ Nonetheless, the sensitivity of the enzyme immunoassays makes them extremely attractive by offering the possibility of developing *in vitro* assays that replicate the *in vivo* response allowing efficient screening of molecular features of nanomaterials and their impact on complement activation.

Critical factors in optimizing complement protein assays

Anticoagulant used for collecting blood

The coagulation cascade and complement pathways are intricately connected as the coagulation components thrombin, and factor Xa can directly activate components of the complement cascade.⁴⁵ So, to ensure that the complement cascade is not activated or blocked due to interference with the coagulation system, the anticoagulant used must be chosen after thorough consideration. Commonly used anticoagulants include Citrate, EDTA, and heparin. Citrating blood prevents coagulation by sequestering Ca^{2+} , while heparin enhances antithrombin activity.⁴⁵ EDTA, on the other hand, works by chelating Ca^{2+} and Mg^{2+} . Hence, EDTA blocks the complement cascade as the metal ions are vital for activating the pathways.⁴⁵ Another anticoagulant that does not inhibit the complement cascade is hirudin. Using

hirudin as an anticoagulant leads to improved complement preservation compared to heparin even at very high concentrations.⁴⁶⁻⁴⁷ Hirudin is a highly specific thrombin inhibitor that leads to lower platelet loss and higher C3a generation, especially with longer incubation times.⁴⁷ However, for both heparin and hirudin, the terminal complex SC5b-9 levels remain similar upon contact with PVC surface.⁴⁷ Also, at lower dosages, heparin does not affect the complement cascade.⁴⁸

Impact of incubation time

The incubation time to be used to generate a response *in vitro* is critical. The time should be adequate for the pathway to proceed and generate sufficient biomarkers to detect the change with accuracy. A computational model addressing time-dependent depletion of C5 and generation of C5a-desArg exhibit an upward trajectory up to 25 minutes, with the rate of change gradually decreasing.⁴⁹ Hence, the time for incubation to generate the response needs to be chosen after thoroughly analyzing what period would lead to biomarker change relevant and matching with the *in vivo* conditions.

Differences in response for whole blood, plasma, and serum

The blood matrix used to generate can significantly affect the amount of biomarkers generated. For instance, in serum, where the coagulation cascade is no longer intact, the level change is faster than in plasma.⁴⁷ Using whole blood in the presence of anticoagulants that do not impact the complement pathways, such as

heparin⁴⁸ or hirudin⁴⁷, would be able to overcome the issues of interference with the complement pathways as well.

The impact of surface architecture and material properties on the complement interaction

Due to the vast surface area exposed, nanomedicines show a fast complement-mediated response. The surface moieties and material properties provide a surface for complement binding, leading to a hypersensitivity response. Many works currently focus on tuning these properties to control complement-mediated reactions starting with modifying the functional groups present or the surface architecture. The orientation or conformation of surface modification (i.e., brush, mushroom, or mushroom-brush orientations) impacts complement activation and the activation pathways.⁵⁰ Particles with brush-like polyethylene oxide (highly dense) or dense dextran brushes are more resistant to binding complement proteins than their counterparts with mushroom-like/ or lightly enveloped surfaces.^{40, 50} Recently, decay-accelerating factors, a type of complement inhibitor, have been investigated as well.⁵¹ Hence surface modification factors like PEGylation, zwitterionic coatings, and coatings such as dextran or surface decoration with complement reaction inhibitors are currently assessed to understand their impact on complement activation.

PEGylation

Covalently grafting, entrapping, or adsorbing Poly(ethylene glycol) (PEG) chains to a molecule or material is known as PEGylation.⁵² Based on one of the earliest theories by Jeon et al. PEGylation of surfaces leads to low protein adsorption due to the fact that PEG has the lowest refractive index among water-soluble synthetic polymers, resulting in low van der Waals forces with proteins.⁵³ Moreover, PEGylation results in a more extended conformation in the presence of water molecules depending on the molecular weight and grafting density, and the hydrophilic nature and flexibility of the PEG chains.⁵²⁻⁵³ A minimum PEG chain molecular weight of 2000 or greater helps in preventing the immediate uptake and clearance of PEGylated nanoparticles.⁵² PEG is a hydrophilic component and this results in a higher chain flexibility. Depending on the molecular weight, PEG coating can lead to the formation of an impermeable cloudlike conformation even from a small number of PEG chains and prevent opsonization.⁵⁴ PEGylation of liposomal nanoformulations enhances the half-life during circulation, and prevents unwanted plasma clearance⁵⁵ and clearance due to reticuloendothelial systems.⁵⁶ Moreover, poly(lactic-co-glycolic acid) PLGA nanoparticles which are coated with polyethylene oxide can impart stealth properties as these form a weak complex with blood albumen and leads to a chameleon effect.⁵⁷ This further results in repulsion of biomolecules in the blood, which are responsible for rapid clearance of the nanoparticles.⁵⁷ Surface modification with innovative coating materials like poly(phosphoester),⁵⁸ and polysaccharides combined with PEG⁵⁹ have been explored as well to enrich the

surfaces of nanomaterials with clusterin. Clusterin is a dysopsonin protein that helps avoiding clearance of nanoparticles by macrophages.⁶⁰ Studies show that increased molecular weight and grafting density of PEG impacts clusterin adsorption, as the dense brush conformation reduces cellular internalization.⁶¹ This is because the grafted PEG chains on the surface impact complement activation and the activation pathways modulating access between nanoparticles and blood proteins.⁵⁰ Thus, particles with brush-like polyethylene oxide (highly dense) or dense dextran brushes are more resistant to binding complement proteins than their counterparts with mushroom-like/ or lightly enveloped surfaces.^{40, 50} Moreover, how PEG remains attached to the surface also plays a pivotal role in determining the extent to which opsonization is blocked, as surface adsorption is reversible, and surface conjugation may lead to insufficient surface coverage.⁵² It is worth noting that the stealth effect is only effective within a PEG size range. The range above 5000Da shows no significant decrease in plasma protein adsorption.⁶² However, increasing the PEG chain length from 2000Da to 5000Da leads to up to 50% reduction in adsorbed proteins.⁶² Recently the concept of combining two different PEG lengths have been explored as well. The concept has been applied previously in microbubbles for improved targeting, as the shorter PEG layer leading to steric repulsion prohibits the approach and adhesion of opsonin, lipoproteins, and other liposomes, and the more extended layer of PEG provides target specificity.⁶³ Recently, PEG pairing has been explored to prevent protein surface adsorption.⁶⁴ The goal was to support the longer chains with the shorter chains and project the longer chains further.⁶⁴ The versatility

in the applications as well as the scope in utilizing the individual properties of PEG, makes PEGylation a very suitable method for achieving stealth properties for nanomaterials.

Zwitterionic coatings

Zwitterionic coatings of phosphorylcholine (PC), carboxybetaine (CB), and sulfobetaine (SB), due to their inertness in blood, are being explored for biomedical applications.⁶⁵ Poly(phosphorylcholine) coatings in oxygenator circuits are able to significantly control fibrinogen adsorption, platelet adhesion, and blood cell activation, as well as thrombus formation during extracorporeal blood circulation.⁶⁶ Carboxybetaine coated biomedical devices show ultra-low fouling to blood proteins and can be further functionalized as well.⁶⁵ Sulfobetaine methacrylate monomers also show anti-biofouling properties *in vitro* and *in vivo*.⁶⁷ Based on their anti-fouling properties, these coatings have gained recognition as probable nanoparticle coatings to impart stealth properties. A comparison between the three zwitterionic coatings mentioned shows that poly(sulfobetaine) coatings can better suppress the formation of hard and soft protein coronas for fluorescent core/multishell quantum dots.⁶⁸ Such studies have been extended to silica nanoparticles⁶⁹ as well. Hence there is much scope to utilize the concept of coating surfaces of nanomaterials with zwitterionic moieties for preventing adsorption of complement proteins and subsequent activation.

Surface functional groups

Functional groups that are present on the surface are critical as they often dictate the interactions with the blood proteins. Studies on crosslinked dextran with surface modification to replace hydroxyl groups into carboxymethyl groups show that the blend of both the functional groups when present instead of just one of the two reduces complement activation based on the amount of C3a observed.⁷⁰ Studies have also shown that while hydroxyl groups on particle surface elicit complement activation, amine modifications do not, based on C3a detected and C1q deposited on the particles.⁷¹ This is due to surface coverage by negative serum proteins interfering with C3b adsorption.⁷¹

Surface decoration with complement inhibitors

Codelivery of complement inhibitors or decay-accelerating factors like CD55 and the synthetic counterpart of the CD55 sequence that leads to the inhibition can inhibit C3 deposition and eventual release of C5a.⁵¹ The use of such inhibitors has been further extended for targeted nano worms with complement inhibitors conjugated to the surface.⁷² Hence, there is potential to further extend such complement pathway controlling entities to be leveraged for stealth properties.

The impact of the core of nanoparticles on complement activation

Nanoparticles based on their composition could be broadly classified as lipid-based, organic, or inorganic. Only nine have been approved by the FDA so far among

the organic polymer-based nanoparticles, with only two approved (Plegridy and ADYNOVATE) over the last decade.⁷³ While surface modification through PEGylation⁷³ or functional groups can impact the complement protein binding,¹⁵ even with stealth coatings, it is not entirely possible to overcome the complement activation. Even single-walled carbon nanotubes lead to elevated complement biomarkers in vitro.⁷⁴ Such complement responses are observed in inorganic nanoparticles like the superparamagnetic iron oxide nanoworms as well.¹³ Hence it becomes critical to investigate the impact of nanoparticle core material and develop nanomaterials with stealth properties. An ideal nanomaterial core should lack recognizable repeat units⁷⁵ that the complement proteins can identify and bind to.

Conclusions

As the complement pathway is a part of the innate immune system responsible for eliminating threats to the immune system, it is always actively at work. However, for therapeutic nanomaterials delivered intravenously, activation of the complement pathways reduces the therapeutic's bioavailability and causes hypersensitivity reactions as severe as anaphylaxis. Hence understanding the mechanism of activation is essential to evaluate what condition could help in preventing such response. The currently deployed methods for quantifying the biomarkers generated from complement activation are not adequate, calling for more sensitive screening tools. Lastly, the role of surface architecture and materials properties need to be evaluated

to design nanomaterials that do not lead to complement-mediated hypersensitivity reactions.

References

1. Dobrovolskaia, M. A.; Aggarwal, P.; Hall, J. B.; McNeil, S. E., Preclinical studies to understand nanoparticle interaction with the immune system and its potential effects on nanoparticle biodistribution. *Mol Pharm* **2008**, *5* (4), 487-95 DOI: 10.1021/mp800032f.
2. Desai, N., Challenges in development of nanoparticle-based therapeutics. *AAPS J* **2012**, *14* (2), 282-95 DOI: 10.1208/s12248-012-9339-4.
3. Szebeni, J.; Simberg, D.; Gonzalez-Fernandez, A.; Barenholz, Y.; Dobrovolskaia, M. A., Roadmap and strategy for overcoming infusion reactions to nanomedicines. *Nat Nanotechnol* **2018**, *13* (12), 1100-1108 DOI: 10.1038/s41565-018-0273-1.
4. Lenz, H. J., Management and preparedness for infusion and hypersensitivity reactions. *Oncologist* **2007**, *12* (5), 601-9 DOI: 10.1634/theoncologist.12-5-601.
5. Anselmo, A. C.; Mitragotri, S., Nanoparticles in the clinic: An update. *Bioengineering & Translational Medicine* **2019**, e10143 DOI: 10.1002/btm2.10143.
6. Anselmo, A. C.; Mitragotri, S., Nanoparticles in the clinic. *Bioengineering & translational medicine* **2016**, *1* (1), 10-29 DOI: 10.1002/btm2.10003.
7. Wibroe, P. P.; Anselmo, A. C.; Nilsson, P. H.; Sarode, A.; Gupta, V.; Urbanics, R.; Szebeni, J.; Hunter, A. C.; Mitragotri, S.; Mollnes, T. E.; Moghimi, S. M., Bypassing adverse injection reactions to nanoparticles through shape modification and attachment to erythrocytes. *Nat Nanotechnol* **2017**, *12* (6), 589-594 DOI: 10.1038/nnano.2017.47.

8. Szebeni, J.; Bedőcs, P.; Csukás, D.; Rosivall, L.; Bünger, R.; Urbanics, R., A porcine model of complement-mediated infusion reactions to drug carrier nanosystems and other medicines. *Advanced Drug Delivery Reviews* **2012**, *64* (15), 1706-1716 DOI: 10.1016/j.addr.2012.07.005.
9. Gustafson, H. H.; Holt-Casper, D.; Grainger, D. W.; Ghandehari, H., Nanoparticle uptake: the phagocyte problem. *Nano today* **2015**, *10* (4), 487-510 DOI: 10.1016/j.nantod.2015.06.006.
10. Szebeni, J.; Bedőcs, P.; Rozsnyay, Z.; Weiszhár, Z.; Urbanics, R.; Rosivall, L.; Cohen, R.; Garbuzenko, O.; Báthori, G.; Tóth, M., Liposome-induced complement activation and related cardiopulmonary distress in pigs: factors promoting reactogenicity of Doxil and AmBisome. *Nanomedicine: Nanotechnology, Biology and Medicine* **2012**, *8* (2), 176-184 DOI: 10.1016/j.nano.2011.06.003.
11. Chanan-Khan, A.; Szebeni, J.; Savay, S.; Liebes, L.; Rafique, N. M.; Alving, C. R.; Muggia, F. M., Complement activation following first exposure to pegylated liposomal doxorubicin (Doxil): possible role in hypersensitivity reactions. *Ann Oncol* **2003**, *14* (9), 1430-7 DOI: 10.1093/annonc/mdg374.
12. Wang, G.; Chen, F.; Banda, N. K.; Holers, V. M.; Wu, L.; Moghimi, S. M.; Simberg, D., Activation of Human Complement System by Dextran-Coated Iron Oxide Nanoparticles Is Not Affected by Dextran/Fe Ratio, Hydroxyl Modifications, and Crosslinking. *Front Immunol* **2016**, *7*, 418 DOI: 10.3389/fimmu.2016.00418.
13. Banda, N. K.; Mehta, G.; Chao, Y.; Wang, G.; Inturi, S.; Fossati-Jimack, L.; Botto, M.; Wu, L.; Moghimi, S. M.; Simberg, D., Mechanisms of complement

activation by dextran-coated superparamagnetic iron oxide (SPIO) nanoworms in mouse versus human serum. *Particle and fibre toxicology* **2014**, *11* (1), 64 DOI: 10.1186/s12989-014-0064-2.

14. De Sousa Delgado, A.; Léonard, M.; Dellacherie, E., Surface Properties of Polystyrene Nanoparticles Coated with Dextrans and Dextran–PEO Copolymers. Effect of Polymer Architecture on Protein Adsorption. *Langmuir* **2001**, *17* (14), 4386-4391 DOI: 10.1021/la001701c.

15. Fornaguera, C.; Caldero, G.; Mitjans, M.; Vinardell, M. P.; Solans, C.; Vauthier, C., Interactions of PLGA nanoparticles with blood components: protein adsorption, coagulation, activation of the complement system and hemolysis studies. *Nanoscale* **2015**, *7* (14), 6045-58 DOI: 10.1039/c5nr00733j.

16. Onwukwe, C.; Maisha, N.; Holland, M.; Varley, M.; Groynom, R.; Hickman, D.; Uppal, N.; Shoffstall, A.; Ustin, J.; Lavik, E., Engineering Intravenously Administered Nanoparticles to Reduce Infusion Reaction and Stop Bleeding in a Large Animal Model of Trauma. *Bioconjugate chemistry* **2018**, *29* (7), 2436-2447 DOI: 10.1021/acs.bioconjchem.8b00335.

17. Szebeni, J., Hemocompatibility testing for nanomedicines and biologicals: predictive assays for complement mediated infusion reactions. *European Journal of Nanomedicine* **2012**, *4* (1), DOI: 10.1515/ejnm-2012-0002.

18. Bertram, J. P.; Williams, C. A.; Robinson, R.; Segal, S. S.; Flynn, N. T.; Lavik, E. B., Intravenous hemostat: nanotechnology to halt bleeding. *Sci Transl Med* **2009**, *1* (11), 11ra22 DOI: 10.1126/scitranslmed.3000397.

19. Shoffstall, A. J.; Atkins, K. T.; Groynom, R. E.; Varley, M. E.; Everhart, L. M.; Lashof-Sullivan, M. M.; Martyn-Dow, B.; Butler, R. S.; Ustin, J. S.; Lavik, E. B., Intravenous Hemostatic Nanoparticles Increase Survival Following Blunt Trauma Injury. *Biomacromolecules* **2012**, *13* (11), 3850-3857 DOI: 10.1021/bm3013023.
20. Noris, M.; Remuzzi, G., Overview of complement activation and regulation. *Semin Nephrol* **2013**, *33* (6), 479-92 DOI: 10.1016/j.semnephrol.2013.08.001.
21. Merle, N. S.; Church, S. E.; Fremeaux-Bacchi, V.; Roumenina, L. T., Complement System Part I - Molecular Mechanisms of Activation and Regulation. *Front Immunol* **2015**, *6*, 262 DOI: 10.3389/fimmu.2015.00262.
22. Merle, N. S.; Noe, R.; Halbwachs-Mecarelli, L.; Fremeaux-Bacchi, V.; Roumenina, L. T., Complement System Part II: Role in Immunity. *Front Immunol* **2015**, *6*, 257 DOI: 10.3389/fimmu.2015.00257.
23. Benjamini, E., *Immunology: a short course*. Vol. 77.
24. Wouters, D.; Wiessenberg, H. D.; Hart, M.; Bruins, P.; Voskuyl, A.; Daha, M. R.; Hack, C. E., Complexes between C1q and C3 or C4: novel and specific markers for classical complement pathway activation. *J Immunol Methods* **2005**, *298* (1-2), 35-45 DOI: 10.1016/j.jim.2004.12.018.
25. Harboe, M.; Mollnes, T. E., The alternative complement pathway revisited. *J Cell Mol Med* **2008**, *12* (4), 1074-84 DOI: 10.1111/j.1582-4934.2008.00350.x.
26. Petersen, S. V.; Thiel, S.; Jensenius, J. C., The mannan-binding lectin pathway of complement activation: biology and disease association. *Molecular immunology* **2001**, *38* (2-3), 133-149 DOI: 10.1016/s0161-5890(01)00038-4.

27. Moghimi, S. M.; Simberg, D., Complement activation turnover on surfaces of nanoparticles. *Nano Today* **2017**, *15*, 8-10 DOI: 10.1016/j.nantod.2017.03.001.
28. Ricklin, D.; Lambris, J. D., Complement in immune and inflammatory disorders: pathophysiological mechanisms. *J Immunol* **2013**, *190* (8), 3831-8 DOI: 10.4049/jimmunol.1203487.
29. Yu, K.; Lai, B. F.; Foley, J. H.; Krisinger, M. J.; Conway, E. M.; Kizhakkedathu, J. N., Modulation of complement activation and amplification on nanoparticle surfaces by glycopolymer conformation and chemistry. *ACS nano* **2014**, *8* (8), 7687-7703.
30. Chen, F.; Wang, G.; Griffin, J. I.; Brenneman, B.; Banda, N. K.; Holers, V. M.; Backos, D. S.; Wu, L.; Moghimi, S. M.; Simberg, D., Complement proteins bind to nanoparticle protein corona and undergo dynamic exchange in vivo. *Nat Nanotechnol* **2017**, *12* (4), 387-393 DOI: 10.1038/nnano.2016.269.
31. Moghimi, S. M.; Simberg, D., Translational gaps in animal models of human infusion reactions to nanomedicines. *Future Medicine*: 2018.
32. Csukás, D.; Urbanics, R.; Wéber, G.; Rosivall, L.; Szebeni, J., Pulmonary intravascular macrophages: prime suspects as cellular mediators of porcine CARPA. *European Journal of Nanomedicine* **2015**, *7* (1), DOI: 10.1515/ejnm-2015-0008.
33. Winkler, G. C., Pulmonary intravascular macrophages in domestic animal species: review of structural and functional properties. *American journal of Anatomy* **1988**, *181* (3), 217-234.

34. Dixon, L. J.; Barnes, M.; Tang, H.; Pritchard, M. T.; Nagy, L. E., Kupffer cells in the liver. *Compr Physiol* **2013**, 3 (2), 785-97 DOI: 10.1002/cphy.c120026.
35. Szebeni, J.; Bawa, R., Human Clinical Relevance of the Porcine Model of Pseudoallergic Infusion Reactions. *Biomedicines* **2020**, 8 (4), DOI: 10.3390/biomedicines8040082.
36. Costabile, M., Measuring the 50% haemolytic complement (CH50) activity of serum. *J Vis Exp* **2010**, (37), DOI: 10.3791/1923.
37. Ekdahl, K. N.; Persson, B.; Mohlin, C.; Sandholm, K.; Skattum, L.; Nilsson, B., Interpretation of Serological Complement Biomarkers in Disease. *Front Immunol* **2018**, 9, 2237 DOI: 10.3389/fimmu.2018.02237.
38. Pham, C. T.; Thomas, D. G.; Beiser, J.; Mitchell, L. M.; Huang, J. L.; Senpan, A.; Hu, G.; Gordon, M.; Baker, N. A.; Pan, D.; Lanza, G. M.; Hourcade, D. E., Application of a hemolysis assay for analysis of complement activation by perfluorocarbon nanoparticles. *Nanomedicine* **2014**, 10 (3), 651-60 DOI: 10.1016/j.nano.2013.10.012.
39. Vu, V. P.; Gifford, G. B.; Chen, F.; Benasutti, H.; Wang, G.; Groman, E. V.; Scheinman, R.; Saba, L.; Moghimi, S. M.; Simberg, D., Immunoglobulin deposition on biomolecule corona determines complement opsonization efficiency of preclinical and clinical nanoparticles. *Nat Nanotechnol* **2019**, 14 (3), 260-268 DOI: 10.1038/s41565-018-0344-3.
40. Coty, J. B.; Eleamen Oliveira, E.; Vauthier, C., Tuning complement activation and pathway through controlled molecular architecture of dextran chains in

nanoparticle corona. *Int J Pharm* **2017**, 532 (2), 769-778 DOI:

10.1016/j.ijpharm.2017.04.048.

41. Kirschfink, M.; Mollnes, T. E., Modern complement analysis. *Clin Diagn Lab Immunol* **2003**, 10 (6), 982-9 DOI: 10.1128/cdli.10.6.982-989.2003.

42. Winzen, S.; Schoettler, S.; Baier, G.; Rosenauer, C.; Mailaender, V.; Landfester, K.; Mohr, K., Complementary analysis of the hard and soft protein corona: sample preparation critically effects corona composition. *Nanoscale* **2015**, 7 (7), 2992-3001 DOI: 10.1039/c4nr05982d.

43. Jaskowski, T. D.; Martins, T. B.; Litwin, C. M.; Hill, H. R., Comparison of three different methods for measuring classical pathway complement activity. *Clin Diagn Lab Immunol* **1999**, 6 (1), 137-9.

44. Guadagnini, R.; Halamoda Kenzaoui, B.; Walker, L.; Pojana, G.; Magdolenova, Z.; Bilanicova, D.; Saunders, M.; Juillerat-Jeanneret, L.; Marcomini, A.; Huk, A.; Dusinska, M.; Fjellsbo, L. M.; Marano, F.; Boland, S., Toxicity screenings of nanomaterials: challenges due to interference with assay processes and components of classic in vitro tests. *Nanotoxicology* **2015**, 9 Suppl 1, 13-24 DOI: 10.3109/17435390.2013.829590.

45. Strobel, L.; Johswich, K. O., Anticoagulants impact on innate immune responses and bacterial survival in whole blood models of *Neisseria meningitidis* infection. *Sci Rep* **2018**, 8 (1), 10225 DOI: 10.1038/s41598-018-28583-8.

46. Kopp, R.; Bensberg, R.; Kashefi, A.; Mottaghy, K.; Rossaint, R.; Kuhlen, R., Effect of hirudin versus heparin on hemocompatibility of blood contacting

biomaterials: an in vitro study. *The International journal of artificial organs* **2005**, 28 (12), 1272-1277.

47. Bexborn, F.; Engberg, A. E.; Sandholm, K.; Mollnes, T. E.; Hong, J.; Nilsson Ekdahl, K., Hirudin versus heparin for use in whole blood in vitro biocompatibility models. *J Biomed Mater Res A* **2009**, 89 (4), 951-9 DOI: 10.1002/jbm.a.32034.

48. Del Tordello, E.; Bottini, S.; Muzzi, A.; Serruto, D., Analysis of the regulated transcriptome of *Neisseria meningitidis* in human blood using a tiling array. *J Bacteriol* **2012**, 194 (22), 6217-32 DOI: 10.1128/JB.01055-12.

49. Zewde, N.; Morikis, D., A computational model for the evaluation of complement system regulation under homeostasis, disease, and drug intervention. *PloS one* **2018**, 13 (6), e0198644.

50. Hamad, I.; Al-Hanbali, O.; Hunter, A. C.; Rutt, K. J.; Andresen, T. L.; Moghimi, S. M., Distinct polymer architecture mediates switching of complement activation pathways at the nanosphere– serum interface: implications for stealth nanoparticle engineering. *ACS nano* **2010**, 4 (11), 6629-6638.

51. Gifford, G.; Vu, V. P.; Banda, N. K.; Holers, V. M.; Wang, G.; Groman, E. V.; Backos, D.; Scheinman, R.; Moghimi, S. M.; Simberg, D., Complement therapeutics meets nanomedicine: overcoming human complement activation and leukocyte uptake of nanomedicines with soluble domains of CD55. *J Control Release* **2019**, 302, 181-189 DOI: 10.1016/j.jconrel.2019.04.009.

52. Owens III, D. E.; Peppas, N. A., Opsonization, biodistribution, and pharmacokinetics of polymeric nanoparticles. *International journal of pharmaceutics* **2006**, *307* (1), 93-102.
53. Jeon, S.; Lee, J.; Andrade, J.; De Gennes, P., Protein—surface interactions in the presence of polyethylene oxide: I. Simplified theory. *Journal of colloid and interface science* **1991**, *142* (1), 149-158.
54. Torchilin, V.; Papisov, M., Why do polyethylene glycol-coated liposomes circulate so long?: Molecular mechanism of liposome steric protection with polyethylene glycol: Role of polymer chain flexibility. *Journal of liposome research* **1994**, *4* (1), 725-739.
55. Harris, J. M.; Chess, R. B., Effect of pegylation on pharmaceuticals. *Nat Rev Drug Discov* **2003**, *2* (3), 214-21 DOI: 10.1038/nrd1033.
56. Gabizon, A.; Martin, F., Polyethylene glycol-coated (pegylated) liposomal doxorubicin. *Drugs* **1997**, *54* (4), 15-21.
57. Vert, M.; Domurado, D., Poly(ethylene glycol): protein-repulsive or albumin-compatible? *J Biomater Sci Polym Ed* **2000**, *11* (12), 1307-17 DOI: 10.1163/156856200744345.
58. Simon, J.; Wolf, T.; Klein, K.; Landfester, K.; Wurm, F. R.; Mailander, V., Hydrophilicity Regulates the Stealth Properties of Polyphosphoester-Coated Nanocarriers. *Angew Chem Int Ed Engl* **2018**, *57* (19), 5548-5553 DOI: 10.1002/anie.201800272.

59. Kang, B.; Okwieka, P.; Schottler, S.; Winzen, S.; Langhanki, J.; Mohr, K.; Opatz, T.; Mailander, V.; Landfester, K.; Wurm, F. R., Carbohydrate-Based Nanocarriers Exhibiting Specific Cell Targeting with Minimum Influence from the Protein Corona. *Angew Chem Int Ed Engl* **2015**, *54* (25), 7436-40 DOI: 10.1002/anie.201502398.
60. Papini, E.; Tavano, R.; Mancin, F., Opsonins and Dysopsonins of Nanoparticles: Facts, Concepts, and Methodological Guidelines. *Front Immunol* **2020**, *11*, 567365 DOI: 10.3389/fimmu.2020.567365.
61. Li, M.; Jiang, S.; Simon, J.; Passlick, D.; Frey, M. L.; Wagner, M.; Mailander, V.; Crespy, D.; Landfester, K., Brush Conformation of Polyethylene Glycol Determines the Stealth Effect of Nanocarriers in the Low Protein Adsorption Regime. *Nano Lett* **2021**, *21* (4), 1591-1598 DOI: 10.1021/acs.nanolett.0c03756.
62. Gref, R.; Lück, M.; Quellec, P.; Marchand, M.; Dellacherie, E.; Harnisch, S.; Blunk, T.; Müller, R., 'Stealth'corona-core nanoparticles surface modified by polyethylene glycol (PEG): influences of the corona (PEG chain length and surface density) and of the core composition on phagocytic uptake and plasma protein adsorption. *Colloids and Surfaces B: Biointerfaces* **2000**, *18* (3-4), 301-313.
63. Kim, D. H.; Klibanov, A. L.; Needham, D., The influence of tiered layers of surface-grafted poly (ethylene glycol) on receptor– ligand-mediated adhesion between phospholipid monolayer-stabilized microbubbles and coated glass beads. *Langmuir* **2000**, *16* (6), 2808-2817.

64. Pannuzzo, M.; Esposito, S.; Wu, L. P.; Key, J.; Aryal, S.; Celia, C.; di Marzio, L.; Moghimi, S. M.; Decuzzi, P., Overcoming Nanoparticle-Mediated Complement Activation by Surface PEG Pairing. *Nano Lett* **2020**, *20* (6), 4312-4321 DOI: 10.1021/acs.nanolett.0c01011.
65. Lin, X.; Jain, P.; Wu, K.; Hong, D.; Hung, H. C.; O'Kelly, M. B.; Li, B.; Zhang, P.; Yuan, Z.; Jiang, S., Ultralow Fouling and Functionalizable Surface Chemistry Based on Zwitterionic Carboxybetaine Random Copolymers. *Langmuir* **2019**, *35* (5), 1544-1551 DOI: 10.1021/acs.langmuir.8b02540.
66. Wang, Y. B.; Shi, K. H.; Jiang, H. L.; Gong, Y. K., Significantly reduced adsorption and activation of blood components in a membrane oxygenator system coated with crosslinkable zwitterionic copolymer. *Acta Biomater* **2016**, *40*, 153-161 DOI: 10.1016/j.actbio.2016.02.036.
67. Hu, Y.; Yang, G.; Liang, B.; Fang, L.; Ma, G.; Zhu, Q.; Chen, S.; Ye, X., The fabrication of superlow protein absorption zwitterionic coating by electrochemically mediated atom transfer radical polymerization and its application. *Acta Biomater* **2015**, *13*, 142-9 DOI: 10.1016/j.actbio.2014.11.023.
68. Debayle, M.; Balloul, E.; Dembele, F.; Xu, X.; Hanafi, M.; Ribot, F.; Monzel, C.; Coppey, M.; Fragola, A.; Dahan, M.; Pons, T.; Lequeux, N., Zwitterionic polymer ligands: an ideal surface coating to totally suppress protein-nanoparticle corona formation? *Biomaterials* **2019**, *219*, 119357 DOI: 10.1016/j.biomaterials.2019.119357.

69. Knowles, B. R.; Wagner, P.; Maclaughlin, S.; Higgins, M. J.; Molino, P. J., Silica Nanoparticles Functionalized with Zwitterionic Sulfobetaine Siloxane for Application as a Versatile Antifouling Coating System. *ACS Appl Mater Interfaces* **2017**, 9 (22), 18584-18594 DOI: 10.1021/acsami.7b04840.
70. Toufik, J.; Labarre, D., Relationship between reduction of complement activation by polysaccharide surfaces bearing diethylaminoethyl groups and their degree of substitution. *Biomaterials* **1995**, 16 (14), 1081-1088.
71. Toda, M.; Kitazawa, T.; Hirata, I.; Hirano, Y.; Iwata, H., Complement activation on surfaces carrying amino groups. *Biomaterials* **2008**, 29 (4), 407-17 DOI: 10.1016/j.biomaterials.2007.10.005.
72. Gaikwad, H.; Li, Y.; Gifford, G.; Groman, E.; Banda, N. K.; Saba, L.; Scheinman, R.; Wang, G.; Simberg, D., Complement Inhibitors Block Complement C3 Opsonization and Improve Targeting Selectivity of Nanoparticles in Blood. *Bioconjug Chem* **2020**, 31 (7), 1844-1856 DOI: 10.1021/acs.bioconjchem.0c00342.
73. Mitchell, M. J.; Billingsley, M. M.; Haley, R. M.; Wechsler, M. E.; Peppas, N. A.; Langer, R., Engineering precision nanoparticles for drug delivery. *Nat Rev Drug Discov* **2021**, 20 (2), 101-124 DOI: 10.1038/s41573-020-0090-8.
74. Andersen, A. J.; Robinson, J. T.; Dai, H.; Hunter, A. C.; Andresen, T. L.; Moghimi, S. M., Single-walled carbon nanotube surface control of complement recognition and activation. *ACS nano* **2013**, 7 (2), 1108-1119.

75. Moghimi, S. M.; Andersen, A. J.; Ahmadvand, D.; Wibroe, P. P.; Andresen, T. L.; Hunter, A. C., Material properties in complement activation. *Adv Drug Deliv Rev* **2011**, *63* (12), 1000-7 DOI: 10.1016/j.addr.2011.06.002.

Chapter 3: Developing a sensitive Assay to Screen

Nanoparticles in vitro for Complement Activation

* The material in this chapter has been published: Maisha, N., Coombs, T., & Lavik, E. (2020). Development of a Sensitive Assay to Screen Nanoparticles in Vitro for Complement Activation. ACS Biomaterials Science & Engineering, 6(9), 4903-4915.

Abstract

Nanomedicines are often recognized by the innate immune system as a threat, leading to unwanted clearance due to complement activation. This adverse reaction not only alters the bioavailability of the therapeutic but can also cause cardiopulmonary complications and death in a portion of the population. There is a need for tools for assessing complement response in the early stage of development of nanomedicines. Currently, quantifying complement-mediated response *in vitro* is limited due to differences between *in vitro* and *in vivo* responses for the same precursors, differences in the complement systems in different species, and lack of highly sensitive tools for quantifying the changes. Hence, we have worked on developing complement assay conditions and sample preparation techniques that can be highly sensitive in assessing the complement-mediated response *in vitro* mimicking the *in vivo* activity. We are screening the impact of incubation time, nanoparticle dosage, anticoagulants, and species of the donor in both blood and blood components. We have validated the optimal assay conditions by replicating the

impact of zeta potential seen *in vivo* on complement activation *in vitro*. As observed in our previous *in vivo* studies, where nanoparticles with neutral zeta-potential were able to suppress complement response, the change in the complement biomarker was least for the neutral nanoparticles as well through our developed guidelines. These assay conditions provide a vital tool for assessing the safety of intravenously administered nanomedicines.

Introduction

Nanoparticle-based therapeutics, despite their therapeutic promise, can trigger a complement-mediated hypersensitivity reaction that can involve cardiopulmonary problems upon intravenous infusion and be, in some cases, fatal.¹⁻² The cardiopulmonary distress ranges from rapid changes in arterial blood gas, vitals and increase blood vessel permeability leading to vasodilation.³⁻⁵ As a result, between 2016 and 2019, only two intravenously delivered nanoparticles have been approved by the FDA and EMA.⁶ This reaction is due, at least in part, to initial intravenous infusion of nanomaterials triggering the complement pathway, a part of the innate immune system.⁶⁻⁸ The complement system is made up of more than thirty plasma and cell surface proteins.⁹ The complement cascade is activated through three distinct pathways and is responsible for primary surveillance against pathogenic entities.¹⁰⁻¹¹ The classical pathway relies on complement protein C1 binding to antigen-antibody complex through recognition of the unit C1q, a part of the component C1.¹² Attachment leading to subsequent proteolysis activates the complement proteins C4

and C2 and formation of initial C3 convertase.¹³ The alternative pathway, the second route of activation, occurs due to the spontaneous hydrolysis of C3 further triggered by the presence of foreign surfaces.¹⁴ The third route of activation is through the lectin pathway as plasma protein mannose-binding lectins attach to carbohydrate structures present in the surface of pathogens.¹⁵ Each of the pathways results in the generation of initial C3 convertase that further triggers the pathway into the generation of anaphylatoxins C3a and C5a.¹⁰ The activity of these potent anaphylatoxins range from its pro-inflammatory functions in degranulation of mast cells and production of histamines,^{12, 16} vasodilation, increased permeability of blood vessels¹⁷ as well as its regenerative roles in tissue restoration,¹⁸ and neuronal development.¹⁹⁻²⁰ The complement system is the first-in-line defense of the immune system against pathogens and active at all times controlled by several complement regulators.^{11, 21} However, if the activation is not inhibited efficiently, it leads to prolonged tissue damage and glomerular disease along with the inflammatory responses mentioned above.¹⁰ As the complement system is directed towards attacking any pathogenic or foreign substance, nanomedicines are reported to elicit complement-mediated initial infusion reaction as well.

When nanoparticles are administered intravenously, they are engulfed with complement and serum proteins. The complement protein C3b either binds directly to nanoparticle surfaces or attach to the serum proteins adsorbed on the surface of the particles, with the attachment being reversible and dynamic.²²⁻²³ C3b deposition on nanoparticles along with factor Bb and Properdin in presence of Magnesium ion will

lead to complement activation and further amplification of C3b.²²⁻²³ This infusion-reaction driven complement-mediated response,^{5, 24} is of concern for nanoparticle systems broadly including liposomal nanoformulation, Doxil,²⁵⁻²⁶ inorganic nanoparticles such as iron oxide and metallic nanoparticles used as contrast agents for imaging,²⁷⁻²⁸ organic nanoparticles such as poly(lactic-co-glycolic acid)-b-poly(ethylene glycol) and polystyrene^{24, 29-31} based nanoparticles. It has been challenging to characterize the complement early in development, as different species show different levels of sensitivity, and the response generated *in vivo* in large animals is difficult to resolve *in vitro*.^{4, 32}

The three most common methods for measuring complement activation are indirect measurement through hemolysis assay,³³⁻³⁵ quantifying the proteins that attach to the nanoparticle surface,^{23, 26-27, 36-37} and through enzyme immunoassays.^{4, 28} These methods use nanoparticle blood interaction to generate complement proteins, and then the proteins that attach directly or indirectly on the surface of nanoparticles is quantified.^{23, 27-28} Hemolysis assays such as CH50 assays and AH50 assays are used to indirectly measure the extent of activation by measuring the amount of serum that causes lysis of 50% of sheep erythrocytes due to exposure of serum to complement activator.³⁴ However, the method can include spontaneous hemolysis and variable affinity of the to-be-lysed erythrocytes.³³ Thus methods like hemolysis assays are often semiquantitative.³⁸ Some of the recent complement studies involve incubating blood matrices with nanoparticles and quantifying the attached complement proteins

through SDS-PAGE and western blots.^{23, 27, 36} Moreover, the protein corona is dynamic due to reversible attachment of proteins, and this can lead to underestimating the overall complement protein levels, mainly quantifying the complement proteins part of the hard corona.³⁹

Enzyme-linked immunoassays (ELISAs) for detecting complement have been available for more than two decades, and the assays are more sensitive than CH50 assays,⁴⁰ but ELISAs are only available for limited species. Moreover, the enzyme immunoassays do not consider interference in signal outputs due to the presence of nanoparticles in the blood, plasma, or serum. Nanoparticles, because of their physiological properties and morphology, may lead to adsorption of assay reagents or biomolecules generating outputs with disturbance.⁴¹ Nonetheless, the sensitivity of the enzyme immunoassays makes these extremely attractive by offering the possibility of developing *in vitro* assays that replicate the *in vivo* response allowing efficient screening of molecular features of nanomaterials and their impact on complement activation. We hypothesized that by optimizing the particle dosage, species of blood matrix, and anticoagulants,⁴² we would be able to develop a set of conditions *in vitro* that correlated with our previous *in vivo* findings and would allow efficient screening of nanomaterials. To test this hypothesis, we investigated the impact of blood matrix conditions, time, and dilution factors to replicate the sensitive response seen *in vivo* in an *in vitro* assay.

Experimental Section

Materials

Assay conditions were developed using heparinized human whole blood, plasma, and complement protected human serum, and heparinized porcine whole blood and plasma obtained from Innovative research Inc (Novi, MI). Porcine citrated plasma and human citrated plasma were also obtained from Innovative research Inc (Novi, MI). Zymosan was obtained from Sigma Aldrich. Dulbecco's phosphate-buffered saline (without phosphate and magnesium) was obtained from Fisher Scientific. C5a human ELISA duo kit (DY2037) was obtained from R&D systems (Minneapolis, MN). Human Complement C3 ELISA Kit (ab108823) and Guinea Pig Complement C3 ELISA Kit (ab157705) were obtained from Abcam plc (Cambridge, MA).

Nanoparticles prepared for validating the assay involved l-lactide from Polysciences Inc (Warrington, PA), heterobifunctional poly(ethylene glycol) with 5000Da molecular weight from Laysan Biosciences (Arab, AL), and d-lactide from Purac Biomaterials (Corbion, Amsterdam, Netherlands). All solvents used were ACS grade and obtained from Fisher Scientific.

Methods

Developing complement assay conditions

Plasma and serum were stored at -80°C until used for the experiments and were thawed by placing them in a 37°C water bath. Whole blood samples were stored at 4°C until used. As a positive control, zymosan, a known complement activator,⁴³ is used. To 500ul aliquots of blood matrices, 100ul of zymosan suspended in Dulbecco's PBS (without calcium and magnesium) (PBS) was added and pipetted gently for mixing. As a negative control, PBS without zymosan was used.

Initially, the role of anticoagulant in blood collection was assessed. The response generated for heparinized and citrated human blood plasma was determined by incubating the samples with zymosan at 1mg/ml dosages for 30 minutes. Next, the differences in complement response in porcine and human blood samples were also investigated for choosing the appropriate species for mimicking the reaction *in vitro*. The optimum incubation times were then determined by incubating the samples with the nanoparticle suspension at 37°C for 30, 45, and 60 minutes, respectively. The response in single donor vs. pooled blood samples was also compared for human serum and heparinized human plasma and whole blood. After incubation, the samples were centrifuged at 4000g for 5 minutes. The serum or plasma was aliquoted in clean tubes and stored on ice until the assay was carried out. Dilutions of the supernatant serum or plasma were prepared, and the assays were carried out following the

protocol for the ELISA assay (C5a ELISA assay duo kit, R&D Systems). For immunoassay quantifying biomarker C5a, the optical density for the samples and standards were measured at a wavelength of 450 nm using SpectraMax M2 Microplate Reader (Molecular Devices LLC) with background correction done using reading obtained at 540 nm. Human C3 ELISA kit and guinea pig C3 ELISA kit from Abcam plc. were used for quantifying the biomarker C3.

The fold change was measured by comparing the level of C5a observed in the sample incubated with PBS and the sample with zymosan.

Fold change

$$= \frac{\text{Biomarker in sample containing zymosan} - \text{Biomarker in sample containing PBS}}{\text{Biomarker in sample containing PBS}}$$

Validating assay's sensitivity to mimic in vivo response in vitro

The developed complement assay was used to determine whether the complement response generated due to differences in surface charge of nanoparticles could be detected precisely. The method of preparing the nanoparticles are summarized in the supplementary data. The nanoparticles fabricated were thoroughly characterized through dynamic light scattering for determining the size and zeta potential using Malvern Zetasizer Nano ZS ((Malvern Panalytical, Malvern, UK).

The ELISA conditions used were identical, as mentioned above. Heparinized human whole blood was incubated with the nanoparticles of various zeta-potential at

a dosage of 0.25mg/ml. As a positive control, zymosan, a known complement activator,⁴³ is used at the same dosage. Aliquoted whole blood in amounts of 500ul was incubated with 100ul of nanoparticles suspended in Dulbecco's PBS (without calcium and magnesium). The samples were incubated at 37°C for 45 minutes and then centrifuged at 4000g for 5 minutes to separate the nanoparticles. The separated plasma was aliquoted in clean tubes and stored on ice until the assay was carried out. The fold-change in each of the samples is quantified comparing the quantity of C5a in whole blood incubated with PBS only to the amount of C5a in samples with nanoparticles or zymosan.

Fold change

$$= \frac{\text{C5a in sample containing zymosan/nanoparticles} - \text{C5a in sample containing PBS}}{\text{C5a in sample containing PBS}}$$

Nanoparticles used for validating the assays

Poly(lactic-co-glycolic acid)-b-poly(l-lysine)-b-poly(ethylene glycol) (PLGA-PLL-PEG) nanoparticles were obtained from the previous study on the response of the nanoparticles *in vivo* in a porcine trauma model.³¹ Three formulations retrieved from the previous study were used in this study, where two of the formulations had peptide cRGD conjugated to the particles. The particles were stored at -20°C and characterized through DLS, ensuring the particle size did not change significantly over the storage time. The zeta-potential was also recorded for these PLGA-PLL-PEG nanoparticles. All protocols involved with the previous study on porcine liver injury

model³¹ were in accordance with animal protocols reviewed and approved by the Institutional Animal Care and Use Committee (IACUC) at Case Western Reserve University. The protocols were developed by Gurney et al⁴⁴ and modified in conjunction with the Trauma Research Laboratory at Massachusetts General Hospital.

Poly(lactic acid)-b-poly(ethylene glycol) (PLA-PEG) nanoparticles with varied zeta-potential were prepared and characterized through DLS. The methods for synthesis, fabrication, and characterization of the nanoparticles are included in supplementary data.

Statistical Analysis

One-way ANOVA was used to determine the statistical significance of the difference of C5a in samples containing nanoparticles and zymosan, compared to samples with PBS. As post-analysis, Dunnett's multiple comparison test was used for comparing to the control group PBS, and Tukey analysis was used for comparing the means for determining which groups displayed statistically significant differences. For donors or blood samples comparing two groups, a t-test was used to determine whether the means were significantly different.

Results

Comparing complement response observed in citrated and heparinized human blood plasma

Two commonly used anticoagulants for collecting blood samples were compared to investigate their impact on complement activation. We analyzed the complement protein C3 which is cleaved when complement activation happens via any of the pathways leading to a short term decrease in C3.^{10-11, 21} Zymosan, a known complement activator,⁴³ was used to generate the response. Heparinized blood matrices preserved C3 more than the citrated matrices (figure 30). This makes heparin the more attractive choice as an anticoagulant because it retains the greater complement response. This result is not entirely surprising. The complex correlation between the coagulation cascade and complement pathways is a significant factor in generating the response as coagulation components thrombin and factor Xa can directly activate components of the complement cascade.⁴⁵ The choice of anticoagulant is essential, to ensure that complement cascade is not activated or blocked as an aftermath. Of the commonly used anticoagulants, citrate prevents coagulation by sequestering Ca^{2+} , while heparin acts by enhancing antithrombin activity.⁴⁵ EDTA, another commonly used anticoagulant, acts by chelating Ca^{2+} and Mg^{2+} entirely, and as a result blocks the complement cascade as well, as the metal ions are essential components for the activation.⁴⁵ Heparin, as an anticoagulant at lower dosages, has been found not concomitantly to impact the complement

cascade.⁴⁶ As a result, the rest of the experiments involved utilizing heparinized blood plasma and whole blood for porcine as well as human donors.

Impact of incubation time in generating complement response in human blood matrices

We investigated the ideal incubation time for generating a complement response initially. The biomarker quantified was the complement protein C5a. In heparinized plasma, we incubated zymosan at concentrations ranging from 1mg/ml to 5mg/ml. The incubation time for generating the response is dependent on several factors. A computational model addressing time-dependent depletion of C5 and generation of C5a-desArg exhibit an upward trajectory up to 25 minutes, with the rate of change gradually decreasing.⁵² The zymosan suspended in phosphate-buffered saline was added to the plasma and incubated for 30, 45, and 60 minutes respectively at 37°C in a rotating shaker. Incubation for 45 minutes showed a concentration dependent response to zymosan (Figure 7). Hence, for further experiments, the incubation time of 45 minutes was chosen for quantifying the change with the greatest sensitivity.

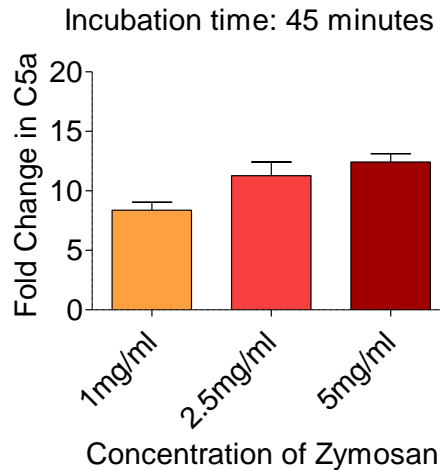


Figure 7. Validation of incubation time at 45 minutes. Statistical analysis using one-way ANOVA shows the fold-change at 5mg/ml dosage for 45 minutes incubation is significantly different from the fold-change for the same time-point at 1mg/ml dosage.

Differences in complement response generated in human blood, plasma, and serum

We subsequently investigated the role of different blood components, i.e., blood plasma, serum, and whole blood obtained from human donors in generating the complement response. The groups include single donor heparinized blood plasma, pooled heparinized blood plasma, single donor serum, and pooled complement-protected serum obtained from human donors. The groups were incubated for 45 minutes at 37 °C in a rotating shaker. Incubating with zymosan at dosages of 0.25mg/ml leads to an increase in C5a as expected due to complement activation in all the groups. The fold-change was calculated relative to the amount of C5a detected in groups incubated with phosphate-buffered saline (Figure 8). While the fold-change

in single donor heparinized plasma was 20-fold, the change in pooled heparinized plasma was 5-fold (Figure 8 B and C). The fold-change in the single donor serum was 12-fold, while pooled complement protected serum had a 14-fold increase (Figure 8 D and E). The anaphylatoxin C5a is generated as the complement cascade advances. The baseline upon incubation with PBS is different for single donor and pooled plasma samples. This difference is attributed to the difference in complement levels among different donors. On the other hand, in serum, as the coagulation cascade is no longer intact, complement protein levels are high due to initial activation followed by the coagulation cascade, and the level change is faster compared to plasma.⁵³

Therefore, from the responses observed from the fold changes for C5a, we can compare the complement response in different matrices. As complement and coagulation cascades often have cross-interaction^{50, 54-55} among themselves, we see a consistent response for fold change in C5a in the pooled and single-donor serum, compared to plasma. Hence, in comparison to plasma, the serum is more suitable for generating the complement response *in vitro*.

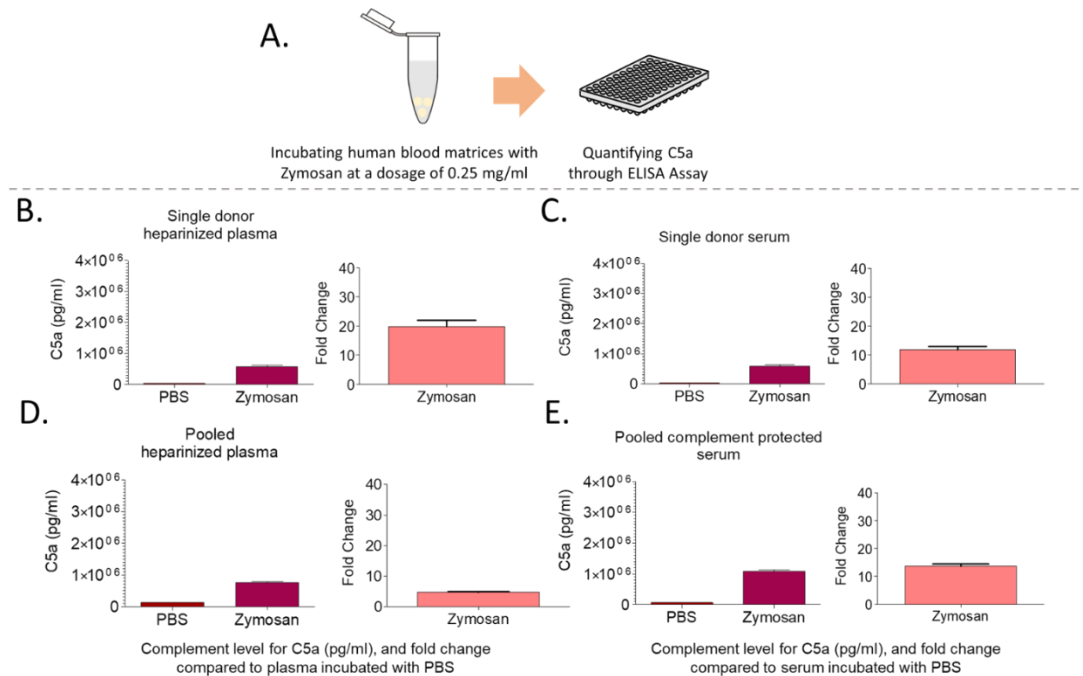


Figure 8. Comparing complement response among single donor and pooled plasma and serum. A. Incubation of blood plasma and serum with zymosan at a dosage of 0.25mg/ml and quantifying complement protein C5a. The C5a levels in the samples are quantified through enzyme immunoassay, and the fold change is determined with respect to the amount of C5a determined in the serum or plasma incubated with PBS. B. The change in complement protein C5a in single donor heparinized plasma resulted in a fold change of 20 ± 4 fold. C. The change in complement protein C5a in single donor serum resulted in 12 ± 2 fold. D. The complement protein C5a changed by 5 ± 0.4 fold in pooled heparinized plasma. E. The complement protein C5a changed by 14 ± 1 fold in pooled serum. Using t-test, the means observed for PBS and zymosan were compared for each sample and the means were significantly different.

The *in vitro* response in whole blood was investigated to further assess the suitable form of blood product for simulating *in vivo* complement response *in vitro*. We studied the impact of the concentration of zymosan by quantifying changes due to zymosan at a concentration as high as 1mg/ml, as well as a lower concentration of 0.25mg/ml (Figure 9). The whole blood was incubated with zymosan suspended in phosphate-buffered saline at the mentioned dosages for 45 minutes at 37°C while shaking. The complement protein C5a was quantified in the samples. When the concentration was lowered to 0.25mg/ml, the fold-changes observed were 14-fold, 31-fold, and 20-fold in samples collected from three different donors. (Fig 9 B, C, and D). While we see a high fold change for C5a for 1mg/ml zymosan, even for the same dosage of 0.25mg/ml, whole heparinized blood showed higher complement response compared to both plasma and serum. Based on the response and higher sensitivity, whole heparinized blood is the most suitable matrix, followed by single-donor and pooled serum for these assays.

We sought to develop a sensitive assay that would be able to simulate the complement response observed *in vivo* using blood products *in vitro*. On comparing whole blood, plasma, and serum, the response generated in whole blood is found to be more sensitive with higher fold changes observed on incubation with Zymosan. Moreover, based on the fold-changes observed, the dosage of 0.25 mg/ml of Zymosan resulted in generating a sensitive response, highlighting the differences in complement response from donor to donor.

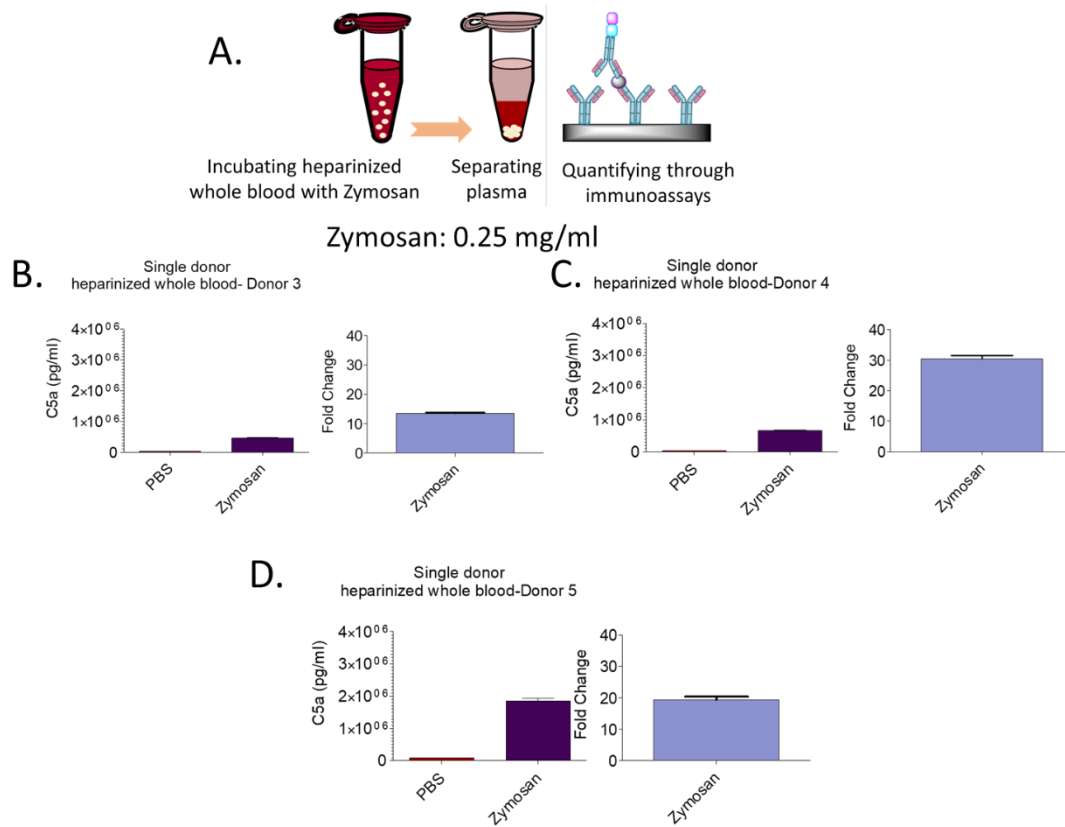


Figure 9. Complement response in heparinized whole blood. A. Schematic of process.

B. Fold change and complement level in donor 3. C. Fold change and complement

level in donor 4. D. Fold change and complement level in donor 5. The changes due

to a dosage of 0.25 mg/ml where 14 ± 6 folds, 31 ± 1.7 and 20 ± 1.9 , respectively.

Using t-test, the means observed for PBS and zymosan were compared for each donor

and the means were significantly different.

Validating impact of zeta-potential of nanoparticles observed in vivo through developed in vitro assay

Based on our observations, we chose the incubation time of 45 minutes and dosage of 0.25mg/ml of zymosan or nanoparticles to investigate further the impact of the nanomaterials in generating a complement response. The impact of dosage of nanoparticles on the complement response are discussed in the supplementary information (Figure 34). The nanoparticles were incubated at 37°C with whole heparinized blood for the incubation time in a rotating shaker (Figure 10). The samples were then prepared following the assay protocol for quantifying the amount of complement protein C5a after incubation with the nanoparticles, positive control zymosan, and negative control phosphate-buffered saline at the dosage of 0.25mg/ml.

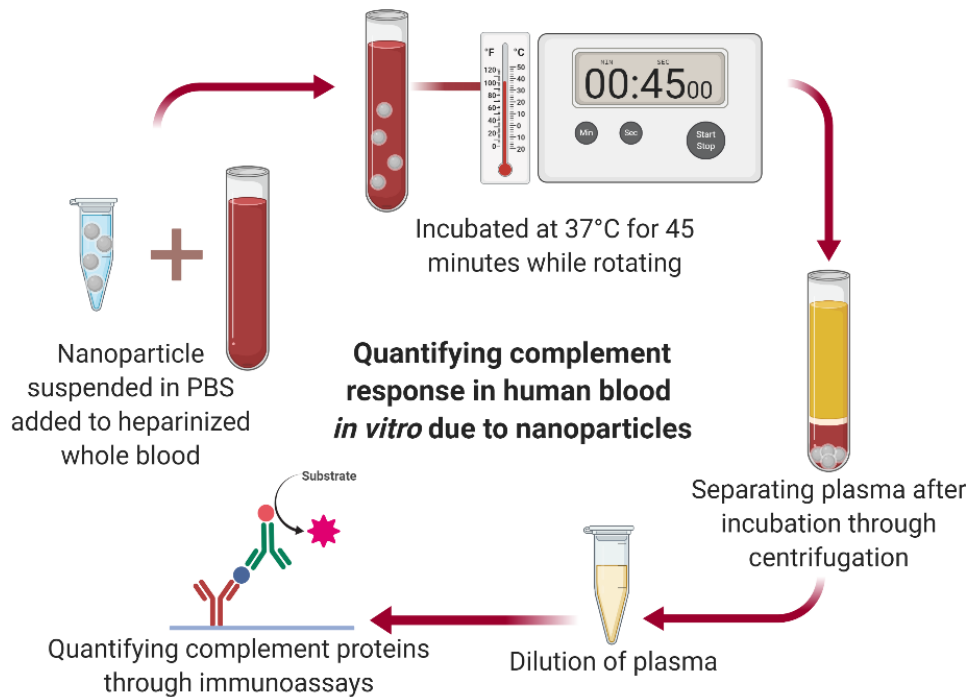


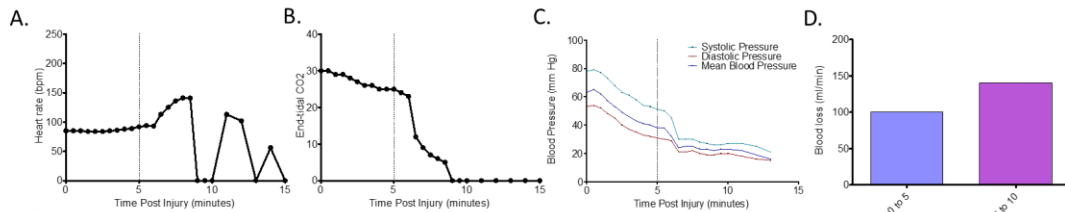
Figure 10. Method for generating complement response *in vitro*. Heparinized whole blood is incubated with nanoparticles suspended in PBS at dosages of 0.25mg/ml for 45 minutes at 37°C in a rotating shaker. The samples are centrifuged to separate the nanoparticles and the supernatant serum is used to quantify the complement activation biomarker C5a through immunoassay.

The objective of our work was to develop an *in vitro* assay that can mimic the complement response observed *in vivo*. As a first step, we investigated whether the developed assay can capture the response observed *in vivo* for poly(lactic-co-glycolic acid)-b-poly(l-lysine)-b-poly(ethylene glycol) (PLGA-PLL-PEG) nanoparticles in a porcine trauma model. We have previously seen that PLGA-PLL-PEG-based hemostatic nanoparticles generate complement response upon infusion in porcine trauma models as well as upon naïve administration.³¹ When the nanoparticles were infused intravenously, the nanoparticles lead to exsanguination in minutes.³¹ While slow infusions can help overcome such hypersensitivity reactions,⁵⁶ even lower dosages lead to complement activation.³¹ Moreover, the hemostatic nanoparticles augment hemostasis by binding with GPIIb/IIIa integrin of activated platelets and subsequently increase survival, and the formulation needs to be administered in bolus to reach targeted efficacy.⁵⁷⁻⁵⁸ As highly negative⁵⁹ or highly positive surface charge of nanoparticles³⁰ can lead to complement mediated hypersensitivity reactions, the role of tuning zeta-potential was investigated. The study showed that nanoparticles with zeta-potential between -3.0 mV and 3.0 mV were able to prevent the hypersensitivity reactions at lower dosages (below 3.3 mg/kg).³¹ We tracked the

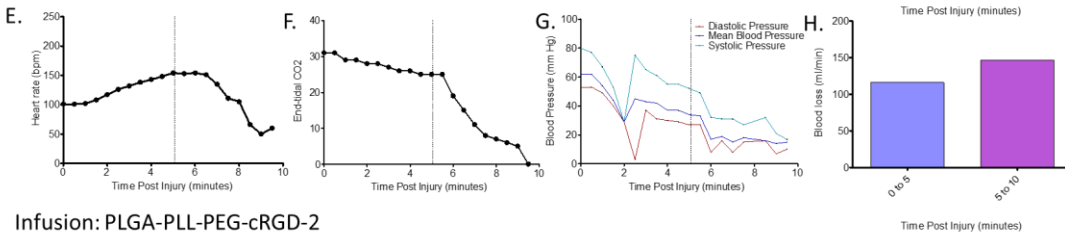
impact of three such PLGA-PLL-PEG nanoparticles on cardiopulmonary vitals and the rate of blood loss upon infusion in porcine animals. The formulations include the PLGA-PLL-PEG-1 without any peptide motif conjugated to it, and two other formulations PLGA-PLL-PEG-CRGD-1 and -2 with same properties but fabricated in different batches. The fabricated nanoparticles were in the neutral range but administering at higher dosages (3.3 and 6.6 mg/kg) had led to complement activation *in vivo*. The formulations PLGA-PLL-PEG-cRGD-1 and PLGA-PLL-PEG-1 lead to exsanguination at 10- and 5-minutes post-infusion showing moderate signs of cardiopulmonary distress, were the nanoparticles were infused at t=5 minutes (i.e. 5 minutes post-injury). (Figure 11 A-H). From figure 11, mild cardiopulmonary distress is visible from the change in heart rate compared to baseline measurements at t=0 minutes as well as abrupt changes in end-tidal CO₂, indicative of respiratory distress and shock.⁶⁰ While the formulation PLGA-PLL-PEG-cRGD-2 did not lead to immediate exsanguination, moderate respiratory as well as cardiac distress was visible post-infusion. In all three infusions, the rate of blood loss increased at 5-10 minutes, i.e., after infusion of nanoparticles, indicating vasodilation and increased permeability leading to subsequent blood loss. When the complement proteins were quantified in the blood samples from the porcine animals receiving the PLGA-PLL-PEG nanoparticles through infusion, there were no significant differences in complement protein C3 and C3a.³¹ However, there was an increase in the C5a level.³¹ Once complement pathway is activated, the complement protein C3 upon complement activation would deplete, leading to the eventual generation of

anaphylatoxins C3a and C5a, where the anaphylatoxins are responsible for cardiopulmonary distress, vasodilation, increased permeability of blood vessels.^{16, 20} Thus, from the *in vivo* response due to the infusion, keeping in mind the complexity of trauma upregulating complement⁶¹ as well, we see moderate complement response from the neutral nanoparticles at high dosages.³¹ This upregulation is mainly from the increased blood loss after infusion, possibly due to anaphylatoxins like C5a acting as vasodilators. Most importantly, the lack of complement detection at the molecular level, even in case of moderate hypersensitivity response observed *in vivo*, highlights the need to develop robust assays for quantifying complement response with high sensitivity.

Infusion: PLGA-PLL-PEG-cRGD-1



Infusion: PLGA-PLL-PEG-1



Infusion: PLGA-PLL-PEG-cRGD-2

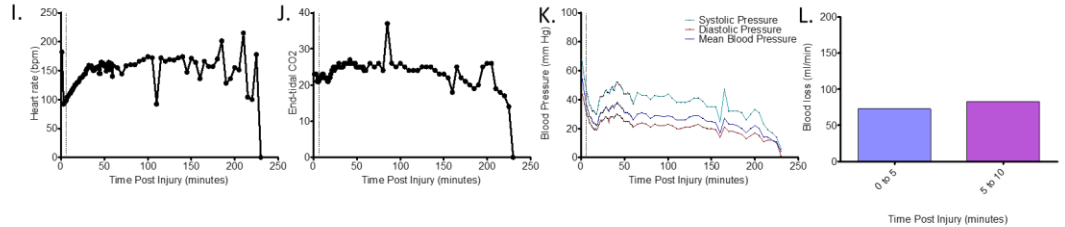


Figure 11. Change in cardiopulmonary vitals upon infusion of PLGA-PLL-PEG nanoparticles in swine. Infusion of the nanoformulation PLGA-PLL-PEG-cRGD-1 resulted in increased rate of blood loss and fluctuations in the vitals with exsanguination at 10 minutes post-infusion. A. Change in heart rate, B. Change in end-tidal CO₂, C. Change in blood pressure, D. Change in rate of blood loss due to PLGA-PLL-PEG-cRGD-1 infusion. Infusion of the nanoformulation PLGA-PLL-PEG 1 increased rate of blood loss and led to exsanguination at 5 minutes post infusion. E. Change in heart rate, F. Change in end-tidal CO₂, G. Change in blood pressure, H. Change in rate of blood loss due to PLGA-PLL-PEG-1 infusion; Infusion of the nanoformulation PLGA-PLL-PEG-cRGD-2 increased rate of blood loss slightly without causing exsanguination, however, fluctuations were exhibited in the vitals. I. Change in heart rate, J. Change in end-tidal CO₂, K. Change in blood pressure, L. Change in rate of blood loss due to PLGA-PLL-PEG-cRGD-2 infusion. These data are from a previous study looking at the impact of modulating zeta potential on the complement response to hemostatic nanoparticles in a porcine model of trauma.³¹

As first step of validating our assay, we determined how the complement protein C5a changes upon incubation with the PLGA-PLL-PEG nanoparticles. The nanoformulations mentioned above resulted in 3.3 ± 0.2 folds change for PLGA-PLL-PEG-cRGD-1, 3.4 ± 0.4 folds for PLGA-PLL-PEG-1, and 4.4 ± 0.5 folds for PLGA-PLL-PEG-cRGD-2 (Figure 12). The differences in the fold changes were statistically significant compared to the response seen in sample incubated with the negative

control, phosphate-buffered saline (PBS). While an increase in complement protein itself does not always lead to a hypersensitivity reaction, a two-four folds increase in terminal complement proteins is observed in the blood samples for cases showing clinical symptoms of complement-mediated hypersensitivity reaction for PEGylated liposomal doxorubicin.^{5, 26} Thus, the developed assay can interpret the molecular response *in vitro* upon incubation with nanoparticles that had shown moderate complement activation *in vivo* based on the observed fold change in complement protein C5a upon incubation of the PLGA-PLL-PEG nanoparticles with whole heparinized human blood.

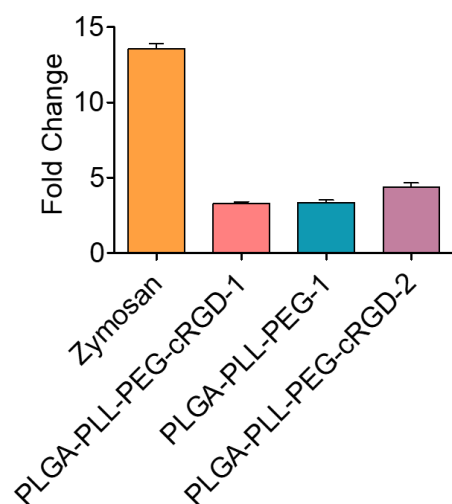


Figure 12. Fold change in complement protein C5a due to incubation of whole blood with PLGA-PLL-PEG nanoparticles. One-way ANOVA followed by Tukey analysis shows that while the means of fold changes are significantly different for the nanoformulations compared to Zymosan, the difference is not statistically significant

for the changes within the three groups PLGA-PLL-PEG-cRGD-1, PLGA-PLL-PEG-1 and the PLGA-PLL-PEG-cRGD-2.

To further validate the responsive assay conditions, we chose to study the difference in complement response in whole blood due to nanoparticles having different zeta potential, as zeta potential, a surface property related to the surface charge of nanoparticles is known to impact complement activation.^{31, 59} We designed nanoparticles with a range of zeta potentials from highly negative to neutral (Figure 13 A and B). The hydrodynamic diameter of the nanoparticles, Z-average, and the zeta potential was determined using dynamic light scattering (Figure 13 C and D). Details of the methods for synthesis, fabrication, and characterization of the nanoparticles are included in supplementary data and supplementary figures 32 and 33. The polymers poly(l-lactic acid)-b-poly(ethylene glycol) with terminal amino and carboxyl groups were used to fabricate the nanoparticles. Nanoparticles with zeta-potential ranging from -1.8 mV to -23.5 mV were prepared (Figure 13D). The nanoparticles have a poly(lactic acid) core, with polyethylene glycol corona on the surface. Adjusting the ratios of the amino and carboxyl groups on the surface helps in controlling the zeta-potential of the nanoparticles.

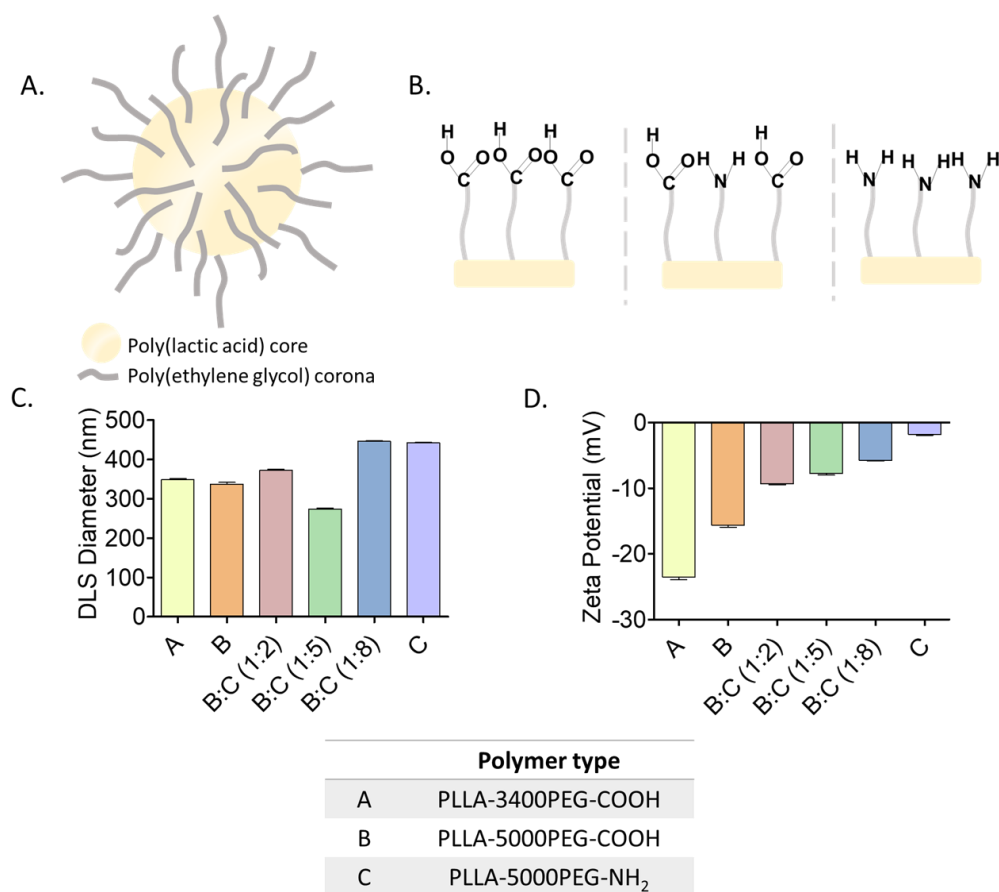


Figure 13. Characterization of nanoparticles with varied zeta-potential. A. Nanoparticles with poly(lactic acid) core and poly(ethylene glycol) corona. B. Varying amino and carboxyl groups to vary zeta-potential. C. Hydrodynamic diameter of nanoparticles. D. Zeta-potential of nanoparticles. 3400PEG indicates PEG with a molecular weight of 3400Da while 5000PEG indicates a molecular weight of 5000Da for the PEG units, respectively.

To validate the assay using the fabricated nanoparticles with a range of zeta-potential, the fold-changes in the incubated samples were determined compared to samples incubated with phosphate-buffered saline. For highly negative zeta-potential, -23.5mV and -15.6 mV, the fold-change was highest, 1.9-fold. As the zeta potential

increases towards the neutral range, i.e., between -3.0 mV and 3.0 mV, the fold-change in C5a also decreases. The observations agree with the reduced complement activation due to the neutral zeta-potential of nanoparticles seen *in vivo*. The fold change is lowest for the neutral nanoparticles at -1.8 mV showing a fold change of -0.02-fold (Figure 14.). There is no statistically significant difference between the C5a levels for PBS and neutral nanoparticles at -1.8 mV. The exchange of carboxyl groups on the exposed nanoparticle surface with amine groups while fabricating the neutral nanoparticles leads to an increase in zeta-potential on the surface resulting in neutral zeta-potential. The lower change in complement protein C5a in whole heparinized blood incubated with these neutral nanoparticles signifies that the complement cascade is not highly activated suggesting that the complement cascade is not treating the incubated nanoparticles as pathogens and trying to clear it out of the system immediately. Whereas the upregulated C5a levels based on the fold change observed for the negative nanoparticles at -23.5 mV and -15.6 mV indicate that the complement system is treating the nanoparticles as a threat and working on the removal of the nanoparticles. Initially, C3b and iC3b binds to the foreign surface, preparing the foreign agent for subsequent clearance,^{23, 62-63} while liberating potent anaphylatoxins and fragments that work in formation of the eventual terminal membrane attack complex. As previously mentioned, two to four-fold change in complement protein is indicative of probable signs of complement-mediated hypersensitivity reaction and related clinical symptoms *in vivo*.^{5, 26} Surface charge is a parameter relevant for complement activation,⁶⁴⁻⁶⁶ and through controlling zeta-

potential a closely related parameter to surface charge, the complement response can be controlled.³¹ The designed assay conditions were able to validate the complement response *in vitro* from the perspective of neutral zeta-potential of nanoparticles and its role in evading complement response. While *in vivo* studies often show only clinical signs and symptoms of hypersensitivity reactions as manifestations of complement activation with the absence of a robust molecular response for the complement proteins itself, we developed an assay that can generate the complement-mediated response *in vitro* mimicking the response associated with changing zeta-potential of nanoparticles.

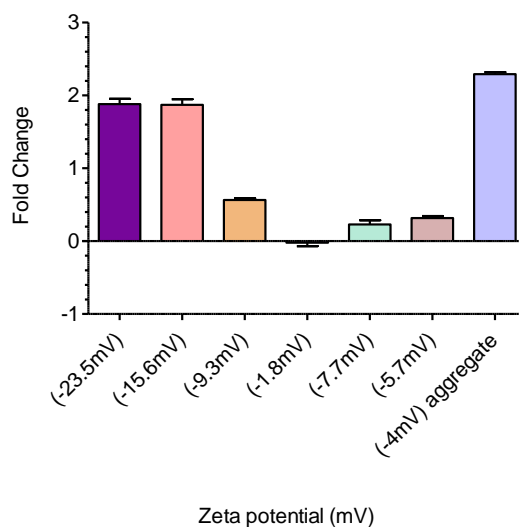


Figure 14. Impact of zeta potential of nanoparticles on complement response. Neutral nanoparticles lead to decreased complement activation *in vitro* leading to lower fold change in complement protein C5a. However, aggregation of particles with a low zeta potential led to an increase in complement protein C5a.

Besides validating the impact of zeta-potential, we quantified the changes in C5a due to aggregation as well. Aggregated nanoparticles with a zeta-potential of -4mV resulted in fold change of C5a (2.3 ± 0.05) equivalent to that observed in more negative unaggregated nanoparticles (2.3 ± 0.05 fold) (Fig 14 and 15). Increasing zeta potential towards neutral range can reduce the change in C5a; however, the aggregated nanoparticles close to neutral range lead to a higher change in C5a compared to unaggregated nanoparticles of similar zeta-potential of -5.7 mV (Figure 14), and C5a comparable to that of the -15.6 mV unaggregated nanoparticles (Figure 15), suggesting the significance of size and aggregation in generating the hypersensitivity reaction as well. Size and curvature of nanoparticles are as a result essential to control complement alongside zeta-potential, as these parameters dictate how the convertase molecules would interact with the surface.⁶⁷⁻⁶⁸ Aggregation of the nanoparticle can lead to higher depositions of C3b, a complement protein essential in forming initial convertase in the complement cascade, as seen for polypropylene sulfide nanoparticles of different size.⁶⁹ Thus, using the assay conditions, we were able to generate the complement response dependency on surface charge as well as size and morphology of nanoparticles *in vitro*.

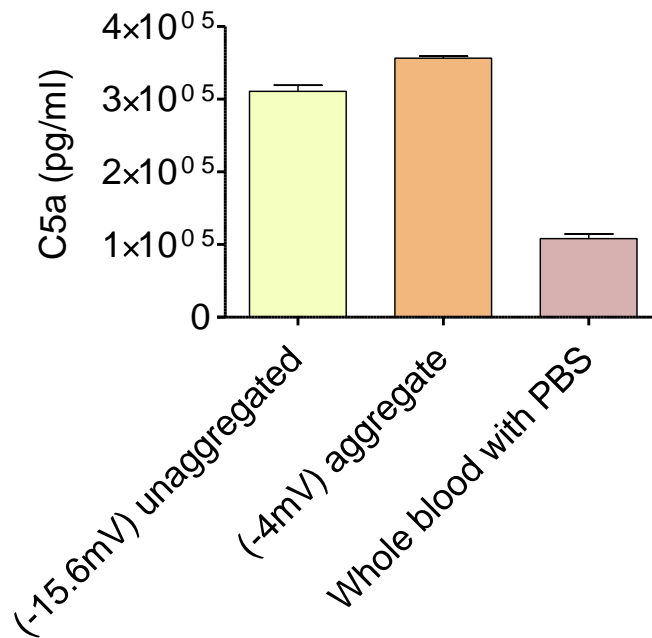


Figure 15. Impact of aggregation of particles. The complement activation as marked by C5a is increased with aggregated particles at levels similar to unaggregated particles with a high zeta potential relative to the whole blood with PBS control.

Discussion

Because of the lack of sensitive assays to quantify complement-mediated response *in vitro*, we worked on developing assays that would be able to detect complement changes *in vitro* with precision and sensitivity, as observed *in vivo*. To determine the optimum assay conditions, we narrowed down the factors that play a critical role in generating the complement response. We chose heparinized blood and blood matrices as citrate and EDTA act as chelators for Ca²⁺ and Mg²⁺ inhibiting the activation of the complement pathway.^{45, 70} The extent of complement activation

is species-dependent, hence while developing assays to quantify changes in complement protein level, a significant challenge is selecting the right species that is hypersensitive. For a liposomal formulation that is known to cause complement activation at a dosage ranging from 0.01-0.3mg/kg in porcine animals, a dosage of 5-25mg/kg is required to get a similar response in rodents and a dose of 0.05-0.1mg/kg in canines. Whereas for reactive human species, which accounts for around 7% of human population, the required dose is comparable to that observed in porcine animals, i.e., 0.01-0.2mg/kg.⁴ Moreover, the blood matrix selected while designing assays, i.e. whole blood vs. plasma vs. serum, is also crucial, due to interplay between complement and coagulation cascades and its impact on the complement protein levels as well as anticoagulant used during a blood draw as that can affect the complement pathway as well.^{45, 70} Complement activation is a dynamic process as the reaction can start in seconds, and hence while designing assays, the role of incubation time plays a critical role as well. Therefore, while developing assays to measure complement activation accurately, factors that play a crucial role include the donor of species, form of blood sample (i.e., plasma, serum, and whole blood), the anticoagulant for collecting blood, the dosage of the nanoparticle, and incubation time for generating the response *in vitro*.

As a control, we have used zymosan for tuning the complement assays. Zymosan can activate the complement system through the alternative pathway as the insoluble yeast cell wall component is able to deplete C3 in presence of Mg^{2+} and

properdin.⁷¹ The surface of zymosan provides immune adherence scope for the complement fragment C3b and enhances phagocytosis.⁷² Complement activation due to biomaterials is dependent on surface coating densities and moieties that impacts covalent binding with the complement protein C3b^{23, 73}, and binding of C3b with the plasma proteins IgG and human serum albumen⁷⁴⁻⁷⁵ that immediately engulf the nanoparticles in the blood stream.²³ As our nanoparticles are PEGylated, and based on correlation between PEGylation density and complement activation pathways⁷³, we suspect complement activation through the alternative pathway to be the significant pathway of activation as the nanosurfaces provide scope of C3b and iC3b binding and subsequent activation.²³

The complement system in pigs and humans are different. Pulmonary intravascular macrophages (PIM), key components of the mononuclear phagocyte system, are responsible for non-IgE mediated hypersensitivity reactions in pigs.⁷⁶ However, the PIMs are morphologically similar to Kupffer cells⁷⁷ in the human liver that are responsible for generating multiple complement receptors and clearance of nanoparticles.⁷⁸ The key difference between the two is how the response is distinct in different species. In comparison to Kupffer cells, PIMs release significant quantities of vasoconstrictors and complement mediators that are responsible for respiratory distress and inflammation.⁷⁶ As a result, porcine *in vivo* models are highly sensitive. However, as only a subset of human population shows the sensitivity, this naturally raises questions on the relevance of the porcine model. But one must also look at the

purpose behind using the porcine *in vivo* model as a guiding tool. The goal of the porcine model is to determine whether a nanomaterial leads to unwanted hypersensitivity reaction at a subtherapeutic dosage.⁷⁹ Thus, as a tool for confirming the safety of a nanoformulation in hypersensitive patients, the porcine *in vivo* model is essential.

However, it is also essential to note that complement factors such as anaphylatoxin receptors can bind with the anaphylatoxins as well.⁸⁰ Time and dosage both are critical in this respect, especially for highly sensitive species such as the pigs. In our assessments using porcine plasma, we see a decrease in complement protein C5a with increasing dosage of complement activator zymosan with increasing incubation time. This could be explained due to the porcine complement system being more robust and generating a response in a short period, especially for a component like C5a that has lower half-life *in vivo*.³⁸ That is, whether the split products in porcine blood samples have a higher propensity in interacting with inhibitors compared to the split products in human blood samples need to be further evaluated. Currently, the *in vitro* assessment of complement biomarkers by immunoassays is highly limited in porcine blood and its matrices. Most often, *in vitro* assessments involve using western blots,⁸¹ and very few immunoassays have been documented in the literature for use *in vitro*. While the response can be tracked through cardiopulmonary vitals observed *in vivo* in porcine matrices^{5, 82}, generating the

response *in vitro* needs to be worked on as a critical step before moving to *in vivo* studies.

While several immunoassays have been developed over the years for quantifying complement, none of them considers interference due to nanoparticles in the blood, plasma, or serum. Nanoparticles itself may lead to adsorption of assay reagents or biomolecules and interfere with the assay outputs.⁴¹ Thus, the samples need to be extensively washed and appropriately groomed to avoid interference in the outputs for the actual complement level detections. The biomarkers quantified are the molecules C3 and the fragment C5a generated due to the depletion of C3. On the event of complement activation, once initial C3-convertase is formed, the convertase catalyzes the breakdown of C3 into the smaller fragment C3a and larger fragment C3b.^{10-11, 21} The pathway proceeds leading to the generation of the anaphylatoxins and eventual terminal complex that works on clearing the threat out of the system.^{10-11, 21} As there is a lack commercially available enzyme immunoassay for different species, the C3 ELISA kit for guinea pig was used to track changes in complement protein *in vitro* in the porcine plasma. This kit was previously used in quantifying changes *in vivo* in the porcine trauma model from the blood samples drawn.³¹ C5a, one of the anaphylatoxins generated, is a potent inflammatory molecule that targets immune and non-immune cell receptors and leads to vasodilation, increased cell permeability, and contraction of smooth muscles.¹⁰ While there are immunoassays for quantifying another potent biomarker C3a, the ELISA assay required subsequent acid-base

neutralization for removal of whole proteins from plasma before quantifying C3a des Arg (Complement C3a des Arg Human ELISA Kit, ab133037) which could lead to degradation of nanoparticles within the samples while processing. Hence, using the biomarker C5a for detection served as a simplified tool for quantifying complement response *in vitro*.

We determined that heparinized human whole blood has higher sensitivity for generating complement response *in vitro*. Compared to plasma, serum shows higher sensitivity as well. This is due to the absence of cells leading to biological turnover, and as a result, the complement pathway is not suppressed in the absence of the coagulation cascade.^{38, 83-84} The differences in fold changes in whole blood due to incubation with zymosan at 0.25 mg/ml can be explained by the difference in responsiveness among individuals, as blood samples are collected from different donors. However, in all cases, there is significant complement activation. For complement split products, patients who show signs of hypersensitivity reaction show at least a two-four fold^{5, 26} increase compared to baseline for PEGylated liposomal doxorubicin. All the whole blood donors showed a more than ten-fold increase in C5a *in vitro*. Hence, the incubation time of 45 minutes for whole heparinized blood at dosages of 0.25mg/ml for complement activator, i.e., either zymosan or nanoparticles were chosen as an optimum scenario for simulating the *in vivo* complement response.

As steps for validation, we generated the response observed *in vivo* in porcine animals for PLGA-PLL-PEG nanoparticles through the *in vitro* assay using human

blood. While porcine animals are more susceptible to complement activation compared to humans,^{4, 85} the pathway of activation, and subsequent response is analogous. The manifestations of complement-mediated hypersensitivity reactions, especially the changes in biomarkers, impacts on cardiopulmonary vitals, along with the time-course of the activation are similar in both humans and porcine animals, with reaction frequency being the point of difference between the two species.⁸⁵ A thorough characterization of the porcine C7 complement protein, one of the complement protein that contributes in the formation of the terminal membrane attack complex in the activated complement pathways, shows that the protein exhibits comparable structural and functional characteristics with the human complement protein C7⁸⁶ and same complement inhibitors can inhibit the catalytic activity of the C5 convertase in human and porcine models *in vitro* and *in vivo*.⁸⁷ The proteins share epitopes across species with cross-reactivity to same detection antibodies,⁸⁸ but the response mostly occurs at different rates, requiring optimization. Moreover, detection antibodies are species-specific and that acts as a limiting factor especially for the commercially available ELISA assays, as such assays could essentially help in safety assessments of the nanomedicines before moving to large animal studies.

While the hypersensitivity response generated due to the PLGA-PLL-PEG nanoparticles is robustly visible *in vivo*, *in vitro* assay did not show strong complement activation previously. Intravenous administration of highly positive and negative poly(lactic-co-glycolic acid)-b-poly(l-lysine)-b-poly(ethylene glycol)

nanoparticles can lead to complement-mediated hypersensitivity reactions, especially in large animals.³¹ For the same nanoparticles, controlling zeta-potential leads to control over the complement response at a specific range of dosages.³¹ Most importantly, tracking the complement proteins *in vivo* did not exhibit any significant change, but the rapid change in blood gas and vitals highlight the hypersensitivity response due to infusion. Through the developed assay, the complement protein C5a change was found to be more than three-fold for all the formulations. As we have mentioned in the previous section as well, patients with visible hypersensitivity reaction symptoms exhibit at least a two-four fold^{5, 26} increase in the complement biomarker.

Zeta-potential is a parameter related to surface charge and relevant for complement activation.⁶⁴⁻⁶⁶ The fact that nanomaterials can elicit such innate immune response is not surprising because of the sheer surface area exposed to complement proteins. A 400-nm particle can provide a surface area of $5 \times 10^5 \text{ nm}^2$. Further introducing functional groups,^{69, 89} and charged moieties³⁰ helps in controlling zeta potential on the surface and subsequent interaction with complement convertase molecules as well. Thus, tuning the surface properties can have an impact on complement activation and the infusion reaction. Once we mimicked the *in vivo* porcine complement response using whole human blood *in vitro*, we applied our developed assay conditions to simulate the change in complement response due to the changing zeta potential of nanoparticles observed *in vivo*.^{31 64} Nanoparticles were

generated with different zeta potential with the polymer poly(lactic acid)-b-poly(ethylene glycol). The zeta-potential observed for the nanoparticles is generated due to the ratio of surface moieties present. We quantified the anaphylatoxin C5a in the blood samples post-incubation and found that the response was least for neutral nanoparticles with zeta-potential of -1.8 mV. The observations confirm what we had seen while investigating the role of zeta-potential in complement response *in vivo* in porcine animals.³¹ Moreover, the designed assay conditions were able to simulate how aggregation and nanoparticle morphology⁶⁹ also dictates interaction with the convertase molecules on the exposed foreign surface. Using the optimum assay conditions determined, we designed an *in vitro* screening tool that can generate reactogenicity observed *in vivo* validated through simulation of complement activation due to zeta-potential and size of nanoparticles.

Conclusions

Highly sensitive immunoassays for quantifying complement response are essential in designing safer nanomedicines. Being able to screen nanomaterials before moving into large animal models, or, potentially, being able to replace large animal models with effective *in vitro* assays has the potential to greatly increase the number of nanomaterials that can be translated to the clinic. We have developed an assay with high sensitivity for evaluating complement response *in vitro*. This is supported by our observations on simulating *in vivo* complement response observed in our previous work³¹ *in vitro* as well as further assessment of the impact of zeta-potential on

complement-mediated hypersensitivity reactions. We believe this optimized assay provides a new method to effectively screen nanomaterials for complement activation so that we can more effectively design nanomaterials that have high safety profiles and the potential to transform medicine.

Acknowledgements

This work was supported by NIH R56 Grant (Project# 1R56NS100732-01) for developing hemostatic nanoparticles for spinal cord injury, and by the AIMM Research award (DOD) (Award Number# W81XWH1820061) for developing intravenously infusible nanoparticles to stop bleeding and increase survival following trauma. Some of the figures were created with Biorender.com.

References

1. Lombardo, D.; Kiselev, M. A.; Caccamo, M. T., Smart Nanoparticles for Drug Delivery Application: Development of Versatile Nanocarrier Platforms in Biotechnology and Nanomedicine. *J Nanomater* **2019**, DOI: 10.1155/2019/3702518.
2. Han, X. J.; Xu, K.; Taratula, O.; Farsad, K., Applications of nanoparticles in biomedical imaging. *Nanoscale* **2019**, *11* (3), 799-819 DOI: 10.1039/c8nr07769j.
3. Markiewski, M. M.; Lambris, J. D., The role of complement in inflammatory diseases from behind the scenes into the spotlight. *The American journal of pathology* **2007**, *171* (3), 715-727 DOI: 10.1016/j.it.2007.02.006.
4. Szebeni, J., Hemocompatibility testing for nanomedicines and biologicals: predictive assays for complement mediated infusion reactions. *European Journal of Nanomedicine* **2012**, *4* (1), DOI: 10.1515/ejnm-2012-0002.
5. Szebeni, J.; Bedőcs, P.; Csukás, D.; Rosivall, L.; Bünger, R.; Urbanics, R., A porcine model of complement-mediated infusion reactions to drug carrier nanosystems and other medicines. *Advanced Drug Delivery Reviews* **2012**, *64* (15), 1706-1716 DOI: 10.1016/j.addr.2012.07.005.
6. Anselmo, A. C.; Mitragotri, S., Nanoparticles in the clinic: An update. *Bioengineering & Translational Medicine* **2019**, e10143 DOI: 10.1002/btm2.10143.
7. Anselmo, A. C.; Mitragotri, S., Nanoparticles in the clinic. *Bioengineering & translational medicine* **2016**, *1* (1), 10-29 DOI: 10.1002/btm2.10003.

8. Gustafson, H. H.; Holt-Casper, D.; Grainger, D. W.; Ghandehari, H., Nanoparticle uptake: the phagocyte problem. *Nano today* **2015**, *10* (4), 487-510 DOI: 10.1016/j.nantod.2015.06.006.
9. Fujita, T., Evolution of the lectin–complement pathway and its role in innate immunity. *Nature Reviews Immunology* **2002**, *2* (5), 346 DOI: 10.1038/nri800.
10. Noris, M.; Remuzzi, G., Overview of complement activation and regulation. *Semin Nephrol* **2013**, *33* (6), 479-92 DOI: 10.1016/j.semnephrol.2013.08.001.
11. Merle, N. S.; Church, S. E.; Fremeaux-Bacchi, V.; Roumenina, L. T., Complement System Part I - Molecular Mechanisms of Activation and Regulation. *Front Immunol* **2015**, *6*, 262 DOI: 10.3389/fimmu.2015.00262.
12. Benjamini, E., *Immunology: a short course*. Vol. 77.
13. Wouters, D.; Wiessenberg, H. D.; Hart, M.; Bruins, P.; Voskuyl, A.; Daha, M. R.; Hack, C. E., Complexes between C1q and C3 or C4: novel and specific markers for classical complement pathway activation. *J Immunol Methods* **2005**, *298* (1-2), 35-45 DOI: 10.1016/j.jim.2004.12.018.
14. Harboe, M.; Mollnes, T. E., The alternative complement pathway revisited. *J Cell Mol Med* **2008**, *12* (4), 1074-84 DOI: 10.1111/j.1582-4934.2008.00350.x.
15. Petersen, S. V.; Thiel, S.; Jensenius, J. C., The mannan-binding lectin pathway of complement activation: biology and disease association. *Molecular immunology* **2001**, *38* (2-3), 133-149 DOI: 10.1016/s0161-5890(01)00038-4.
16. Peng, Q.; Li, K.; Sacks, S. H.; Zhou, W., The role of anaphylatoxins C3a and C5a in regulating innate and adaptive immune responses. *Inflammation & Allergy-*

- Drug Targets (Formerly Current Drug Targets-Inflammation & Allergy)* **2009**, 8 (3), 236-246 DOI: 10.2174/187152809788681038.
17. Ember, J.; Jagels, M.; Hugli, T.; Volanakis, J.; Frank, M., The human complement system in health and disease. *Marcel Dekker* **1998**, 241-84.
 18. Mastellos, D.; Papadimitriou, J. C.; Franchini, S.; Tsonis, P. A.; Lambris, J. D., A novel role of complement: mice deficient in the fifth component of complement (C5) exhibit impaired liver regeneration. *J Immunol* **2001**, 166 (4), 2479-86 DOI: 10.4049/jimmunol.166.4.2479.
 19. Bénard, M.; Gonzalez, B. J.; Schouft, M.-T.; Falluel-Morel, A.; Vaudry, D.; Chan, P.; Vaudry, H.; Fontaine, M., Characterization of C3a and C5a receptors in rat cerebellar granule neurons during maturation neuroprotective effect of C5a against apoptotic cell death. *Journal of Biological Chemistry* **2004**, 279 (42), 43487-43496 DOI: 10.1074/jbc.M404124200.
 20. Klos, A.; Tenner, A. J.; Johswich, K.-O.; Ager, R. R.; Reis, E. S.; Köhl, J., The role of the anaphylatoxins in health and disease. *Molecular immunology* **2009**, 46 (14), 2753-2766 DOI: 10.1016/j.molimm.2009.04.027.
 21. Merle, N. S.; Noe, R.; Halbwachs-Mecarelli, L.; Fremeaux-Bacchi, V.; Roumenina, L. T., Complement System Part II: Role in Immunity. *Front Immunol* **2015**, 6, 257 DOI: 10.3389/fimmu.2015.00257.
 22. Moghimi, S. M.; Simberg, D., Complement activation turnover on surfaces of nanoparticles. *Nano Today* **2017**, 15, 8-10 DOI: 10.1016/j.nantod.2017.03.001.

23. Chen, F.; Wang, G.; Griffin, J. I.; Brenneman, B.; Banda, N. K.; Holers, V. M.; Backos, D. S.; Wu, L.; Moghimi, S. M.; Simberg, D., Complement proteins bind to nanoparticle protein corona and undergo dynamic exchange in vivo. *Nat Nanotechnol* **2017**, *12* (4), 387-393 DOI: 10.1038/nnano.2016.269.
24. Wibroe, P. P.; Anselmo, A. C.; Nilsson, P. H.; Sarode, A.; Gupta, V.; Urbanics, R.; Szebeni, J.; Hunter, A. C.; Mitragotri, S.; Mollnes, T. E.; Moghimi, S. M., Bypassing adverse injection reactions to nanoparticles through shape modification and attachment to erythrocytes. *Nat Nanotechnol* **2017**, *12* (6), 589-594 DOI: 10.1038/nnano.2017.47.
25. Szebeni, J.; Bedőcs, P.; Rozsnyay, Z.; Weiszhar, Z.; Urbanics, R.; Rosivall, L.; Cohen, R.; Garbuzenko, O.; Báthori, G.; Tóth, M., Liposome-induced complement activation and related cardiopulmonary distress in pigs: factors promoting reactogenicity of Doxil and AmBisome. *Nanomedicine: Nanotechnology, Biology and Medicine* **2012**, *8* (2), 176-184 DOI: 10.1016/j.nano.2011.06.003.
26. Chanan-Khan, A.; Szebeni, J.; Savay, S.; Liebes, L.; Rafique, N. M.; Alving, C. R.; Muggia, F. M., Complement activation following first exposure to pegylated liposomal doxorubicin (Doxil): possible role in hypersensitivity reactions. *Ann Oncol* **2003**, *14* (9), 1430-7 DOI: 10.1093/annonc/mdg374.
27. Wang, G.; Chen, F.; Banda, N. K.; Holers, V. M.; Wu, L.; Moghimi, S. M.; Simberg, D., Activation of Human Complement System by Dextran-Coated Iron Oxide Nanoparticles Is Not Affected by Dextran/Fe Ratio, Hydroxyl Modifications, and Crosslinking. *Front Immunol* **2016**, *7*, 418 DOI: 10.3389/fimmu.2016.00418.

28. Banda, N. K.; Mehta, G.; Chao, Y.; Wang, G.; Inturi, S.; Fossati-Jimack, L.; Botto, M.; Wu, L.; Moghimi, S. M.; Simberg, D., Mechanisms of complement activation by dextran-coated superparamagnetic iron oxide (SPIO) nanoworms in mouse versus human serum. *Particle and fibre toxicology* **2014**, *11* (1), 64 DOI: 10.1186/s12989-014-0064-2.
29. De Sousa Delgado, A.; Léonard, M.; Dellacherie, E., Surface Properties of Polystyrene Nanoparticles Coated with Dextrans and Dextran–PEO Copolymers. Effect of Polymer Architecture on Protein Adsorption. *Langmuir* **2001**, *17* (14), 4386-4391 DOI: 10.1021/la001701c.
30. Fornaguera, C.; Caldero, G.; Mitjans, M.; Vinardell, M. P.; Solans, C.; Vauthier, C., Interactions of PLGA nanoparticles with blood components: protein adsorption, coagulation, activation of the complement system and hemolysis studies. *Nanoscale* **2015**, *7* (14), 6045-58 DOI: 10.1039/c5nr00733j.
31. Onwukwe, C.; Maisha, N.; Holland, M.; Varley, M.; Groynom, R.; Hickman, D.; Uppal, N.; Shoffstall, A.; Ustin, J.; Lavik, E., Engineering Intravenously Administered Nanoparticles to Reduce Infusion Reaction and Stop Bleeding in a Large Animal Model of Trauma. *Bioconjugate chemistry* **2018**, *29* (7), 2436-2447 DOI: 10.1021/acs.bioconjchem.8b00335.
32. Moghimi, S. M.; Simberg, D., Translational gaps in animal models of human infusion reactions to nanomedicines. *Future Medicine*: 2018.
33. Costabile, M., Measuring the 50% haemolytic complement (CH50) activity of serum. *J Vis Exp* **2010**, (37), DOI: 10.3791/1923.

34. Ekdahl, K. N.; Persson, B.; Mohlin, C.; Sandholm, K.; Skattum, L.; Nilsson, B., Interpretation of Serological Complement Biomarkers in Disease. *Front Immunol* **2018**, *9*, 2237 DOI: 10.3389/fimmu.2018.02237.
35. Pham, C. T.; Thomas, D. G.; Beiser, J.; Mitchell, L. M.; Huang, J. L.; Senpan, A.; Hu, G.; Gordon, M.; Baker, N. A.; Pan, D.; Lanza, G. M.; Hourcade, D. E., Application of a hemolysis assay for analysis of complement activation by perfluorocarbon nanoparticles. *Nanomedicine* **2014**, *10* (3), 651-60 DOI: 10.1016/j.nano.2013.10.012.
36. Vu, V. P.; Gifford, G. B.; Chen, F.; Benasutti, H.; Wang, G.; Groman, E. V.; Scheinman, R.; Saba, L.; Moghimi, S. M.; Simberg, D., Immunoglobulin deposition on biomolecule corona determines complement opsonization efficiency of preclinical and clinical nanoparticles. *Nat Nanotechnol* **2019**, *14* (3), 260-268 DOI: 10.1038/s41565-018-0344-3.
37. Coty, J. B.; Eleamen Oliveira, E.; Vauthier, C., Tuning complement activation and pathway through controlled molecular architecture of dextran chains in nanoparticle corona. *Int J Pharm* **2017**, *532* (2), 769-778 DOI: 10.1016/j.ijpharm.2017.04.048.
38. Kirschfink, M.; Mollnes, T. E., Modern complement analysis. *Clin Diagn Lab Immunol* **2003**, *10* (6), 982-9 DOI: 10.1128/cdli.10.6.982-989.2003.
39. Winzen, S.; Schoettler, S.; Baier, G.; Rosenauer, C.; Mailaender, V.; Landfester, K.; Mohr, K., Complementary analysis of the hard and soft protein

corona: sample preparation critically effects corona composition. *Nanoscale* **2015**, 7 (7), 2992-3001 DOI: 10.1039/c4nr05982d.

40. Jaskowski, T. D.; Martins, T. B.; Litwin, C. M.; Hill, H. R., Comparison of three different methods for measuring classical pathway complement activity. *Clin Diagn Lab Immunol* **1999**, 6 (1), 137-9.

41. Guadagnini, R.; Halamoda Kenzaoui, B.; Walker, L.; Pojana, G.; Magdolenova, Z.; Bilanicova, D.; Saunders, M.; Juillerat-Jeanneret, L.; Marcomini, A.; Huk, A.; Dusinska, M.; Fjellsbo, L. M.; Marano, F.; Boland, S., Toxicity screenings of nanomaterials: challenges due to interference with assay processes and components of classic in vitro tests. *Nanotoxicology* **2015**, 9 Suppl 1, 13-24 DOI: 10.3109/17435390.2013.829590.

42. Dobrovolskaia, M. A.; McNeil, S. E., Understanding the correlation between in vitro and in vivo immunotoxicity tests for nanomedicines. *J Control Release* **2013**, 172 (2), 456-66 DOI: 10.1016/j.jconrel.2013.05.025.

43. Keystone, E.; Schorlemmer, H.; Pope, C.; Allison, A., Zymosan—induced arthritis. *Arthritis & Rheumatism: Official Journal of the American College of Rheumatology* **1977**, 20 (7), 1396-1401.

44. Gurney, J.; Philbin, N.; Rice, J.; Arnaud, F.; Dong, F.; Wulster-Radcliffe, M.; Pearce, L. B.; Kaplan, L.; McCarron, R.; Freilich, D., A hemoglobin based oxygen carrier, bovine polymerized hemoglobin (HBOC-201) versus Hetastarch (HEX) in an uncontrolled liver injury hemorrhagic shock swine model with delayed evacuation. *J Trauma* **2004**, 57 (4), 726-38 DOI: 10.1097/01.ta.0000147520.84792.b4.

45. Strobel, L.; Johswich, K. O., Anticoagulants impact on innate immune responses and bacterial survival in whole blood models of *Neisseria meningitidis* infection. *Sci Rep* **2018**, 8 (1), 10225 DOI: 10.1038/s41598-018-28583-8.
46. Del Tordello, E.; Bottini, S.; Muzzi, A.; Serruto, D., Analysis of the regulated transcriptome of *Neisseria meningitidis* in human blood using a tiling array. *J Bacteriol* **2012**, 194 (22), 6217-32 DOI: 10.1128/JB.01055-12.
47. Moghimi, S. M., Nanomedicine safety in preclinical and clinical development: focus on idiosyncratic injection/infusion reactions. *Drug Discov Today* **2018**, 23 (5), 1034-1042 DOI: 10.1016/j.drudis.2017.11.006.
48. Skotland, T., Injection of nanoparticles into cloven-hoof animals: Asking for trouble. *Theranostics* **2017**, 7 (19), 4877-4878 DOI: 10.7150/thno.22420.
49. Szebeni, J.; Alving, C. R.; Rosivall, L.; Bunger, R.; Baranyi, L.; Bedocs, P.; Toth, M.; Barenholz, Y., Animal models of complement-mediated hypersensitivity reactions to liposomes and other lipid-based nanoparticles. *J Liposome Res* **2007**, 17 (2), 107-17 DOI: 10.1080/08982100701375118.
50. Oikonomopoulou, K.; Ricklin, D.; Ward, P. A.; Lambris, J. D., Interactions between coagulation and complement--their role in inflammation. *Semin Immunopathol* **2012**, 34 (1), 151-65 DOI: 10.1007/s00281-011-0280-x.
51. Norda, R.; Schött, U.; Berséus, O.; Åkerblom, O.; Nilsson, B.; Ekdahl, K.; Stegmayr, B. G.; Knutson, e. F., Complement activation products in liquid stored plasma and C3a kinetics after transfusion of autologous plasma. *Vox Sanguinis* **2012**, 102 (2), 125-133 DOI: 10.1111/j.1423-0410.2011.01522.x.

52. Zewde, N.; Morikis, D., A computational model for the evaluation of complement system regulation under homeostasis, disease, and drug intervention. *PloS one* **2018**, *13* (6), e0198644.
53. Bexborn, F.; Engberg, A. E.; Sandholm, K.; Mollnes, T. E.; Hong, J.; Nilsson Ekdahl, K., Hirudin versus heparin for use in whole blood in vitro biocompatibility models. *J Biomed Mater Res A* **2009**, *89* (4), 951-9 DOI: 10.1002/jbm.a.32034.
54. Lupu, F.; Keshari, R. S.; Lambris, J. D.; Coggeshall, K. M., Crosstalk between the coagulation and complement systems in sepsis. *Thromb Res* **2014**, *133 Suppl 1*, S28-31 DOI: 10.1016/j.thromres.2014.03.014.
55. Markiewski, M. M.; Nilsson, B.; Ekdahl, K. N.; Mollnes, T. E.; Lambris, J. D., Complement and coagulation: strangers or partners in crime? *Trends Immunol* **2007**, *28* (4), 184-92 DOI: 10.1016/j.it.2007.02.006.
56. Moghimi, S. M., Nanomedicine safety in preclinical and clinical development: focus on idiosyncratic injection/infusion reactions. *Drug discovery today* **2018**, *23* (5), 1034-1042.
57. Shoffstall, A. J.; Atkins, K. T.; Groynom, R. E.; Varley, M. E.; Everhart, L. M.; Lashof-Sullivan, M. M.; Martyn-Dow, B.; Butler, R. S.; Ustin, J. S.; Lavik, E. B., Intravenous Hemostatic Nanoparticles Increase Survival Following Blunt Trauma Injury. *Biomacromolecules* **2012**, *13* (11), 3850-3857 DOI: 10.1021/bm3013023.
58. Shoffstall, A. J.; Everhart, L. M.; Varley, M. E.; Soehnlen, E. S.; Shick, A. M.; Ustin, J. S.; Lavik, E. B., Tuning Ligand Density on Intravenous Hemostatic

Nanoparticles Dramatically Increases Survival Following Blunt Trauma.

Biomacromolecules **2013**, *14* (8), 2790-2797 DOI: 10.1021/bm400619v.

59. Mayer, A.; Vadon, M.; Rinner, B.; Novak, A.; Wintersteiger, R.; Frohlich, E., The role of nanoparticle size in hemocompatibility. *Toxicology* **2009**, *258* (2-3), 139-47 DOI: 10.1016/j.tox.2009.01.015.

60. Aminiahidashti, H.; Shafiee, S.; Kiasari, A. Z.; Sazgar, M., Applications of End-Tidal Carbon Dioxide (ETCO₂) Monitoring in Emergency Department; a Narrative Review. *Emergency* **2018**, *6* (1).

61. Chakraborty, S.; Karasu, E.; Huber-Lang, M., Complement After Trauma: Suturing Innate and Adaptive Immunity. *Front Immunol* **2018**, *9*, 2050 DOI: 10.3389/fimmu.2018.02050.

62. Ricklin, D.; Hajishengallis, G.; Yang, K.; Lambris, J. D., Complement: a key system for immune surveillance and homeostasis. *Nature immunology* **2010**, *11* (9), 785-797.

63. Moghimi, S. M.; Szebeni, J., Stealth liposomes and long circulating nanoparticles: critical issues in pharmacokinetics, opsonization and protein-binding properties. *Progress in lipid research* **2003**, *42* (6), 463-478.

64. Szebeni, J.; Muggia, F.; Gabizon, A.; Barenholz, Y., Activation of complement by therapeutic liposomes and other lipid excipient-based therapeutic products: prediction and prevention. *Adv Drug Deliv Rev* **2011**, *63* (12), 1020-30 DOI: 10.1016/j.addr.2011.06.017.

65. Pham, C. T.; Mitchell, L. M.; Huang, J. L.; Lubniewski, C. M.; Schall, O. F.; Killgore, J. K.; Pan, D.; Wickline, S. A.; Lanza, G. M.; Hourcade, D. E., Variable antibody-dependent activation of complement by functionalized phospholipid nanoparticle surfaces. *J Biol Chem* **2011**, 286 (1), 123-30 DOI: 10.1074/jbc.M110.180760.
66. Socha, M.; Bartecki, P.; Passirani, C.; Sapin, A.; Damgé, C.; Lecompte, T.; Barré, J.; Ghazouani, F. E.; Maincent, P., Stealth nanoparticles coated with heparin as peptide or protein carriers. *Journal of Drug Targeting* **2009**, 17 (8), 575-585 DOI: 10.1080/10611860903112909.
67. Moghimi, S. M.; Andersen, A. J.; Ahmadvand, D.; Wibroe, P. P.; Andresen, T. L.; Hunter, A. C., Material properties in complement activation. *Adv Drug Deliv Rev* **2011**, 63 (12), 1000-7 DOI: 10.1016/j.addr.2011.06.002.
68. Szeto, G. L.; Lavik, E. B., Materials design at the interface of nanoparticles and innate immunity. *J Mater Chem B* **2016**, 4 (9), 1610-1618 DOI: 10.1039/C5TB01825K.
69. Thomas, S. N.; van der Vlies, A. J.; O'Neil, C. P.; Reddy, S. T.; Yu, S. S.; Giorgio, T. D.; Swartz, M. A.; Hubbell, J. A., Engineering complement activation on polypropylene sulfide vaccine nanoparticles. *Biomaterials* **2011**, 32 (8), 2194-203 DOI: 10.1016/j.biomaterials.2010.11.037.
70. Mollnes, T.; Garred, P.; Bergseth, G., Effect of time, temperature and anticoagulants on in vitro complement activation: consequences for collection and

preservation of samples to be examined for complement activation. *Clinical and experimental immunology* **1988**, 73 (3), 484.

71. Pillemer, L.; Blum, L.; Lepow, I. H.; Ross, O. A.; Todd, E. W.; Wardlaw, A. C., The properdin system and immunity: I. Demonstration and isolation of a new serum protein, properdin, and its role in immune phenomena. *Science* **1954**, 120 (3112), 279-285.

72. Fearon, D. T.; Austen, K. F., Activation of the alternative complement pathway due to resistance of zymosan-bound. *Proceedings of the National Academy of Sciences* **1977**, 74 (4), 1683-1687.

73. Hamad, I.; Al-Hanbali, O.; Hunter, A. C.; Rutt, K. J.; Andresen, T. L.; Moghimi, S. M., Distinct polymer architecture mediates switching of complement activation pathways at the nanosphere– serum interface: implications for stealth nanoparticle engineering. *ACS nano* **2010**, 4 (11), 6629-6638.

74. Nilsson, B.; Ekdahl, K. N.; Mollnes, T. E.; Lambris, J. D., The role of complement in biomaterial-induced inflammation. *Molecular immunology* **2007**, 44 (1-3), 82-94.

75. Andersson, J.; Ekdahl, K. N.; Lambris, J. D.; Nilsson, B., Binding of C3 fragments on top of adsorbed plasma proteins during complement activation on a model biomaterial surface. *Biomaterials* **2005**, 26 (13), 1477-85 DOI: 10.1016/j.biomaterials.2004.05.011.

76. Csukás, D.; Urbanics, R.; Wéber, G.; Rosivall, L.; Szebeni, J., Pulmonary intravascular macrophages: prime suspects as cellular mediators of porcine CARPA. *European Journal of Nanomedicine* **2015**, 7 (1), DOI: 10.1515/ejnm-2015-0008.
77. Winkler, G. C., Pulmonary intravascular macrophages in domestic animal species: review of structural and functional properties. *American journal of Anatomy* **1988**, 181 (3), 217-234.
78. Dixon, L. J.; Barnes, M.; Tang, H.; Pritchard, M. T.; Nagy, L. E., Kupffer cells in the liver. *Compr Physiol* **2013**, 3 (2), 785-97 DOI: 10.1002/cphy.c120026.
79. Szebeni, J.; Bawa, R., Human Clinical Relevance of the Porcine Model of Pseudoallergic Infusion Reactions. *Biomedicines* **2020**, 8 (4), DOI: 10.3390/biomedicines8040082.
80. Szebeni, J., Mechanism of nanoparticle-induced hypersensitivity in pigs: complement or not complement? *Drug Discov Today* **2018**, 23 (3), 487-492 DOI: 10.1016/j.drudis.2018.01.025.
81. Meszaros, T.; Kozma, G. T.; Shimizu, T.; Miyahara, K.; Turjeman, K.; Ishida, T.; Barenholz, Y.; Urbanics, R.; Szebeni, J., Involvement of complement activation in the pulmonary vasoactivity of polystyrene nanoparticles in pigs: unique surface properties underlying alternative pathway activation and instant opsonization. *Int J Nanomedicine* **2018**, 13, 6345-6357 DOI: 10.2147/IJN.S161369.
82. Szebeni, J.; Bedőcs, P.; Dézsi, L.; Urbanics, R., A porcine model of complement activation-related pseudoallergy to nano-pharmaceuticals: Pros and cons

of translation to a preclinical safety test. *Precision Nanomedicine* **2018**, *1* (1), 63-73
DOI: 10.29016/180427.1.

83. Yang, S.; McGookey, M.; Wang, Y.; Cataland, S. R.; Wu, H. M., Effect of blood sampling, processing, and storage on the measurement of complement activation biomarkers. *Am J Clin Pathol* **2015**, *143* (4), 558-65 DOI: 10.1309/AJCPXPD7ZQXNTIAL.

84. Ekdahl, K. N.; Fromell, K.; Mohlin, C.; Teramura, Y.; Nilsson, B., A human whole-blood model to study the activation of innate immunity system triggered by nanoparticles as a demonstrator for toxicity. *Science and technology of advanced materials* **2019**, *20* (1), 688-698 DOI: 10.1080/14686996.2019.1625721.

85. Urbanics, R.; Bedőcs, P.; Szebeni, J., Lessons learned from the porcine CARPA model: constant and variable responses to different nanomedicines and administration protocols. *European Journal of Nanomedicine* **2015**, *7* (3), DOI: 10.1515/ejnm-2015-0011.

86. Agah, A.; Montalto, M. C.; Kiesecker, C. L.; Morrissey, M.; Grover, M.; Whoolery, K. L.; Rother, R. P.; Stahl, G. L., Isolation, characterization, and cloning of porcine complement component C7. *J Immunol* **2000**, *165* (2), 1059-65 DOI: 10.4049/jimmunol.165.2.1059.

87. Barratt-Due, A.; Thorgersen, E. B.; Lindstad, J. K.; Pharo, A.; Lissina, O.; Lambris, J. D.; Nunn, M. A.; Mollnes, T. E., Ornithodoros moubata complement inhibitor is an equally effective C5 inhibitor in pigs and humans. *J Immunol* **2011**, *187* (9), 4913-9 DOI: 10.4049/jimmunol.1101000.

88. Salvesen, B.; Mollnes, T. E., Pathway-specific complement activity in pigs evaluated with a human functional complement assay. *Mol Immunol* **2009**, *46* (8-9), 1620-5 DOI: 10.1016/j.molimm.2009.02.028.
89. Toda, M.; Kitazawa, T.; Hirata, I.; Hirano, Y.; Iwata, H., Complement activation on surfaces carrying amino groups. *Biomaterials* **2008**, *29* (4), 407-17 DOI: 10.1016/j.biomaterials.2007.10.005.

Chapter 4: Engineering PEGylated polyester nanoparticles to reduce complement-mediated infusion reaction

* The material in this chapter has been submitted for review. Maisha, N., Naik, N., Okesola, M., Coombs, T., & Lavik, E.* Engineering PEGylated polyester nanoparticles to reduce complement-mediated infusion reaction (2021)

Abstract

Translation of intravenously administered nanomaterials to the clinic is limited due to adverse infusion reactions. While these reactions are infrequent, with up to 10% prone to experiencing infusion reactions, the reactions can be severe and life-threatening. One of the innate immune pathways, the complement activation pathway, plays a significant role in mediating this response. Nanoparticle surface properties are a relevant design feature, as they control the blood proteins the nanoparticles interact with and allow the nanoparticles to evade the immune reaction. PEGylation of nano-surfaces is critical in improving the blood circulation of nanoparticles and reducing opsonization. Our goal was to understand whether modifying the surface architecture by varying the PEG density and architecture can impact the complement response in vitro. We utilized block-copolymers of poly(lactic acid)-b-poly(ethylene glycol) prepared with poly(ethylene glycol) macroinitiators of molecular weights 3400Da and 5000Da. Tracking the complement biomarker C5a, we monitored the impact of changing PEGylation of the

nanoparticles. We also investigated how the changing PEG length on the nanoparticle surface impacts further strengthening the stealth properties. Lastly, we determined which cytokines change upon blood incubation with nanoparticles in vitro to understand the extent to which inflammation may occur and the crosstalk between the complement and immune responses. This study's overall objective is to determine the parameters essential to develop stealth nanoparticles that do not lead to infusion reactions upon intravenous administration.

Introduction

Infusion reactions are complex immune responses that are set in motion minutes after intravenous infusions.¹ While only 10% of humans appear to exhibit infusion responses,² the symptoms can range from mild hypersensitivity issues to severe cardiovascular complications and fatality in a subset of the population.³ Intravenously administered nanomedicines are engulfed in proteins as soon as they come in contact with bodily fluids, forming a protein corona.^{4 5} The immune system can recognize either the nanoparticle surface or the protein corona formed which initiates the complement pathways resulting in infusion reactions.⁴

The complement system is a vital component of the innate host defense⁶ and is associated with the onset of hypersensitivity reactions and subsequent clearance of nanoparticles from the bloodstream.¹ The complement activation occurs through either the classical, alternative, or lectin pathway.⁷⁻⁸ The initiating molecule is different for each of the pathways. The classical pathway is initiated through C1

binding to antigen-antibody complex,⁹ while the spontaneous hydrolysis of C3 triggers the alternative pathway.¹⁰ The lectin pathway is initiated through plasma protein mannose-binding lectins attaching to carbohydrate structures present in the surface of pathogens.¹¹ Each of the pathways converges with the formation of initial C3 convertase, eventually leading to the generation of anaphylatoxins C3a and C5a.¹⁰ The anaphylatoxins are responsible for many of the symptoms associated with the onset of infusion reactions, including the degranulation of mast cells and production of histamines,^{9, 12} vasodilation, and increased permeability of blood vessels.¹³ Hence, a change in the anaphylatoxins can be a suitable biomarker for tracking the immune response to nanoparticles upon intravenous infusion. While identifying stealth properties, tracking cytokines, especially pro-inflammatory chemokines, can be helpful to evaluate the immunotoxicity.¹⁴ However, therapeutics delivered intravenously results in immediate protein corona formation and receptor recognition for subsequent clearance, and data regarding how the biomolecules governing inflammation change when nanoparticles encounter blood matrices is inadequate.

PEGylation refers to covalently grafting, entrapping, or adsorbing Poly(ethylene glycol) (PEG) chains to a molecule or material.¹⁵ One of the earliest theories by Jeon et al. regarding why PEGylation of surfaces leads to protein resistance is because PEG has the lowest refractive index among water-soluble synthetic polymers, resulting in low van der Waal's force.¹⁶ Based on molecular weight, grafting density, the hydrophilic nature, and flexibility of the PEG chains, PEGylation leads to a more extended conformation in the presence of water

molecules.¹⁵⁻¹⁶ Owing to the hydrophilic nature and higher chain flexibility based on molecular weight, the PEG coating can lead to the formation of an impermeable cloud-like conformation even from a small number of PEG chains and prevent opsonization.¹⁷ PEGylation of liposomal nanoformulations has increased the half-life during circulation, decreased plasma clearance,¹⁸ and reduced clearance due to reticuloendothelial systems.¹⁹ While PEGylation has been extensively studied for making stealth nanomaterials, the details of the density and molecular weight of the chains that are critical for this, particularly in response to infusion reactions, have not been studied thoroughly. Surface coverage of Poly(lactic-co-glycolic acid) PLGA nanoparticles with polyethylene oxide can impart stealth properties by forming a weak complex with blood albumen leading to the chameleon effect and repulsion to biomolecules in the blood responsible for rapid clearance of the nanoparticles.²⁰ Surface modification with poly(phosphoester),²¹ and polysaccharides combined with PEG²² can lead to surface enrichment with clusterin. This dysopsonin protein helps avoid clearance by macrophages.²³ Increased molecular weight and grafting density for PEG have been found to enhance clusterin adsorption while reducing cellular internalization as well.²⁴ This is because the grafted PEG chains on the surface impact complement activation and the activation pathways modulating access between nano surfaces and blood proteins.²⁵ Thus, particles with brush-like polyethylene oxide (highly dense) or dense dextran brushes are more resistant to binding complement proteins than their counterparts with mushroom-like/ or lightly enveloped surfaces.²⁵⁻²⁶ Moreover, how PEG remains attached to the surface also plays a pivotal role in

determining the extent to which opsonization is blocked, as surface adsorption is reversible, and surface conjugation may lead to insufficient surface coverage.¹⁵ Owing to its hydrophilicity and chain flexibility, PEGylation with 2000Da molecular weight PEG can lower protein adsorption on poly(lactic acid) nanoparticles by 57%.²⁷

Because degradable polyesters have been used extensively in developing drug delivery systems, we were interested in understanding the details of how PEGylation might reduce or eliminate infusion reactions. To investigate the impact of PEGylation on polyesters, we developed polylactic acid (PLA) nanoparticles as well as a series of PLA-based nanoparticles with different densities and architectures of PEG arms. We quantified C5a, a biomarker of the complement activation, *in vitro*, as we incubated the surface-modified nanoparticles with the blood matrices. Our goal was to understand how the extent of surface PEGylation modulates the innate immune response and further comprehend what role PEG chain length plays in imparting the stealth properties. Moreover, we investigated the impact PEGylation plays on cytokine levels upon *in vitro* incubation to understand better the overall immune response between blood matrices and PLA-*b*-PEG nanoparticles.

Materials and Methods

Materials

Poly(lactic acid)-*b*-poly(ethylene glycol) block copolymer was synthesized using L-lactide from Polysciences Inc. (Warrington, PA), heterobifunctional poly(ethylene glycol) with 5000 Da and 3400Da molecular weight from Laysan

Biosciences (Arab, AL), and D-lactide from Purac Biomaterials (Corbion, Amsterdam, Netherlands). All solvents used were of ACS grade and obtained from Fisher Scientific.

We monitored Complement protein C5a using a C5a human ELISA duo kit (DY2037) obtained from R&D Systems (Minneapolis, MN). We measured cytokine levels in vitro using Proteome Profiler Human Cytokine Array Kit (R and D Systems, catalog number ARY005B). For generating the responses in vitro, we used heparinized human blood and complement protected human serum from Innovative Research Inc. (Novi, MI).

Synthesis and characterization of nanoparticles

Block copolymers of Poly(lactic acid)-b-poly(ethylene glycol) with either 3400 or 5000Da PEG macroinitiators were synthesized through a ring-opening polymerization reaction.²⁸⁻²⁹ Poly(D-lactic acid) (PDLA) was also synthesized using a ring-opening polymerization but with methanol as the initiator. The molecular weight was determined using gel permeation chromatography in Tetrahydrofuran (THF) and Dimethylformamide (DMF).

The nanoparticles were prepared using different ratios of poly(L-lactic acid)-b-poly(ethylene glycol) (PLLA-b-PEG5000, PLLA- b-PEG3400), Poly(D-lactic acid)-b-poly(ethylene glycol) (PDLA-b-PEG5000, PDLA-b-PEG3400) and PDLA through nanoprecipitation.²⁹ The nanoparticle groups used in this study, along with the variation in the polymers used, are summarized in table 1 and table 2.

Table 1: Altering amount of surface PEG by varying ratio of block copolymer PLLA-*b*-PEG5000 and PDLA (%w/w)

	Polymers used
Very low-density PEG brush	10% PLLA- <i>b</i> -PEG5000 +90%PDLA
Low-density PEG brush	50% PLLA- <i>b</i> -PEG5000 +50%PDLA
Medium-density PEG brush	75% PLLA- <i>b</i> -PEG5000 +25%PDLA
High-density PEG brush	75% PLLA- <i>b</i> -PEG5000 +25% PDLA- <i>b</i> -PEG3400

Table 2: Combining surface PEG of different molecular by varying ratio of block copolymer PLA-*b*-PEG5000 and PLA-*b*-PEG3400 (%w/w)

	PEG length	Polymers used
A	3400Da PEG	75% PLLA- <i>b</i> -PEG3400+ 25% PDLA- <i>b</i> -PEG3400
B	75% 3400Da PEG	75% PLLA- <i>b</i> -PEG3400+ 25% PDLA- <i>b</i> -PEG5000
C	75% 5000Da PEG	75% PLLA- <i>b</i> -PEG5000+ 25% PDLA- <i>b</i> -PEG3400
D	5000Da PEG	75% PLLA- <i>b</i> -PEG5000+ 25% PDLA- <i>b</i> -PEG5000

The polymer dissolved in the organic phase, i.e., Tetrahydrofuran (THF), at a concentration of 20mg/ml was added dropwise to double the phosphate-buffered saline's volumetric amount. This was stir-hardened to form the nanoparticles. After stir-hardening for 3 hours, excess THF was removed by exposing the solution to air and poloxamer was added as the stabilizer. The nanoparticles were then collected through centrifugation at 4000XG for 10 minutes at 4°C and resuspended in phosphate-buffered saline. The particles were characterized through dynamic light scattering for determining the hydrodynamic diameter and the zeta-potential for nanoparticles in dilute potassium chloride solution (10mM). The extent of PEGylation was determined through ¹H-NMR as well. PLA nanoparticles were prepared by dissolving the polymer in THF, and adding to PVA solution dropwise. Th mixture was briefly sonicated and then added to a larger volume of PVA solution

to further stir harden the nanoparticles overnight. Size and Zeta-potential was determined using DLS.

Generating complement response in vitro and quantification through complement assay

The change in complement protein C5a was quantified following previously established protocol.³⁰ The blood matrix was incubated with nanoparticles suspended in Dulbecco's PBS (without calcium and magnesium). As a positive control, Zymosan was used. The dosage used for the nanoparticles and Zymosan was 0.25mg/ml in serum. The samples were incubated at 37°C for 45 minutes and then centrifuged at 4000g for 5 minutes to separate the nanoparticles. The plasma was aliquoted in clean tubes and stored on ice until assay was carried out using the C5a ELISA assay duo kit (R&D Systems). The optical density for the samples and standards were measured at a wavelength of 450 nm using SpectraMax M2 Microplate Reader (Molecular Devices LLC) with background correction done using reading obtained at 540 nm. The normalized change was measured by comparing the level of C5a observed in the sample incubated with PBS.

$$\text{Normalized Change} = \frac{\text{Biomarker in sample incubated with Zymosan or nanoparticles}}{\text{Biomarker in sample incubated with PBS}}$$

Generating immune response in vitro and quantification through cytokine array

Nanoparticles resuspended in Minimum essential medium (MEM) were added to whole blood to reach a final concentration of 0.25mg/ml. The blood to the

nanoparticle in MEM ratio was 5:1. The blood was gently pipetted with the nanoparticle resuspension and incubated for 45 at 37 °C in a rotating shaker. Immediately after incubation, samples were placed on ice and then centrifuged at 4000G for 5 minutes. The supernatant plasma was collected in clean microcentrifuge tubes. For the cytokine array panel, 200µl of plasma was used to prepare samples following the protocol, and subsequent steps given in the protocol were followed for the human cytokine array panel (R&D Systems). The final image was taken using a Bio-Rad imager. For further analysis, ImageJ was used. Integrated density gives the sum of total pixels within a region. Following this method, each dot blot within the membrane was quantified for each sample. The levels of the detected cytokines were expressed as a percentage of the pixel density determined for the reference spot.³¹

Detecting the levels of IL-6 generated from rat endothelial cells exposed to PLA and PLA-PEG nanoparticles

Rat endothelial cells were seeded at a density of 150,000 cells/well in treated 24-well plates and left overnight at incubator operating at 37C and 5% CO₂. Nanoparticles resuspended in MEM or Zymosan resuspended in MEM was added to reach a concentration of 0.25mg/ml and incubated further for 24 hours. The supernatant was removed and centrifuged to separate the nanoparticle pellet, and the collected supernatant was used to quantify the IL-6 levels using the Rat IL-6 Quantikine ELISA Kit (R&D systems, R6000B). The normalized change was determined as follows.

$$\text{Normalized Change} = \frac{\text{Biomarker in sample incubated with Zymosan or nanoparticles}}{\text{Biomarker in sample incubated with MEM only}}$$

Statistical Analysis

We used Chi-square analysis to calculate the p-value within groups. As the expected value, the C5a level for blood or serum incubated with PBS or MEM was used.

Results

Characterization of nanoparticles with changing amount of surface PEGylation and combination of different PEG lengths

First, we tracked the change in complement protein C5a for PLA nanoparticles. The nanoparticles prepared had an average size of 324.3 ± 4.7 nm and a zeta-potential of -25.4 ± 0.66 mV. Our goal was to design a set of nanoparticles with different amounts of PEGylation on the surface to compare with the complement response observed for the PLA nanoparticles. We blended block copolymer of poly(l-lactic acid)-*b*-(polyethylene glycol) and poly(d-lactic acid) at different ratios to generate these nanoparticles. (Figure 16)

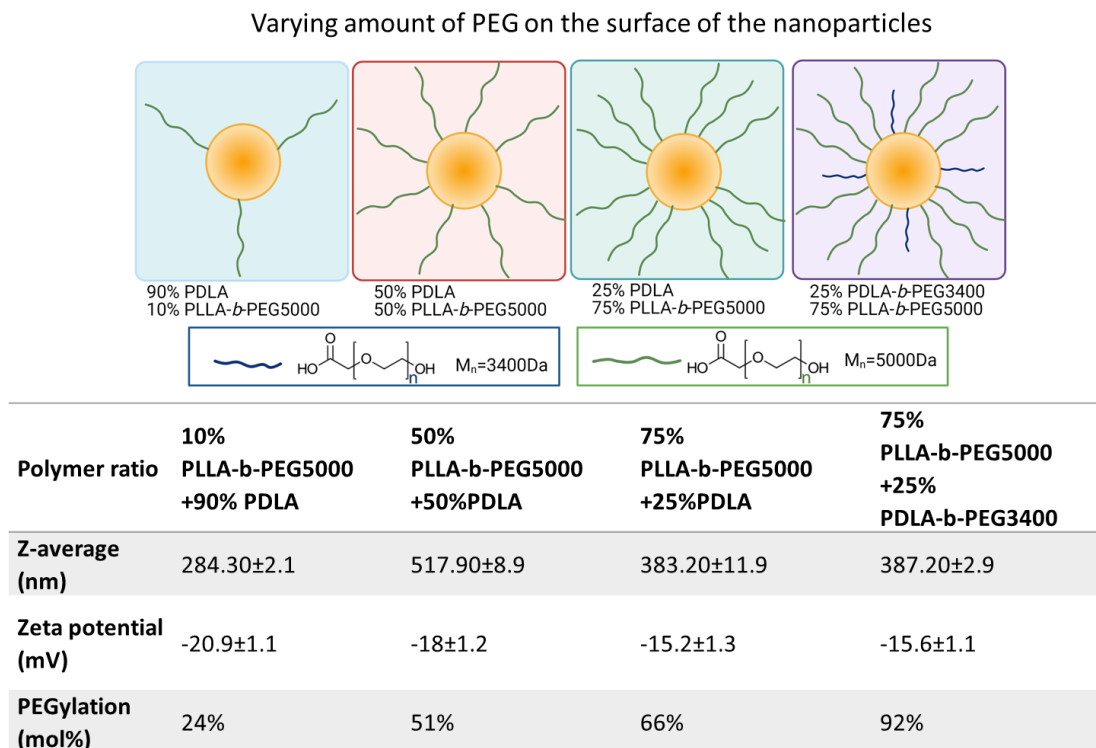


Figure 16: Summary of characterization data for nanoparticles with varying amounts of surface PEG

To further understand how PEGylation can help generate stealth properties, we also prepared nanoparticles combining PEG of different molecular weights on the surface. To achieve this variation, we combined block copolymers of poly(l-lactic acid)-*b*-(polyethylene glycol) with PEG molecular weights of 5000Da and 3400Da. (Figure 17)

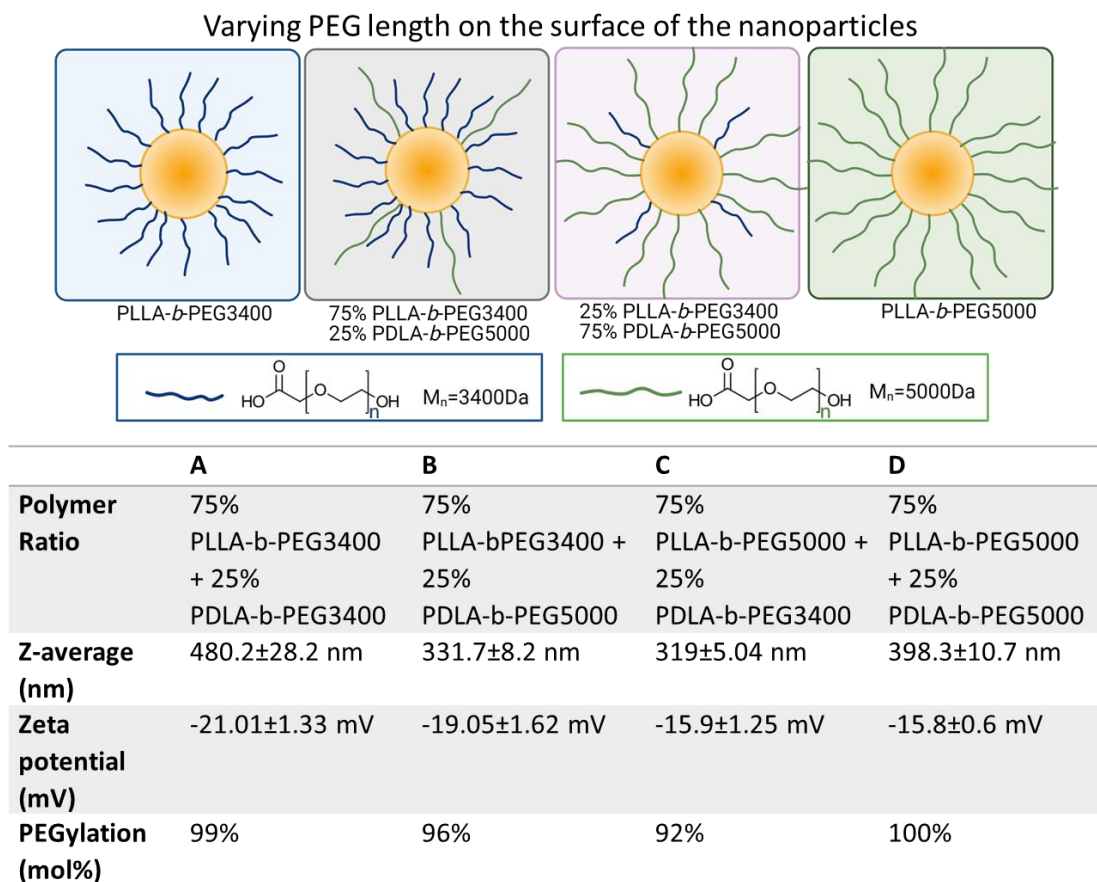


Figure 17: Summary of DLS data for nanoparticles with a combination of PEG lengths in the corona

The nanoparticles prepared were characterized using dynamic light scattering (Malvern ZetaSizer (Nano ZS90), Malvern Panalytical Ltd). The nanoparticles' average size and the Zeta-potential in 10mM KCl solution are summarized below in Figure 1 and Figure 2. As the extent of PEGylation increases, the zeta-potential increases, as the more negatively charged surface of the PLA nanoparticles getting cloaked by the PEG chains. The extent of PEGylation calculated using ^1H NMR is also summarized in these tables. The extent of PEGylation is measured as the

percentage of moles of PLA with a PEG chain attached to it. We determined the values based on the ^1H NMR peak integrated areas observed for PLA segments and PEG segments in deuterated Chloroform (Supplementary figure 35 and 36).

Change in complement protein C5a in vitro for different PEG corona structures

We measured the change in complement protein C5a in vitro in human whole heparinized blood and complement protected human serum by incubating the blood matrices with the nanoparticles suspended in PBS at a concentration of 0.25mg/ml. The preparation method is based on our previously established protocol for sensitively quantifying complement proteins in vitro.³⁰ The complement-mediated response is highly donor sensitive. Heparinized whole blood is more sensitive as the complement pathways are not impacted by the anticoagulant itself,³² while in serum, as the coagulation cascade is no longer intact, the complement pathway is not suppressed, due to the absence of cells leading to biological turnover.³³⁻³⁵ As a result, in serum, complement protein levels are high due to initial activation, and the level change is faster.³⁶ Hence the complement-mediated response was measured in both heparinized whole blood and complement protected human serum. Polylactic acid nanoparticles without any surface modifications, when incubated with heparinized whole blood, led to the highest amount of complement protein C5a generated within the samples. (Figure 18) The level observed was comparable to the amount of C5a generated for the positive control zymosan. Statistical analysis was carried out using

the Chi-square analysis, and the change in C5a detected was significantly different for the positive control Zymosan and the PLA nanoparticles.

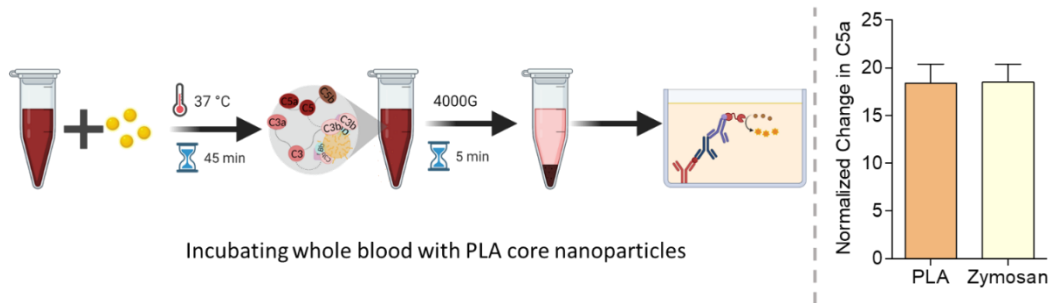


Figure 18: Change in complement protein C5a upon incubation of heparinized whole blood with PLA nanoparticles. Using Chi-square analysis, p-value obtained was less $p < 0.05$ when compared against an expected value of 1 for the level in sample incubated with PBS.

As we cloaked the surface with the PEG corona, the increasing extent of PEGylation on the surface leads to a decrease in C5a detected within the samples in heparinized human whole blood. Even the lowest amount of PEGylation tested led to 10 times lower C5a generation within the sample. As the extent of PEGylation increases, the C5a generation further decreases with the samples. The result summarized is the response observed in whole heparinized blood. (Figure 19). Based on the Chi-square analysis, for the PEGylated nanoparticles, a p-value lower than 0.05 was obtained, indicating the significant difference for the nanoparticles with 24 and 51% PEGylation. However, the p-value was greater than 0.05 for 66 and 92% PEGylation, indicating lower differences observed than the sample incubated with PBS. Hence, the increasing extent of PEGylation can control the C5a generation in

vitro and prevent complement activation. In complement-protected human serum, the nanoparticles with high-density PEG had a lower change in C5a when compared to the nanoparticles with 66% PEGylation (Supplementary figure 37). Based on the Chi-square analysis, the observed change in C5a was not significantly different from the serum incubated with PBS, as observed in the whole blood.

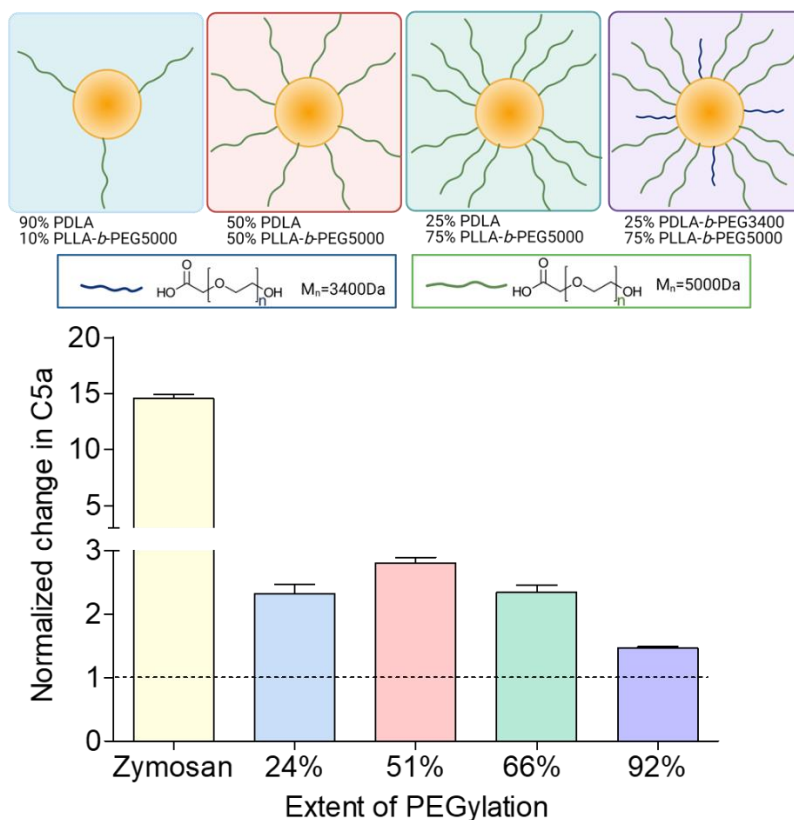


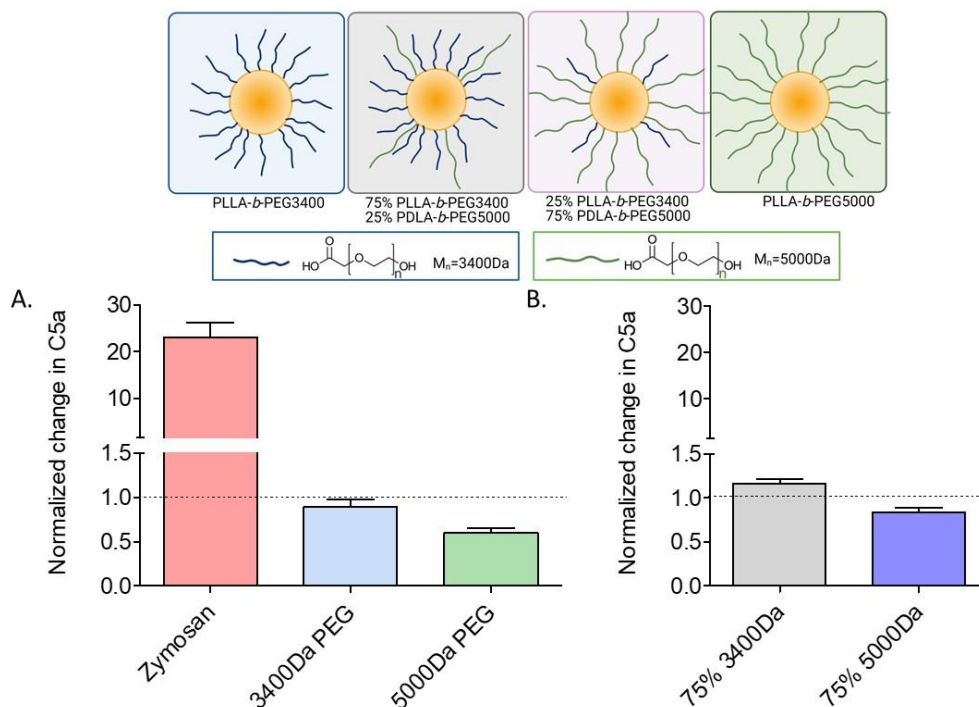
Figure 19: Impact of the extent of PEGylation on the normalized change in complement protein C5a in vitro upon incubation of heparinized human blood with nanoparticles at a concentration of 0.25mg/ml. As a positive control, Zymosan was used. The normalized change was calculated in comparison to the sample incubated

with PBS. Using Chi-square analysis, p-value obtained was less $p < 0.05$ when compared against an expected value of 1 for the level in sample incubated with PBS for the 24 and 51% PEGylation but not for the other groups.

Change in complement response in vitro for changing ratio of PEGs with different lengths

While increasing the extent of PEGylation reduced changes in C5a, we also investigated the impact of the PEG chain length. We compared four variations, ranging from highly PEGylated nanoparticles with a PEG chain length of 3400 Da to nanoparticles with a dual PEG brush combining 3400 and 5000Da PEG chains and nanoparticles with a PEG chain length of 5000 Da. We investigated this change in both whole blood and complement protected human serum at a nanoparticle concentration of 0.25mg/ml. The C5a levels detected were lowest for nanoparticles with 5000Da PEG in human whole heparinized blood (Figure 20) and complement protected serum (Supplementary figure 38) compared to 3400 Da PEG. In the case of the dual-PEG corona, the molecular weight of the dominant PEG in presence seemed to be the controlling factor. For nanoparticles with a higher presence of 3400Da PEG chain, the C5a detected was higher than the amount detected for nanoparticles with a higher fraction of 5000Da PEG chain in both blood and serum. The C5a level detected remained close to the levels detected in the control sample incubated with PBS only. There was no significant difference in the means observed; however, the means were significantly different from the positive control Zymosan in all the cases.

This was confirmed through the Chi-square analysis, where calculated p-values were greater than 0.05.



Keeping constant PEG length in the corona Mixing PEG of different lengths in the corona

Figure 20: Impact of PEG chain length on normalized change of complement protein C5a in vitro upon incubation of heparinized human blood with highly PEGylated nanoparticles at a concentration of 0.25mg/ml. As a positive control, Zymosan was used. The normalized change was calculated in comparison to the sample incubated with PBS. A. The normalized change in C5a observed for PEG lengths of 3400Da and 5000Da. B. The normalized change in C5a observed for mixing different PEG lengths. Using the Chi-square analysis, the p-value>0.05 was obtained, indicating the C5a levels observed are similar to the levels observed in samples incubated with PBS.

Change in cytokine response for PEGylated nanoparticles

To better understand the crosstalk between complement and the other inflammatory responses in vitro, we quantified the changes in cytokine levels in heparinized human whole blood through dot blot using a cytokine array kit. We incubated the nanoparticles with heparinized human whole blood at a concentration of 0.25mg/ml to detect the presence of the cytokines. We compared the impact of PEG corona conformation and identified whether the cytokines were upregulated or downregulated for PEGylated and non-PEGylated nanocapsules. (Figure 21)

The change observed in C5/C5a biomarker was the greatest, with the value being significantly higher for the non-PEGylated PLA nanoparticles and Zymosan. PEGylation of PLA-*b*-PEG nanoparticles lowered the levels of C5/C5a detected. The levels observed were significantly higher based on the Chi-square analysis. Anaphylatoxin C5a is a potent mediator of inflammation.³⁷ The pro-inflammatory biomarkers that were detected primarily include IL-8 and IL-16. Interleukin-16 (IL-16) is a chemoattractant factor,³⁸ released in response to mitogens, antigens, or vasoactive amines such as histamine or serotonin.³⁸ IL-16 is responsible for the upregulation of pro-inflammatory cytokines (IL-1 β , IL-6, and TNF- α) or cytokines that can cause pro-inflammatory activity.³⁹ The levels observed remained low for IL-16 in all cases. IL-8 levels remain elevated but not significantly compared to the MEM for PLA-PEG nanoparticles. IL-16 levels remain downregulated for Zymosan, PLA, and PLA-PEG compared to MEM, and the downregulation is significant, based on the Chi-square analysis. Receptor antagonist for IL-1 (IL-1ra)dampening

inflammation,⁴⁰ can be downregulated due to complement activation.⁴¹ The anti-inflammatory cytokine IL-1ra remains close to levels observed for MEM. Chemokine protein CXCL-12 is known to trigger anti-inflammatory molecular cascades.⁴² It is critical in the recruitment of leucocytes and fundamental in inflammation.⁴³ While CXCL-12 levels remain similar for PLA, PLA-PEG, and MEM, the detected level is lower for Zymosan. The regulators for the innate and acquired immune system, Macrophage migration inhibitory factor (MIF), remain lower for the PEGylated nanoparticles, and the level of downregulation is significant. MIF is a critical upstream regulator of the innate and acquired immune response,⁴⁴ induces pro-inflammatory cytokine expression.⁴⁴ PAI-1 levels also remain close to the level observed in blood incubated with MEM, slightly decreasing for Zymosan. As mentioned, other than C5/C5a and IL-16, none of the cytokines showed significant upregulation or downregulation in the whole heparinized blood.

For intravenous infusion, it is critical to understand how the cytokines may change upon exposure to nanoparticles *in vivo*. As a preliminary assessment, we sought to understand how the biomarkers change *in vitro* in whole heparinized blood and whether complement-mediated infusion reactions and inflammation can be prevented. The method of detecting the cytokine is pseudo-quantitative, as the absolute values are not obtained, rather the intensities are determined. It should also be noted that using whole human blood introduces variability in response, as the response could be donor-specific. However, for detecting an overview of cytokine profiles, whole blood assays are found to be as effective as quantifications were done

using peripheral blood mononuclear cells.⁴⁵ It should also be noted that the collected blood storage time may impact the sensitivity of the assay as well. Hence, the detection of upregulation or downregulation of cytokines used is mainly a risk assessment tool. Overall, the nanoparticles did not upregulate the pro-inflammatory cytokines in the whole heparinized blood. The greatest change was observed for C5/C5a, and the trend observed is similar to what we have seen in ELISA as well, where PLA and Zymosan had resulted in the highest level of changes.

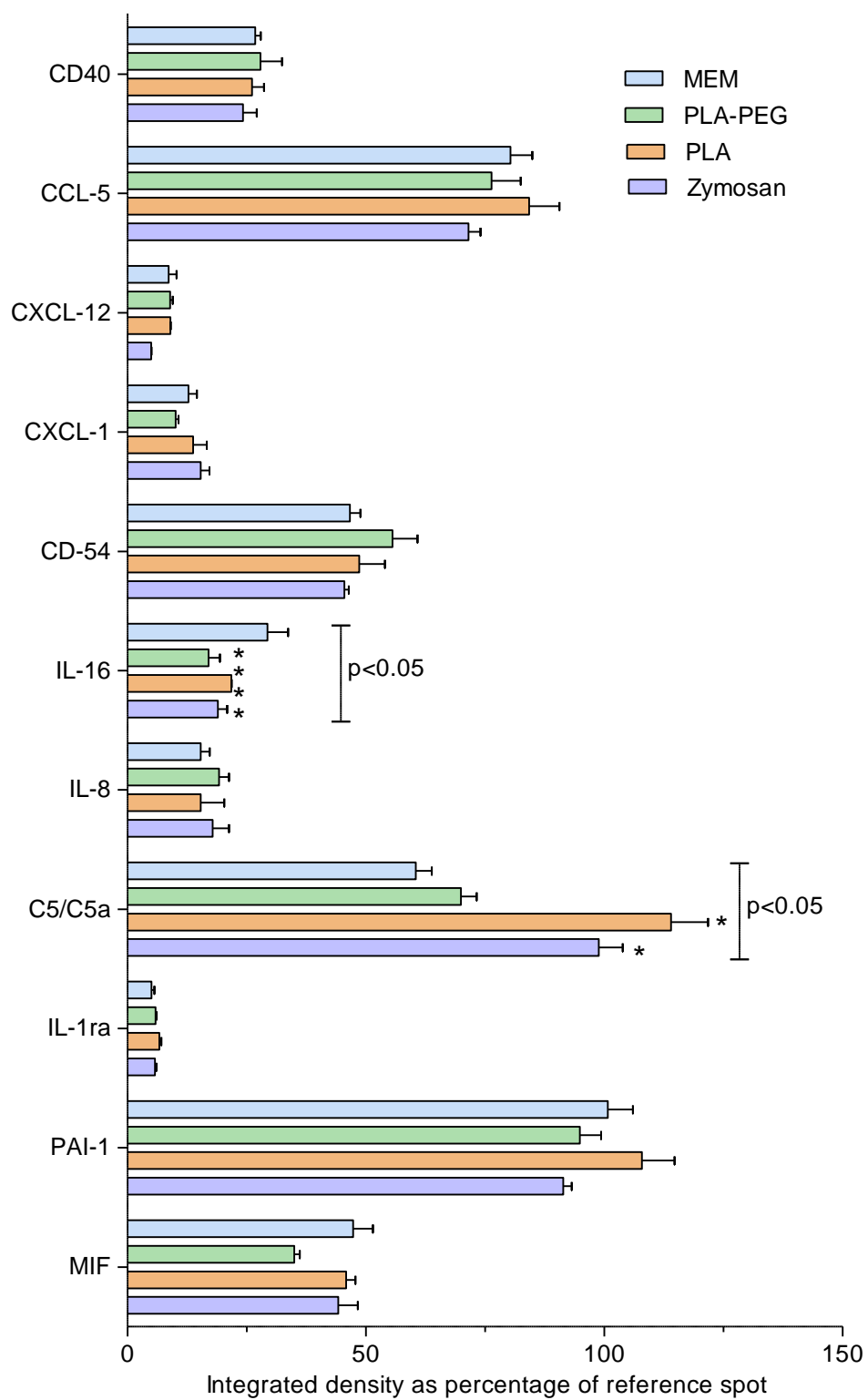


Figure 21: Impact of extent of PEGylation of nanoparticles on the cytokine levels in heparinized human whole blood.

Change in IL-6 for nanoparticles incubated with rat endothelial cells

We further quantified the changes in IL-6 levels when rat endothelial cells were incubated with PLA and PLA-PEG nanoparticles. As a positive control, Zymosan was used, and resulted in the highest level of IL-6 observed. (Figure 22) The normalized change was calculated compared to the observations for rat endothelial cells incubated with MEM. The change was statistically significant as well based on the chi-square analysis resulting in $p < 0.05$. Both PLA and PLA-PEG nanoparticles did not lead to significant changes in IL-6, and the values remained even lower than the observation for the MEM.

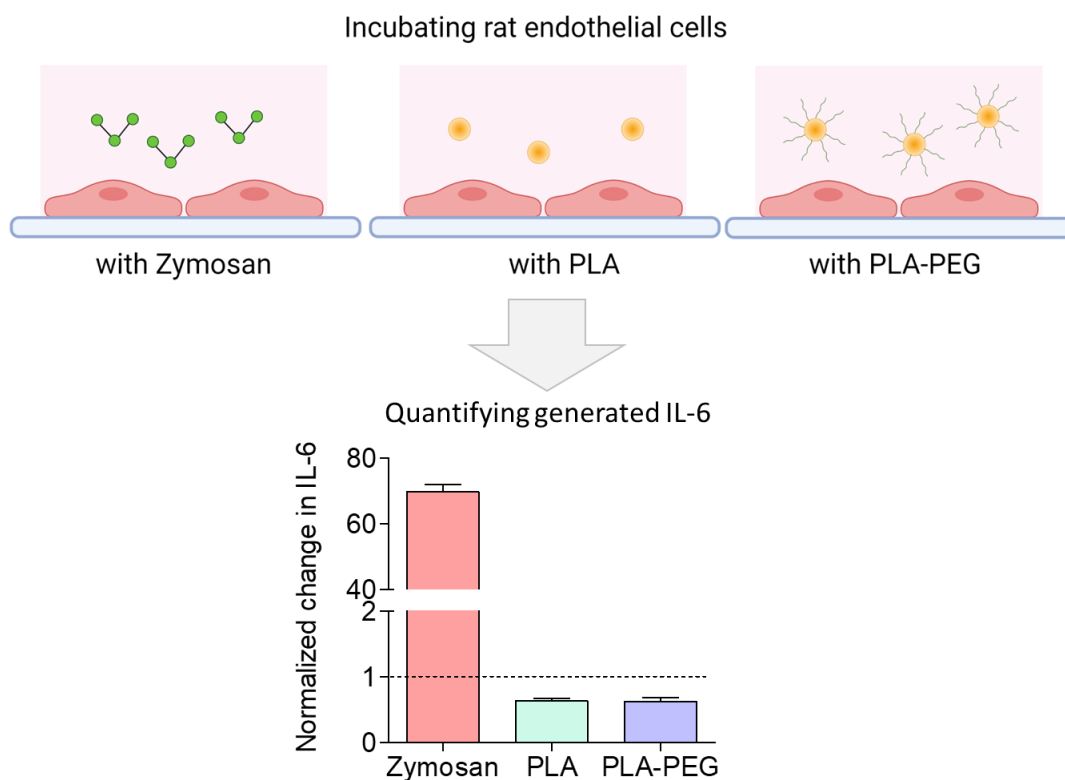


Figure 22: Change in IL-6 due to encounter of nanoparticles with rat endothelial cells.

The change in IL-6 was significantly higher for the positive control Zymosan but remained downregulated for the PLA and PLA-PEG nanoparticles.

Discussion

PEGylation has been essential in preventing aggregation of nanoparticles, opsonization, and phagocytosis.⁴⁶ Due to the highly hydrophilic nature and chain flexibility, PEG chains of 2000Da can lower protein adsorption on poly(lactic acid) nanoparticles by 57%.²⁷ Our goal was to understand how the extent of PEGylation impacts changes in complement proteins and cytokines *in vitro*. We hypothesized that increasing the extent of PEGylation will lead to an impenetrable cloud-like

conformation covering maximum surface and impart stealth properties to develop nanoparticles that do not lead to complement-mediated infusion reactions. We also investigated the role PEG chain length plays in imparting the stealth property. The biomarker tracked *in vitro* was the complement protein C5a, the anaphylatoxin produced due to complement activation. We also quantified the pro-inflammatory cytokines and chemokines generated *in vitro* upon contact with blood matrices to further understand the crosstalk between the complement system and the immune system and what that may imply upon *in vivo* administration.

First, we generated nanoparticles with varied amounts of PEG on the surface. It is critical how PEG is attached to the nanoparticle. As adsorption is a reversible process, it can often lead to desorption and result in exposed nano surface, while covalent attachment can often lead to insufficient surface coverage.¹⁵ We prepared block copolymer of poly(lactic acid)-*b*-poly(ethylene glycol) with the heterobifunctional PEG as the macroinitiator through ring-opening polymerization.²⁸⁻²⁹ By mixing ratios of PLA and PLA-*b*-PEG, we generated nanoparticles with different extents of PEGylation. The extent was a measure of the density of the PEG corona. The highest density conformation was for the nanoparticle formulation with a combination of PLLA-*b*-PEG and PDLA-*b*-PEG.

Upon quantifying the biomarker C5a *in vitro*, we found the C5a levels were lowest for nanoparticles with the greatest extent of PEGylation. The density of surface graft is a crucial component of surface protein adsorption and subsequent complement activation. As the surface density changes from mushroom-like lateral

chains to brush-like conformations, nanoparticles lead to lower complement activation products.²⁵ The brush conformation can be confirmed even for the lowest density, which leads to a 4.8wt% PEG on the nanoparticles. In the case of PLGA-PEG nanoparticles with 3wt% PEG on the surface, a brush configuration was observed, with the brush getting denser for 5wt% PEG.⁴⁶ While PEGylation can reduce the biomolecule adsorption it cannot prevent it entirely. Compared to bare PLA nanoparticles with the most significant change in C5a levels, all the PEGylated nanoparticles resulted in lower complement activation, .i.e., generation of biomarker C5a. Hence, we identified that increased PEGylation leads to the lowest complement protein adsorption and subsequent complement activation *in vitro*. This agrees with our previous observation of PLGA-PLL-PEG nanoparticles with 10-15% PEGylation⁴⁷ showing higher levels of C5a as well *in vitro*.³⁰

As we figured out that combining PLLA-b-PEG and PDLA-b-PEG resulted in the lowest complement activation, quantified through the change in biomarker C5a, we investigated the role PEG chain length plays. While it may seem that the longer the chain, the higher the flexibility would lead to better repulsion, the range above 5000Da has shown no significant decrease in plasma protein adsorption.²⁷ Whereas, as PEG chain length increased from 2000Da to 5000Da, 50% reduction was seen in adsorbed protein amounts.²⁷ Based on the pattern, we investigated whether increasing PEG chain length from 3400Da to 5000Da would reduce the change in complement protein C5a. The C5a detected in samples incubated with 5000Da PEG was lowest in both blood and serum. At the same time, we also explored the approach of combining

two different PEG lengths. The concept has been applied for microbubbles, the shorter PEG layer leading to steric repulsion prohibiting the approach and adhesion of opsonin, lipoproteins, and other liposomes, and the more extended layer of PEG providing target specificity.⁴⁸ Recently, PEG pairing has also been explored to support longer chains with the shorter chains and project the longer chains further to prevent protein surface adsorption.⁴⁹ We found that in combining 5000Da PEG and 3400Da PEG, the impact of chain length of the PEG present in a higher ratio was dominant. When the ratio of 5000Da PEG to 3400Da PEG increased, the complement protein C5a detected decreased in both blood and serum.

We tracked how cytokine levels change *in vitro* in heparinized human whole blood to validate the stealth property of the nanomaterial surfaces. The physiological properties of nanoparticles and the cytokine profiles observed are mostly related.¹⁴ Understanding how the changing PEGylation impacts cytokine levels can help further engineering the nanoparticles to evade complement-mediated infusion reactions. Complement proteins like C5a can stimulate Plasminogen activator inhibitor-1 (PAI-1) leading to vascular injury.⁵⁰ The release of cytokines has been detected for several nanoformulations as well. Iron-based nanomedicine and carbon nanotubes depending on the physicochemical properties of the final formulation, can lead to an elevation in IFN- γ and TNF- α along with IL-1 β .⁵¹⁻⁵³ We did not detect any changes in the mentioned pro-inflammatory cytokines that are found to be elevated for the iron and carbon nanotubes. For the detected cytokines, the levels observed are not significantly different in heparinized human whole blood compared to the observations for the

negative control MEM, showing statistically significant differences mainly for the complement protein C5/C5a only. Based on our observations, immediately after nanoparticles encounter blood, the cytokine levels do not change significantly for the pro-inflammatory cytokines in whole heparinized blood. On further assessment with rat endothelial cells, we determined that the cytokine IL-6, a potent biomarker of inflammation was upregulated for zymosan, however it remained downregulated for the PLA and PLA-PEG nanoparticles.

While nanoparticle PEGylation primarily increases blood circulation time and prevents opsonization, it can be utilized to inhibit complement-mediated infusion reactions as well. Since surface architecture is crucial for surface coverage and subsequent cloud-like conformation that can reduce protein adsorption, we worked on tracking this change with changing amount of PEG on the surface. Once we figured that higher PEGylation leads to lesser complement activation, we investigated the role PEG chain length plays in further extending that stealth property. Looking into the cytokine profiles, we get a picture of the pro and anti-inflammatory chemokines that are elevated or downregulated upon nanoparticles encountering blood. Further incorporating the nanoparticle core role and similarly exploring coatings other than PEG, along with this study, can be vital to developing nanoparticles that do not lead to complement-mediated infusion reactions upon intravenous administration.

Conclusion

We have developed a study to track the impact of PEGylation on complement activation *in vitro*. To achieve that, we quantified the changes in anaphylatoxin C5a, produced upon complement activation, as a biomarker. We utilized block copolymers of PLA-b-PEG to generate the nanoparticles. The highest possible PEGylation with this block copolymer led to the least amount of C5a detected in the blood *in vitro*. We investigated the impact of PEG chain length as well. The increasing PEG length from 3400Da to 5000Da leads to the least amount of C5a within the sample *in vitro*. How PEG pairing impacted the change in C5a was intriguing as we can leverage this to design stealth nanoparticles with better targeting capability. Lastly, we generated the cytokine profiles *in vitro* for these nanoparticles to mark the chemokines critical in the inflammation process. As nanoparticles' physiochemical properties are essential regulators of the interaction between the nanomaterials and blood proteins, we can further extend this study to include the nanoparticle core's role. Combining the knowledge gathered can lead to the detection of the properties that strengthen the stealth behavior to prevent nanotherapeutics' complement-mediated infusion reactions once they encounter blood proteins.

Acknowledgements

This work was supported by the AIMM Research award (DOD) (Award Number# W81XWH1820061) for developing intravenously infusible nanoparticles to stop bleeding and increase survival following trauma. We would like to thank

Binapani Mahaling for providing the PLA nanoparticles. Some of the figures were created with Biorender.com.

References

1. Szebeni, J.; Simberg, D.; Gonzalez-Fernandez, A.; Barenholz, Y.; Dobrovolskaia, M. A., Roadmap and strategy for overcoming infusion reactions to nanomedicines. *Nat Nanotechnol* **2018**, *13* (12), 1100-1108 DOI: 10.1038/s41565-018-0273-1.
2. Fulop, T.; Kozma, G. T.; Vashegyi, I.; Meszaros, T.; Rosivall, L.; Urbanics, R.; Storm, G.; Metselaar, J. M.; Szebeni, J., Liposome-induced hypersensitivity reactions: Risk reduction by design of safe infusion protocols in pigs. *J Control Release* **2019**, *309*, 333-338 DOI: 10.1016/j.jconrel.2019.07.005.
3. Szebeni, J., Hemocompatibility testing for nanomedicines and biologicals: predictive assays for complement mediated infusion reactions. *European Journal of Nanomedicine* **2012**, *4* (1), DOI: 10.1515/ejnm-2012-0002.
4. Szeto, G. L.; Lavik, E. B., Materials design at the interface of nanoparticles and innate immunity. *J Mater Chem B* **2016**, *4* (9), 1610-1618 DOI: 10.1039/C5TB01825K.
5. Ritz, S.; Schottler, S.; Kotman, N.; Baier, G.; Musyanovych, A.; Kuharev, J.; Landfester, K.; Schild, H.; Jahn, O.; Tenzer, S.; Mailander, V., Protein corona of nanoparticles: distinct proteins regulate the cellular uptake. *Biomacromolecules* **2015**, *16* (4), 1311-21 DOI: 10.1021/acs.biomac.5b00108.
6. Dunkelberger, J. R.; Song, W. C., Complement and its role in innate and adaptive immune responses. *Cell Res* **2010**, *20* (1), 34-50 DOI: 10.1038/cr.2009.139.

7. Noris, M.; Remuzzi, G., Overview of complement activation and regulation. *Semin Nephrol* **2013**, 33 (6), 479-92 DOI: 10.1016/j.semnephrol.2013.08.001.
8. Merle, N. S.; Church, S. E.; Fremeaux-Bacchi, V.; Roumenina, L. T., Complement System Part I - Molecular Mechanisms of Activation and Regulation. *Front Immunol* **2015**, 6, 262 DOI: 10.3389/fimmu.2015.00262.
9. Benjamini, E., *Immunology: a short course*. Vol. 77.
10. Harboe, M.; Mollnes, T. E., The alternative complement pathway revisited. *J Cell Mol Med* **2008**, 12 (4), 1074-84 DOI: 10.1111/j.1582-4934.2008.00350.x.
11. Petersen, S. V.; Thiel, S.; Jensenius, J. C., The mannan-binding lectin pathway of complement activation: biology and disease association. *Molecular immunology* **2001**, 38 (2-3), 133-149 DOI: 10.1016/s0161-5890(01)00038-4.
12. Peng, Q.; Li, K.; Sacks, S. H.; Zhou, W., The role of anaphylatoxins C3a and C5a in regulating innate and adaptive immune responses. *Inflammation & Allergy-Drug Targets (Formerly Current Drug Targets-Inflammation & Allergy)* **2009**, 8 (3), 236-246 DOI: 10.2174/187152809788681038.
13. Ember, J.; Jagels, M.; Hugli, T.; Volanakis, J.; Frank, M., The human complement system in health and disease. *Marcel Dekker* **1998**, 241-84.
14. Elsabahy, M.; Wooley, K. L., Cytokines as biomarkers of nanoparticle immunotoxicity. *Chem Soc Rev* **2013**, 42 (12), 5552-76 DOI: 10.1039/c3cs60064e.
15. Owens III, D. E.; Peppas, N. A., Opsonization, biodistribution, and pharmacokinetics of polymeric nanoparticles. *International journal of pharmaceutics* **2006**, 307 (1), 93-102.

16. Jeon, S.; Lee, J.; Andrade, J.; De Gennes, P., Protein—surface interactions in the presence of polyethylene oxide: I. Simplified theory. *Journal of colloid and interface science* **1991**, *142* (1), 149-158.
17. Torchilin, V.; Papisov, M., Why do polyethylene glycol-coated liposomes circulate so long?: Molecular mechanism of liposome steric protection with polyethylene glycol: Role of polymer chain flexibility. *Journal of liposome research* **1994**, *4* (1), 725-739.
18. Harris, J. M.; Chess, R. B., Effect of pegylation on pharmaceuticals. *Nat Rev Drug Discov* **2003**, *2* (3), 214-21 DOI: 10.1038/nrd1033.
19. Gabizon, A.; Martin, F., Polyethylene glycol-coated (pegylated) liposomal doxorubicin. *Drugs* **1997**, *54* (4), 15-21.
20. Vert, M.; Domurado, D., Poly(ethylene glycol): protein-repulsive or albumin-compatible? *J Biomater Sci Polym Ed* **2000**, *11* (12), 1307-17 DOI: 10.1163/156856200744345.
21. Simon, J.; Wolf, T.; Klein, K.; Landfester, K.; Wurm, F. R.; Mailander, V., Hydrophilicity Regulates the Stealth Properties of Polyphosphoester-Coated Nanocarriers. *Angew Chem Int Ed Engl* **2018**, *57* (19), 5548-5553 DOI: 10.1002/anie.201800272.
22. Kang, B.; Okwieka, P.; Schottler, S.; Winzen, S.; Langhanki, J.; Mohr, K.; Opatz, T.; Mailander, V.; Landfester, K.; Wurm, F. R., Carbohydrate-Based Nanocarriers Exhibiting Specific Cell Targeting with Minimum Influence from the

Protein Corona. *Angew Chem Int Ed Engl* **2015**, *54* (25), 7436-40 DOI:

10.1002/anie.201502398.

23. Papini, E.; Tavano, R.; Mancin, F., Opsonins and Dysopsonins of Nanoparticles: Facts, Concepts, and Methodological Guidelines. *Front Immunol* **2020**, *11*, 567365 DOI: 10.3389/fimmu.2020.567365.
24. Li, M.; Jiang, S.; Simon, J.; Passlick, D.; Frey, M. L.; Wagner, M.; Mailander, V.; Crespy, D.; Landfester, K., Brush Conformation of Polyethylene Glycol Determines the Stealth Effect of Nanocarriers in the Low Protein Adsorption Regime. *Nano Lett* **2021**, *21* (4), 1591-1598 DOI: 10.1021/acs.nanolett.0c03756.
25. Hamad, I.; Al-Hanbali, O.; Hunter, A. C.; Rutt, K. J.; Andresen, T. L.; Moghimi, S. M., Distinct polymer architecture mediates switching of complement activation pathways at the nanosphere– serum interface: implications for stealth nanoparticle engineering. *ACS nano* **2010**, *4* (11), 6629-6638.
26. Coty, J. B.; Eleamen Oliveira, E.; Vauthier, C., Tuning complement activation and pathway through controlled molecular architecture of dextran chains in nanoparticle corona. *Int J Pharm* **2017**, *532* (2), 769-778 DOI: 10.1016/j.ijpharm.2017.04.048.
27. Gref, R.; Lück, M.; Quellec, P.; Marchand, M.; Dellacherie, E.; Harnisch, S.; Blunk, T.; Müller, R., ‘Stealth’corona-core nanoparticles surface modified by polyethylene glycol (PEG): influences of the corona (PEG chain length and surface density) and of the core composition on phagocytic uptake and plasma protein adsorption. *Colloids and Surfaces B: Biointerfaces* **2000**, *18* (3-4), 301-313.

28. Connor, E. F.; Nyce, G. W.; Myers, M.; Möck, A.; Hedrick, J. L., First Example of N-Heterocyclic Carbenes as Catalysts for Living Polymerization: Organocatalytic Ring-Opening Polymerization of Cyclic Esters. *Journal of the American Chemical Society* **2002**, *124* (6), 914-915 DOI: 10.1021/ja0173324.
29. Lashof-Sullivan, M.; Holland, M.; Groynom, R.; Campbell, D.; Shoffstall, A.; Lavik, E., Hemostatic Nanoparticles Improve Survival Following Blunt Trauma Even after 1 Week Incubation at 50 (°)C. *ACS biomaterials science & engineering* **2016**, *2* (3), 385-392 DOI: 10.1021/acsbiomaterials.5b00493.
30. Maisha, N.; Coombs, T.; Lavik, E., Development of a Sensitive Assay to Screen Nanoparticles in Vitro for Complement Activation. *ACS Biomaterials Science & Engineering* **2020**, *6* (9), 4903-4915 DOI: 10.1021/acsbiomaterials.0c00722.
31. Lategan, K.; Alghadi, H.; Bayati, M.; de Cortalezzi, M. F.; Pool, E., Effects of Graphene Oxide Nanoparticles on the Immune System Biomarkers Produced by RAW 264.7 and Human Whole Blood Cell Cultures. *Nanomaterials (Basel)* **2018**, *8* (2), DOI: 10.3390/nano8020125.
32. Del Tordello, E.; Bottini, S.; Muzzi, A.; Serruto, D., Analysis of the regulated transcriptome of *Neisseria meningitidis* in human blood using a tiling array. *J Bacteriol* **2012**, *194* (22), 6217-32 DOI: 10.1128/JB.01055-12.
33. Kirschfink, M.; Mollnes, T. E., Modern complement analysis. *Clin Diagn Lab Immunol* **2003**, *10* (6), 982-9 DOI: 10.1128/cdli.10.6.982-989.2003.
34. Yang, S.; McGookey, M.; Wang, Y.; Cataland, S. R.; Wu, H. M., Effect of blood sampling, processing, and storage on the measurement of complement

activation biomarkers. *Am J Clin Pathol* **2015**, *143* (4), 558-65 DOI:

10.1309/AJCPXPD7ZQXNTIAL.

35. Ekdahl, K. N.; Fromell, K.; Mohlin, C.; Teramura, Y.; Nilsson, B., A human whole-blood model to study the activation of innate immunity system triggered by nanoparticles as a demonstrator for toxicity. *Science and technology of advanced materials* **2019**, *20* (1), 688-698 DOI: 10.1080/14686996.2019.1625721.

36. Bexborn, F.; Engberg, A. E.; Sandholm, K.; Mollnes, T. E.; Hong, J.; Nilsson Ekdahl, K., Hirudin versus heparin for use in whole blood in vitro biocompatibility models. *J Biomed Mater Res A* **2009**, *89* (4), 951-9 DOI: 10.1002/jbm.a.32034.

37. Horiuchi, T.; Tsukamoto, H., Complement-targeted therapy: development of C5- and C5a-targeted inhibition. *Inflamm Regen* **2016**, *36*, 11 DOI: 10.1186/s41232-016-0013-6.

38. Cruikshank, W. W.; Kornfeld, H.; Center, D. M., Interleukin-16. *Journal of leukocyte biology* **2000**, *67* (6), 757-766.

39. Mathy, N.; Scheuer, W.; Lanzendörfer, M.; Honold, K.; Ambrosius, D.; Norley, S.; Kurth, R., Interleukin-16 stimulates the expression and production of pro-inflammatory cytokines by human monocytes. *Immunology* **2000**, *100* (1), 63-69.

40. Arend, W. P., The balance between IL-1 and IL-1Ra in disease. *Cytokine & growth factor reviews* **2002**, *13* (4-5), 323-340.

41. Lappegard, K. T.; Christiansen, D.; Pharo, A.; Thorgersen, E. B.; Hellerud, B. C.; Lindstad, J.; Nielsen, E. W.; Bergseth, G.; Fadnes, D.; Abrahamsen, T. G.; Hoiby, E. A.; Schejbel, L.; Garred, P.; Lambris, J. D.; Harboe, M.; Mollnes, T. E., Human

genetic deficiencies reveal the roles of complement in the inflammatory network:

lessons from nature. *Proc Natl Acad Sci U S A* **2009**, *106* (37), 15861-6 DOI:

10.1073/pnas.0903613106.

42. Katz, M. G.; Gubara, S. M.; Bridges, C. R.; Hajjar, R. J.; Fargnoli, A. S.,
Gene and protein-based therapies for improving cardiac performance and
regeneration. In *Emerging Technologies for Heart Diseases*, Elsevier: 2020; pp 311-
332.

43. Berahovich, R. D.; Zabel, B. A.; Lewen, S.; Walters, M. J.; Ebsworth, K.;
Wang, Y.; Jaen, J. C.; Schall, T. J., Endothelial expression of CXCR7 and the
regulation of systemic CXCL12 levels. *Immunology* **2014**, *141* (1), 111-22 DOI:
10.1111/imm.12176.

44. Lolis, E.; Bucala, R., Macrophage migration inhibitory factor. *Expert opinion
on therapeutic targets* **2003**, *7* (2), 153-164.

45. Silva, D.; Ponte, C. G.; Hacker, M. A.; Antas, P. R., A whole blood assay as a
simple, broad assessment of cytokines and chemokines to evaluate human immune
responses to Mycobacterium tuberculosis antigens. *Acta Trop* **2013**, *127* (2), 75-81
DOI: 10.1016/j.actatropica.2013.04.002.

46. Suk, J. S.; Xu, Q.; Kim, N.; Hanes, J.; Ensign, L. M., PEGylation as a strategy
for improving nanoparticle-based drug and gene delivery. *Adv Drug Deliv Rev* **2016**,
99 (Pt A), 28-51 DOI: 10.1016/j.addr.2015.09.012.

47. Onwukwe, C.; Maisha, N.; Holland, M.; Varley, M.; Groynom, R.; Hickman,
D.; Uppal, N.; Shoffstall, A.; Ustin, J.; Lavik, E., Engineering Intravenously

Administered Nanoparticles to Reduce Infusion Reaction and Stop Bleeding in a Large Animal Model of Trauma. *Bioconjugate chemistry* **2018**, 29 (7), 2436-2447 DOI: 10.1021/acs.bioconjchem.8b00335.

48. Kim, D. H.; Klibanov, A. L.; Needham, D., The influence of tiered layers of surface-grafted poly (ethylene glycol) on receptor– ligand-mediated adhesion between phospholipid monolayer-stabilized microbubbles and coated glass beads. *Langmuir* **2000**, 16 (6), 2808-2817.

49. Pannuzzo, M.; Esposito, S.; Wu, L. P.; Key, J.; Aryal, S.; Celia, C.; di Marzio, L.; Moghimi, S. M.; Decuzzi, P., Overcoming Nanoparticle-Mediated Complement Activation by Surface PEG Pairing. *Nano Lett* **2020**, 20 (6), 4312-4321 DOI: 10.1021/acs.nanolett.0c01011.

50. Wojta, J.; Kaun, C.; Zorn, G.; Ghannadan, M.; Hauswirth, A. W.; Sperr, W. R.; Fritsch, G.; Printz, D.; Binder, B. R.; Schatzl, G., C5a stimulates production of plasminogen activator inhibitor-1 in human mast cells and basophils. *Blood, The Journal of the American Society of Hematology* **2002**, 100 (2), 517-523.

51. Andersen, A. J.; Wibroe, P. P.; Moghimi, S. M., Perspectives on carbon nanotube-mediated adverse immune effects. *Adv Drug Deliv Rev* **2012**, 64 (15), 1700-5 DOI: 10.1016/j.addr.2012.05.005.

52. Murphy, F. A.; Schinwald, A.; Poland, C. A.; Donaldson, K., The mechanism of pleural inflammation by long carbon nanotubes: interaction of long fibres with macrophages stimulates them to amplify pro-inflammatory responses in mesothelial cells. *Part Fibre Toxicol* **2012**, 9, 8 DOI: 10.1186/1743-8977-9-8.

53. Verhoef, J. J.; de Groot, A. M.; van Moorsel, M.; Ritsema, J.; Beztsinna, N.; Maas, C.; Schellekens, H., Iron nanomedicines induce Toll-like receptor activation, cytokine production and complement activation. *Biomaterials* **2017**, *119*, 68-77.

Chapter 5: Designing polyurethane-based hemostatic nanocapsules to evade complement-mediated initial infusion reactions

* The material in this chapter has been submitted for review. Maisha, N., Rubenstein, M., Bieberich, C., & Lavik, E.* Hemostatic nanocapsules to control bleeding and circumvent infusion reactions (2021)

Abstract

Hemostatic nanomaterials have the potential of increasing survivability after traumatic injuries, which is a leading cause of death for people under 46. However, like many other intravenously administered nanomaterials, hemostatic nanomaterials can also lead to complement-mediated infusion reactions. While rare, such hypersensitivity is observed in about 10% of the population. The response itself leads to significant morbidity, increased healthcare costs, and the inability to take the nanoparticles to avoid adverse reactions despite its better therapeutic effects in susceptible patients. As materials properties and surface architecture are some of the governing factors on how the blood proteins and the nanoparticles interact, we have developed a polyurethane-based nanocapsule system that could be designed as a hemostatic nanomaterial while evading complement-mediated initial infusion reaction. We have utilized *in vitro* screening tools to validate that the polyurethane

nanocapsules with and without PEGylation do not activate the complement pathways. We have also evaluated the hemostatic activity of these nanocapsules *in vitro* using ROTEM-based coagulation assays. This study is a critical step in developing hemostatic polyurethane nanocapsules for traumatic injuries, especially before starting *in vivo* studies in small and large animal trauma models, and making the nanomaterials clinically translatable in the long run.

Introduction

With almost 30 to 40% of trauma mortality caused due to blood loss, and 33 to 56% of this percentage occurring during the prehospital period, trauma is a leading cause of death, especially for ages under 46.¹ The time immediately following trauma is critical, as, in case of blunt trauma, the ‘golden hour’ could be utilized for a positive impact to improve survival chances.²⁻³ An immediate on-field response can provide the scope of controlling exsanguination and saving lives by prolonging the time to move and stabilize the patient following catastrophic trauma incidents. Controlling hemorrhage is the first step in managing casualties. While first responders can play a role in controlling external bleeding through pressure, in case of internal bleeding, the application of intravenous hemostats is not possible until a medical facility is reached. Hemostatic nanoparticles are designed to mimic the role of fibrinogen consisting of a polymeric core, with poly(ethylene glycol) corona, with a peptide sequence GRGDS conjugated to it. The peptide motif binds with glycoprotein IIb/IIIa in the activated platelets and helps in forming clots faster to reduce bleeding.⁴

⁵ The nanoparticles effectively reduce bleeding and improve survival significantly in small animal models,⁵ and these can mitigate internal bleeding and improve the pathologic outcomes after traumatic brain injuries following blast trauma in small animals.⁶ However, it can trigger the complement system in large animal trauma models even at very low dosages.⁷ Our goal is to develop a non-complement triggering nanoparticle system for effectively transferring our hemostatic nanoparticle to large animal trauma models and eventually to the clinic.

The complement system is the first-in-line defense of the immune system against pathogens, and it is active at all times controlled by several complement regulators. However, uninhibited complement activation may eventually lead to inflammatory responses as severe as anaphylaxis, an acute life-threatening respiratory failure.⁸ As the complement system attacks all components that are not recognized as healthy or familiar, nanomedicines such as the hemostatic nanoparticles may elicit complement-mediated initial infusion reactions as well. Such immune response leads to vasodilation, increased tissue permeability, edema, and drastic fall in blood pressure leading to shock, and symptoms appear in minutes after exposure to an allergen and can occur within 30 minutes.⁹⁻¹⁰ While it is more reproducibly present in porcine animals, the complement-mediated response is observed in a particular part of the human population. A complement-mediated response incidence rate is 7% for humans, with a 0.3% chance of fatality.¹¹ Hence, while developing hemostatic nanoparticles, it would be crucial to ensure that the first infusion reaction can be avoided for successfully translating the nanoparticles to clinic.

As materials properties frequently dictate complement-surface interactions leading to the activation, this raises the question of whether these can be altered to achieve stealth properties. One of the earliest cases of complement mediated response was due to the liposomal formulation Doxil, an FDA approved PEGylated liposomal formulation of Doxorubicin, a chemotherapy drug for treating several types of malignancies.¹² Slower infusion rates and premedication with antihistamines and glucocorticoids, as well as repeated administration, can control the hypersensitivity reaction but not prevent it entirely.¹² The reaction itself leads to significant morbidity, increased healthcare costs, as well as the inability to take the nanoparticles to avoid adverse reactions despite its better therapeutic effects in highly sensitive patients.¹² Hypersensitivity reactions have also caused the withdrawal of few inorganic iron oxide nanoparticles used as contrast agents in imaging.¹³⁻¹⁴ Several liposomal and micellar formulations have shown infusion reactions as well after initial administration, with incidence ranging between 3% and 45%.¹¹ The structure of nanomaterials, as well as surface moieties, can impact surface protein adsorption. So, the choice of materials is critical in ensuring that initial infusion reactions can be avoided.

Polyurethane nanocapsules have the potential of being used as dental resins and bone cement encapsulating self-healing components.¹⁵ The materials properties and nanoparticle systems can be modified for controlled release triggered enzymatically,¹⁶ leveraging thermo-sensitivity¹⁷ or through pH,¹⁸ among many other probable stimuli. Polyurethane nanocapsules formed from macromers of Isophorone

diisocyanate (IPDI) and 1,6 hexanediol can be used to encapsulate therapeutics that are released on demand through sonication, most likely due to cavitation.¹⁹ Moreover, polyurethanes, especially with further surface modifications, impart biocompatibility²⁰ and hemocompatibility²¹, making them suitable prospects for the core material of nanoparticles intravenously administered. In our endeavor to find the properties of the materials that can prevent complement-mediated infusion reactions, we developed polyurethane-based nanocapsules. The nanocapsules' core was modified through PEGylation for later conjugating peptide motifs of interest. These nanocapsules can encapsulate therapeutics for targeted release using stimuli and increase the scope of further incorporating antioxidants and anti-inflammatory molecules. Our objective was to develop polyurethane hemostatic nanocapsules such that they do not lead to complement-mediated initial infusion reactions. As our validation tool during the early stages of development, we have used *in vitro* assays for quantifying the changes in complement proteins and detect changes in proinflammatory cytokines. Finally, we also evaluated the hemostatic efficacy through an *in vitro* coagulation assay to verify that the system can enhance clotting in the presence of activated platelets. This study is the first step in designing polyurethane-based hemostatic nanocapsules that would not lead to complement-mediated infusion reactions *in vivo*.

Materials and methods

Materials

For preparing the nanocapsules, monomers Isophorone diisocyanate (IPDI) 98% (ACROS Organics), 1,6-hexanediol (HDOH) 97% (ACROS Organics), surfactant Sodium dodecyl sulfate (SDS) (Fisher Scientific), and co-stabilizer 99% pure hexadecane we used without further purification. For bioconjugation, peptide motif GRGDS was obtained from Selleckchem (Houston, TX). N-hydroxy succinimide (NHS) and 1-Ethyl-3-(3-dimethylaminopropyl) carbodiimide (EDC) were obtained from Sigma Aldrich (Merck KGaA, Darmstadt, Germany).

Methods

Developing PEGylated polyurethane nanocapsules

First, PEGylated nanocapsules were prepared through interfacial polycondensation by modifying an existing method of preparing polyurethane nanocapsules.¹⁹ An oil-water emulsion was prepared using 1.1 g SDS dissolved in 70ml DI water and 1.145ml n-hexadecane. The oil-water emulsion was stirred at 40°C for 1 hour at 300rpm. To that 2.094 mL of IPDI mixed with 7ml DI water was added and stirred. As the IPDI solution entered the pre-emulsification solution, the stirring speed was increased to 400 rpm. The solution was mixed at 400 rpm and 40°C for 10 minutes. The solution was then sonicated using a 130-Watt Ultrasonic Processor with Thumb-actuated Pulser at an amplitude of 38% to break up any IPDI

molecules for 1 minute. Following immediately and still under sonication, over 40 seconds, an aqueous solution of 5.9 g of HDOH and 10 mL of DI water was added into the system. The reaction mixture was transferred to 40°C stirring at 300rpm. Immediately, HO-PEG-COOH/ HO-PEGm dissolved in DI water was added. The nanocapsules were collected through centrifugation at 10000rpm for 10 minutes, and then resuspended in DI water. This step was repeated two more times, for a total of three washes. The nanocapsules resuspended in DI water were flash frozen and lyophilized.

Characterization of the nanocapsules

Nanocapsules prepared were characterized to determine the size and zeta-potential using the Malvern ZetaSizer (Nano ZS90). The nanocapsules were resuspended in 190 proof ethanol for sizing. The zeta-potential was determined by resuspending the nanocapsules in 10 mM potassium chloride (KCl). Both the size and zeta potential measurements were run in triplicates

Determining amount of PEG in the nanocapsules

To determine the amount of PEG present, ¹H-NMR was used. The nanocapsules were resuspended in deuterated water and the peaks generated were used to calculate the moles of PEG present in the sample.

Conjugating with GRGDS peptide motif to develop hemostatic nanocapsules

The PEGylated nanocapsules were conjugated with the GRGDS peptide motif through NHS/EDC bioconjugation. First, nanocapsules resuspended in DI water were allowed to react with NHS and EDC in dissolved in DI water, where utilizing the carboxyl end group of the PEG, an intermediate complex is generated. The nanocapsules were collected by centrifugation to discard unreacted NHS and EDC, and then resuspended in DI water again. To that, GRGDS dissolved in DI water was added and through the primary amine of the peptide, the bioconjugation takes place. The nanocapsules were then collected through centrifugation, resuspended in DI water and flash frozen to lyophilize.

Quantifying amount of peptide through ortho-phthalaldehyde assay

The amount of peptide conjugated was calculated through ortho-phthalaldehyde assay. The compound ortho-phthalaldehyde in presence of mercaptoethanol reacts with primary amines to form a fluorophore that absorbs at 340nm and emits at 455nm. The optical densities were measured for blank and peptide conjugated nanocapsules in a fluorescent plate reader (Molecular Devices, SpectraMax M2). Based on the standard curve prepared, the amount of peptide within the samples were determined.

Generating complement response in vitro and quantification through complement assay

The change in complement protein C5a was quantified following previously established protocol.²² The blood matrix was incubated with nanoparticles suspended

in Dulbecco's PBS (without calcium and magnesium). As a positive control, Zymosan was used. The dosage used for the nanoparticles and Zymosan was 0.25mg/ml in serum. The samples were incubated at 37°C for 45 minutes and then centrifuged at 4000g for 5 minutes to separate the nanoparticles. The supernatant was aliquoted in clean tubes and stored on ice until assay was carried out using the C5a ELISA assay duo kit (R&D Systems). The optical density for the samples and standards were measured at a wavelength of 450 nm using SpectraMax M2 Microplate Reader (Molecular Devices LLC) with background correction done using reading obtained at 540 nm. The normalized change was measured by comparing the level of C5a observed in the sample incubated with PBS.

Normalized Change

$$= \frac{\text{Biomarker in sample incubated with Zymosan or nanoparticles}}{\text{Biomarker in sample incubated with PBS}}$$

Generating immune response in vitro and quantification through cytokine array

Nanoparticles resuspended in MEM were added to whole blood to reach a final concentration of 0.25mg/ml. The blood to the nanoparticle in MEM ratio was 5:1. The blood was gently pipetted with the nanoparticle resuspension and incubated for 45 minutes at 37 °C in a rotating shaker. Immediately after incubation, samples were placed on ice and then centrifuged at 4000G for 5 minutes. The supernatant plasma was collected in clean microcentrifuge tubes. For the cytokine array panel, 200µl of plasma was used to prepare samples following the protocol, and subsequent steps given in the protocol were followed for the human cytokine array panel (R&D

Systems). The final image was taken using a Bio-Rad imager. For further analysis, ImageJ was used. Integrated density gives the sum of total pixels within a region. Following this method, each dot blot within the membrane was quantified for each sample. The levels of the detected cytokines were expressed as a percentage of the pixel density determined for the reference spot.²³

Evaluating coagulation in vitro using whole blood through rotational thromboelastometry

To evaluate the coagulation in vitro, rodent blood collected through cardiac puncture was used. Using rotational thromboelastometry (ROTEM), the clotting time and clot formation time, and maximum clot firmness were determined. The groups in this study include: the vehicle (minimum essential media), control nanocapsules and hemostatic nanocapsules. The nanocapsules were resuspended in the minimum essential media, and the dosages investigated were 5mg/ml and 2.5mg/ml. The normalized changes were determined based on the values observed for the vehicle control.

Statistical analysis

We used Chi-square analysis to calculate the p-value within groups for the complement protein C5a. As the expected value, the C5a level for serum incubated with PBS or MEM was used. In case of the ROTEM data, t-test was used to determine the p-values between the two groups.

Results

Synthesis and characterization of PEGylated polyurethane nanocapsules

To develop hemostatic nanoparticles that do not lead to hypersensitivity reactions, we first prepared PEGylated polyurethane nanocapsules through interfacial polymerization by modifying a previously published protocol.^{19, 24} To achieve the hemostatic attribute, we then utilized NHS/EDC-based bioconjugation technique to conjugate the carboxyl end group of the exposed PEG on the nano surface with the primary amine group of the peptide motif GRGDS. (Figure 23) The method of preparing these nanocapsules is a modified form of synthesizing the on-demand and long-term drug delivery nanocapsules.¹⁹ So, there is further scope of encapsulating therapeutics within this system to target inflammation at the site of injury utilizing stimuli such as sonication.

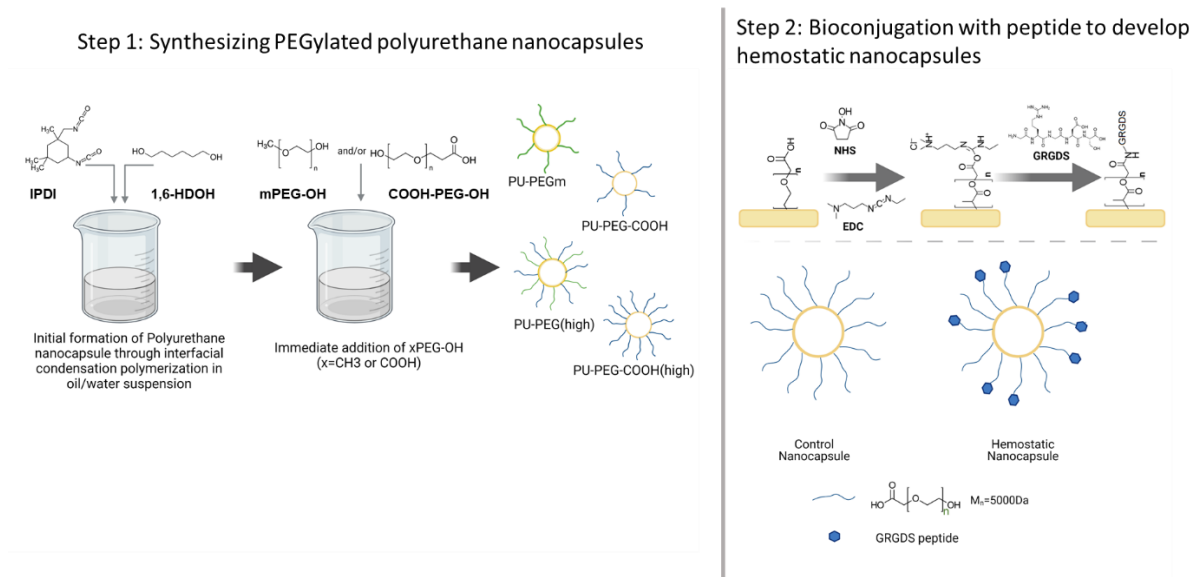


Figure 23: Synthesizing PEGylated polyurethane nanocapsules and consequent bioconjugation to prepare hemostatic nanocapsules. In the first step, polyurethane nanocapsules are synthesized through interfacial condensation polymerization between Isophorone diisocyanate (IPDI) in the oil phase and 1,6 hexanediol (1,6 HDOH) in the aqueous phase. Immediately adding poly(ethylene glycol) with hydroxyl end group allows conjugation of PEG chain to the surface. In the second step, hemostatic nanocapsules are prepared by utilizing NHS/EDC zero-length linkers; peptide motif GRGDS is conjugated to the carboxyl end groups present in the PEG chains.

We characterized the nanocapsules to determine the size and zeta-potential and to confirm the presence of PEG. The dynamic light scattering data for the nanocapsules show that the nanocapsules are close to 150-250 nm in size and the zeta-potential changes based on the surface composition. (figure 24 B) As previously observed,¹⁹ the nanocapsules in DLS show two peaks, with most nanocapsules in size range mentioned. A very small population of the nanocapsules appears with a smaller size of less than 10nm. As the nanocapsules are PEGylated, the zeta-potential increases from the highly negative zeta-potential of -47.3 mV observed in the non-PEGylated nanocapsules with increasing amount of PEG. The TEM of the nanocapsules was also consistent with the size of the particles observed in DLS. (Figure 24 C) As we modified the nanocapsules by PEGylation, we used ¹H-NMR to confirm the presence of the PEG and then quantify the amount present on the surface. To do that, we resuspended the lyophilized nanocapsules in deuterated water and used

the PEGylated and non-PEGylated samples to generate the peaks. The peak corresponding to PEG appears at 3.572ppm, which remains absent in the NMR peak for non-PEGylated polyurethane nanocapsules. (Supplementary figure 39-42). The moles of PEG in the sample are calculated compared to the IPDI moles in the sample based on the peak observed for its cyclohexyl ring at 1.41-1.42ppm. Increasing the amount of PEG to the synthesis leads to an increase in the amount of the chain conjugated to the surface (Figure 24 B).

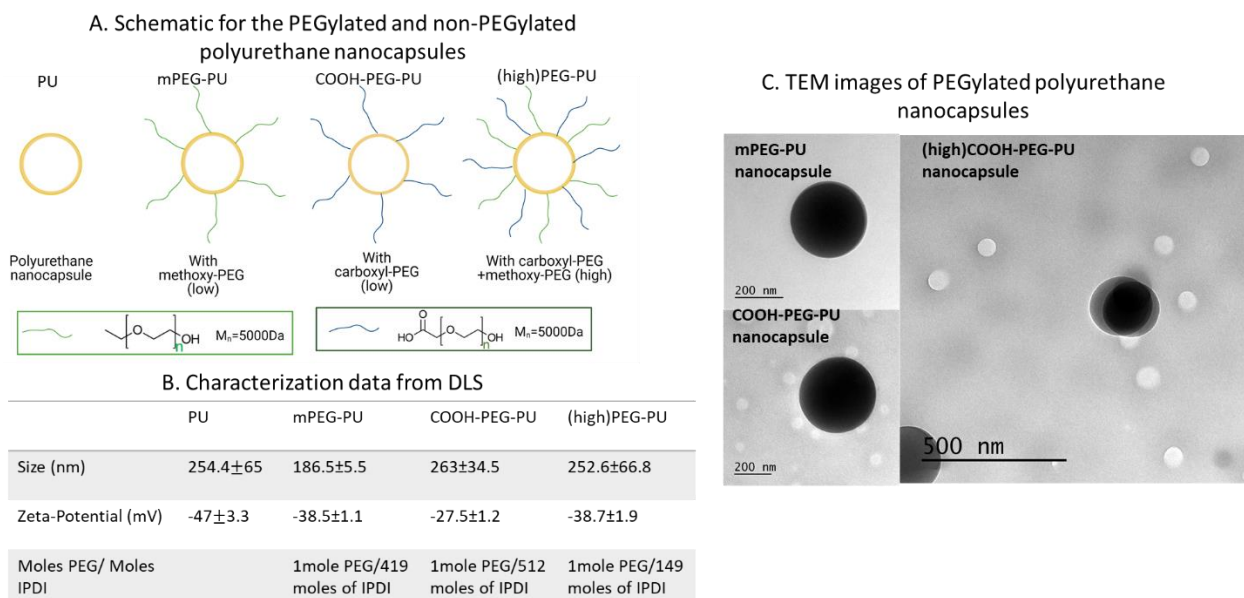


Figure 24: Characterization of PEGylated polyurethane nanocapsules. A. Schematic representation of polyurethane nanocapsules with and without PEGylation. B. A summary of the size and surface charge of the PEGylated and non-PEGylated nanocapsules. The presence of PEG was confirmed through ^1H -NMR in deuterated water. C. TEM images of the nanocapsules confirm the size observed through DLS.

Evaluating changes in complement protein C5a in vitro

To further confirm that the nanomaterials do not lead to hypersensitivity responses due to initial infusion reactions, we quantified how the complement proteins change in vitro. We incubated complement-protected human serum with the PEGylated and non-PEGylated nanocapsules based on our previously established protocol.²² The normalized change was determined compared to the C5a levels observed for complement-protected human serum incubated with PBS only. The change in complement protein remained least for the highly PEGylated polyurethane nanocapsule and the non-PEGylated nanocapsules. We observed the highest change for zymosan, a known complement activator,²⁵ and positive control in this study. In our previous study, we had established that PEGylation could help in controlling complement activation in vitro. For highly PEGylated polyurethane nanocapsules with a dual brush length of 5000Da PEG and 3400Da PEG, with the former molecular weight present at a higher ratio, the complement protein C5a changes the least. Moreover, bare PLA nanocapsules can lead to as much activation as observed for the complement activator zymosan. With the polyurethane nanocapsules, changes observed for both the PEGylated and non-PEGylated counterparts remained lower than the PEG-PLA nanocapsules and even close to the observed levels for the serum incubated with PBS only. (Figure 25) Hence, the polyurethane nanocapsules based on their in vitro findings should lead to the least level of changes in complement proteins upon contact with blood and avoid complement-mediated infusion reactions in vivo.

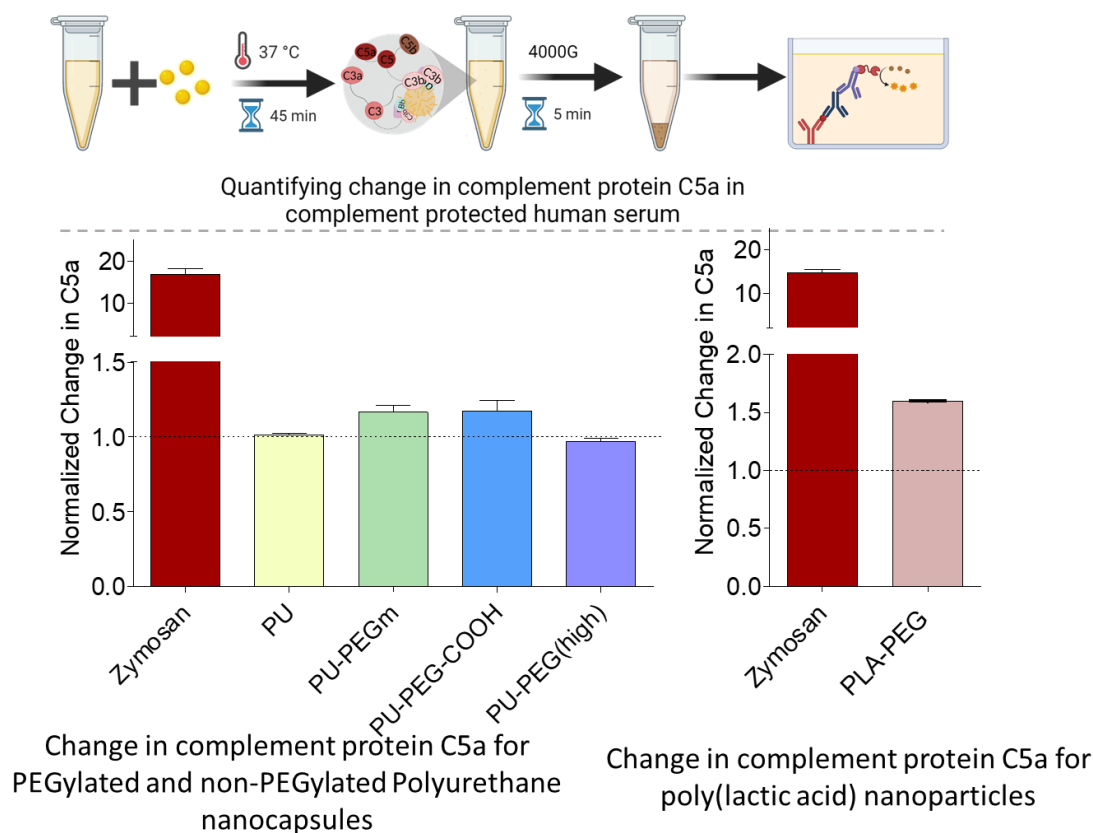


Figure 25: Quantifying complement protein in vitro for polyurethane nanocapsules.

Polyurethane nanocapsules lead to low levels of complement protein C5a in vitro.

Nanocapsules were incubated with complement protected human serum and incubated for 45 minutes at 37°C. The complement protein C5a was least for the non-PEGylated nanocapsules and the highly PEGylated nanocapsules.

Identifying the changes in cytokines in vitro upon incubation with polyurethane nanocapsules

Quantifying and detecting the pro-inflammatory cytokines when nanoparticles are incubated with blood is critical, as it would lead to a better mechanistic

understanding of hypersensitivity responses. To understand the crosstalk between the complement system and the immune system and its implication upon in vivo administration, we identified the inflammatory cytokines produced in vitro as the biological fluids encounter the nanocapsules. As a guide for comparing materials, both poly(lactic acid) and polyurethane-based nanomaterials were investigated. First, we detected the cytokines generated, and based on the integrated densities observed, the upregulation or downregulation was confirmed. This approach was more qualitative as the exact amounts of chemokines generated were not determined, but it was thorough as multiple cytokines could be screened simultaneously. As a control, the integrated pixel density for heparinized human whole blood incubated with MEM was used. The change in complement protein biomarker C5/C5a was most elevated for PLA, while the level remained close to control for the PU and PU-PEG (Figure 26). The other pro-inflammatory cytokines detected in the blood and had shown upregulation for at least one of the groups tested include IL-8 and IL-16. The levels detected for IL-8 remained close to observed level for MEM, while IL-16 observed was low for all the blood samples incubated with nanoparticles. The change in C5/C5a was significantly highest for Zymosan and PLA nanoparticles based on the Chi-square analysis. While PEGylation of PU nanocapsules slightly increased the C5/C5a levels, the C5/C5a levels were similar to the observation for PU nanocapsules and MEM for the PU-PEG-GRGDS nanoparticles.

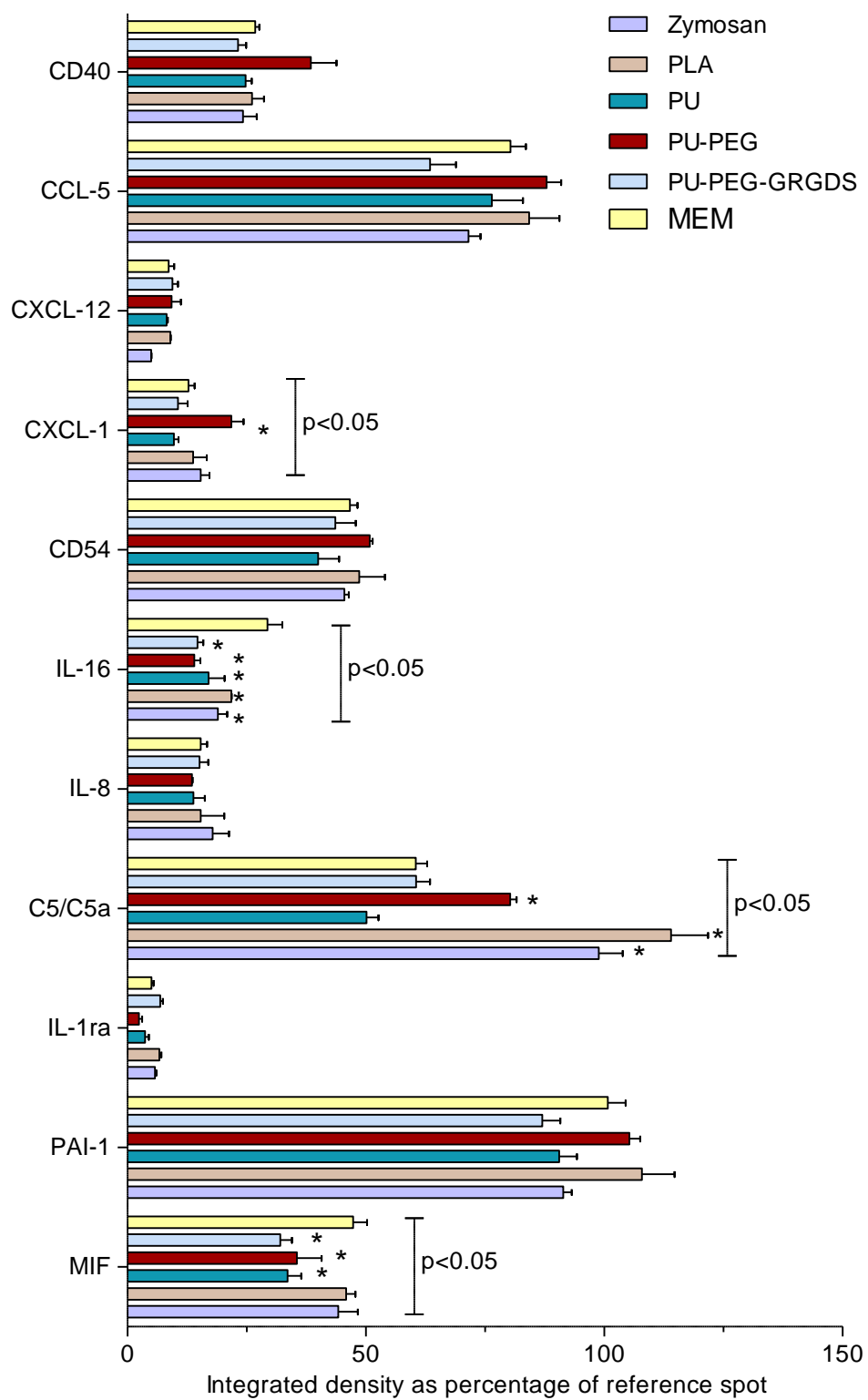


Figure 26: Normalized changes in the integrated pixel densities for the detected cytokines in vitro in heparinized human whole blood.

Validating the hemostatic activity through in vitro coagulation assay

As hemostatic nanocapsules are administered intravenously, the nanoparticles would immediately encounter blood proteins. As a result, the PEGylated polyurethane nanocapsules seem like a feasible choice based on the low levels of complement proteins detected in vitro. So, we utilized the PEGylated nanocapsules for conjugating the peptide motif GRGDS. We then evaluated the hemostatic activity of these nanocapsules in vitro. The in vitro coagulation assay was carried out using the NATEM test of ROTEM for citrated blood collected from Sprague-Dawley rats through cardiac puncture. The clotting time and clot formation time in total give the time required to reach a 20mm clot thickness, and that is used as a parameter in this study to understand how the hemostatic nanocapsules impact that. The vehicle solution, the minimum essential medium supplemented with l-glutamine only, was used as a control. The normalized change was determined compared to the vehicle control for the control nanocapsules without any peptide motif attached and the hemostatic nanocapsules. (Figure 27) The change was significantly different and lower for the hemostatic nanocapsules at a 5mg/ml concentration. At a lower concentration of 2.5mg/ml, the hemostatic nanocapsules still result in a lower value for normalized CT+CFT; however, the change is not significantly different. Therefore, the polyurethane-based hemostatic nanocapsules are not only able to avoid

complement-mediated infusion reactions but also able to display effective hemostatic activity.

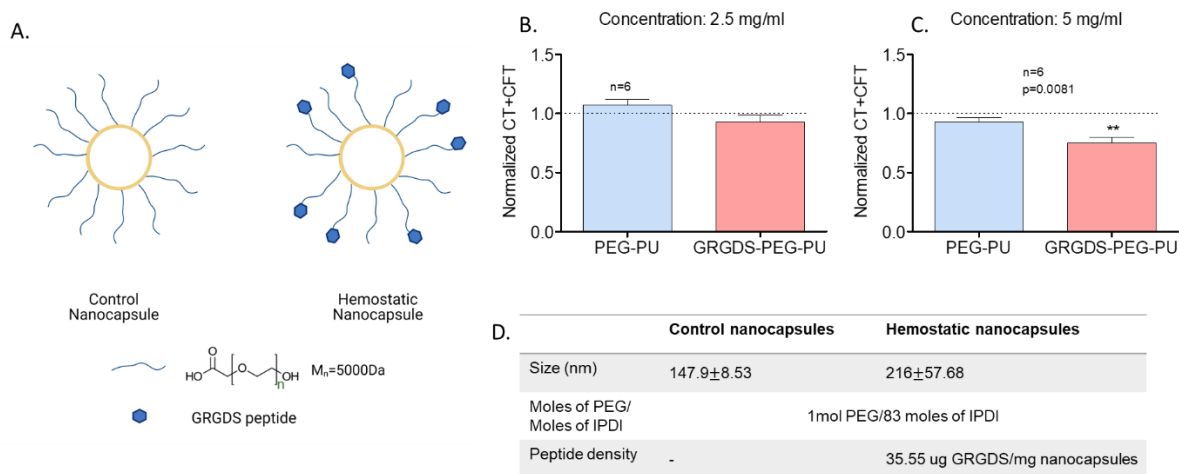


Figure 27: Evaluating the impact on coagulation in vitro. A. A schematic representation of the control and hemostatic nanocapsules. B. The clotting time was lower for the hemostatic nanocapsules at 2.5mg/ml concentration but not significantly different. C. The clotting time was the least for the hemostatic nanocapsules at 5mg/ml concentration and significantly different as evaluated using t-test.

Discussion

Nanoparticle upon intravenous infusion gets immediately engulfed in a protein corona, and the subsequent interaction can lead to complement-mediated hypersensitivity responses. This complement-mediated response, often termed an infusion reaction²⁶⁻²⁷, is of concern for nanoparticle systems broadly, including liposomal nanoformulation Doxil^{12, 28}, inorganic nanoparticles such as iron oxide and metallic nanoparticles used as contrast agents for imaging^{13, 29}, organic nanoparticles

such as poly(lactic-co-glycolic acid)-b-poly(ethylene glycol) and polystyrene^{7, 26, 30-31} based nanoparticles. The vast differences in materials and surface architecture indicate that materials properties impact this innate immune response.^{13, 29, 32-34} The hypersensitivity reaction is usually due to the first infusion, and as the system gets multiple exposures through subsequent bolus administrations, such reactions can be controlled.³⁵ However, for many nanoparticle infusions, the dosage must be high enough and delivered as a single bolus dose, where desensitization would not be possible. One such nanoparticle system is the hemostatic nanoparticles. The nanoparticles can reduce bleeding by almost 50% and significantly improve survival in major femoral artery injury models for rodents following intravenous administration.⁵ Moreover, the hemostatic nanoparticles are designed such that they are safe and stable at room temperature.³⁶ Administering the hemostatic nanoparticles after traumatic injury due to blasts can mitigate internal bleeding and improve the pathologic outcomes.⁶ However, the PLGA based hemostatic nanoparticles may lead to hypersensitivity reactions, especially in large animal models.⁷ Previous work with the hemostatic nanoparticle has shown that highly negative or highly positive nanoparticles cause complement activation leading to vasodilation.⁷ Tuning the zeta-potential of the nanoparticles modulated the hypersensitivity responses; however, the effectiveness in avoiding the complement activation was only within a low particle dosage range.⁷ Hence, there is a growing need for safer materials for nanomedicine that do not lead to initial infusion reactions, not only for the hemostatic nanoparticles but for nanomedicine in general that would be administered intravenously. To address

that, we have designed a polyurethane-based hemostatic nanocapsule system and evaluated the impact of polyurethane nanocapsules on complement activation and coagulation activity in vitro.

We prepared polyurethane nanocapsules by forming polyurethane linkages between aromatic isocyanate groups and aliphatic diols,¹⁹ and the materials based on the ratio of the hard and soft segments³⁷ present leads to soft rubbery elastomers. Polyurethane nanocapsules as drug delivery vehicles have gained popularity due to the scope of controlled release profile for therapeutics of interest utilizing stimuli. Based on the macromers selected to form the nanomaterial, there is scope to modulate the system to achieve biocompatibility.³⁷ One of the earlier polyurethane applications as a biomaterial is as coatings on the implant to release antibodies in a controlled manner while preventing pathogen colonization and virulence in implant sites.³⁸ Polyurethanes with different hard and soft segments and surface modifications have been investigated in the past for their hemocompatibility.²¹ We seek to understand whether polyurethane nanomaterials developed with the goal of intravenous administration would lead to complement-mediated hypersensitivity response. We assessed the change in complement protein C5a in vitro as a validation. As the complement pathways are activated, it results in the generation of C3 convertase, which triggers the release of anaphylatoxins C3a and C5a.¹⁰ The anaphylatoxins are pro-inflammatory and lead to degranulation of mast cells and production of histamines,^{9, 39} vasodilation, increased permeability of blood vessels⁴⁰ among some of many impacts of complement activation. We compared the polyurethane-based

systems with and without PEGylation to poly(lactic acid) based nanomaterials which are more prone to complement activation. We found that compared to highly reactive poly(lactic acid) cores, both PEGylated and non-PEGylated polyurethane lead to the least amount of complement protein C5a. The levels remained close to the observations in heparinized human whole blood incubated with PBS. Compared to previous studies involving PLGA-PLL-PEG hemostatic nanomaterials, where signs of complement activation were observed *in vivo*⁷, the change in complement protein C5a was 3-4 folds higher *in vitro*²² as well. As a result, the lesser complement activation *in vitro* indicates that the polyurethane nanoparticles could be expected to modulate the initial infusion reaction *in vivo*, making the system translatable and suitable for the hemostatic nano-systems.

We have also evaluated the impact of the nanomaterials in generating pro-inflammatory cytokines mainly through cytokine arrays to understand the cytokines that change *in vitro* upon incubation with the nanocapsules, specifically in whole heparinized blood. When blood encounters nanoparticles, distinct complement proteins can further exacerbate inflammation, which could be detected from the generated pro-inflammatory cytokines. For example, complement protein C5a can stimulate Plasminogen activator inhibitor-1 (PAI-1) production and lead to vascular injury.⁴¹ Some of the iron-based nanomedicine depending on the physicochemical properties of the final formulation can lead to an elevation in IL-1 β and IL-6.⁴² Some of the other mediators of inflammation includes the cytokines IFN- γ and TNF- α along with IL-1 β generated at higher amounts *in vitro* from lymphocytes due to carbon

nanotubes.⁴³ Moreover, IL-1 β , TNF α , IL-6, and IL-8 are found to be upregulated from mesothelial cells and THP-1 macrophages upon incubation with carbon nanotubes as well.⁴⁴ We tracked whether the polyester and polyurethane-based organic nanoparticles lead to the releasing pro-inflammatory entities in vitro from whole blood. Of the cytokines observed after incubating heparinized human whole blood with the nanocapsules, other than the complement protein C5/C5a, pro-inflammatory biomarkers IL-8 and IL-16 were detected. IL-16 remained downregulated while IL-8 remained in similar levels to MEM. The pro-inflammatory cytokines IL-6, IL-1 β , IFN- γ , and TNF- α , were not detected for any of the nanoparticles. While C5/C5a levels slightly increased for the PEGylated nanocapsules, addition of peptide on the surface was able to decrease the C5/C5a levels. This highlights further that unlike PLA, PU as a core material itself is better able to suppress the C5/C5a generation. Moreover, the hemostatic nanocapsules do not further increase the C5/C5a level as well compared to MEM.

Finally, we evaluated the hemostatic activity of the nanocapsules with this newly designed polyurethane system through an in vitro coagulation assay using the NATEM test of ROTEM. The hemostatic nanocapsules have the peptide motif GRGDS conjugated to the PEG on the surface, which leads to the nanocapsules mimicking the role of fibrinogen and attach to activated platelets at the site of injury through the GPIIb/IIIa integrin. The citrated blood collected from Sprague Dawley rats was used to mimic those conditions, where the citration was reversed using the CaCl₂ reagent. The hemostatic nanocapsules at a concentration of 5mg/ml could

decrease the time required to form a 20mm clot significantly compared to the control nanoparticles. This outcome highlights that we can develop a nanocapsule system that would potentially not lead to complement activation and at the same time able to impart hemostatic activity. There is further scope for tuning the peptide density and determining the optimum dosage required for the hemostatic nanocapsules. We have previously seen peptide density⁴⁵ as crucial in determining the optimum dosage in vivo. Moreover, encapsulating anti-inflammatory molecules and triggering the release could be critical in controlling inflammation at the injury site.

Conclusion

One of the critical aspects of intravenously administered nanomaterials is that these encounter blood proteins immediately. That could often cause initial infusion reactions as the body recognizes these as foreign materials. Hence understanding the properties of the material and how it interacts with the blood proteins can significantly impact the development and design of nanomaterials. We developed a PEGylated polyurethane nanocapsule system in our quest to identify the materials that would lead to the least amount of changes in the complement system. We utilized that to generate the new generation of hemostatic nanocapsules. Our initial assessment and comparison with conventional polyester-based nanomaterials indicate that the polyurethane nanocapsules lead to lower complement activation in vitro. Moreover, the peptide conjugated hemostatic nanocapsules lead to lower clot formation time in vitro, indicating that the system can form a stable clot plug faster to

vehicle control and control nanoparticles. The outcomes of this study are significant as it would guide future studies for testing these in vivo in small and large animal models and for eventual clinical translation.

Acknowledgements

This work was supported by the AIMM Research award (DOD) (Award Number# W81XWH1820061) for developing intravenously infusible nanoparticles to stop bleeding and increase survival following. We would like to thank Tagide deCarvalho, PhD and Sara Larson for assisting with the TEM imaging. We would also like to thank Binapani Mahaling for providing the PLA nanoparticles.

References

1. Kauvar, D. S.; Lefering, R.; Wade, C. E., Impact of hemorrhage on trauma outcome: an overview of epidemiology, clinical presentations, and therapeutic considerations. *Journal of Trauma and Acute Care Surgery* **2006**, *60* (6), S3-S11.
2. Cloonan, C. C., Treating traumatic bleeding in a combat setting. *Mil Med* **2004**, *169* (12 Suppl), s8-s10.
3. Okada, K.; Matsumoto, H.; Saito, N.; Yagi, T.; Lee, M., Revision of 'golden hour' for hemodynamically unstable trauma patients: an analysis of nationwide hospital-based registry in Japan. *Trauma Surg Acute Care Open* **2020**, *5* (1), e000405 DOI: 10.1136/tsaco-2019-000405.
4. Bertram, J. P.; Williams, C. A.; Robinson, R.; Segal, S. S.; Flynn, N. T.; Lavik, E. B., Intravenous hemostat: nanotechnology to halt bleeding. *Sci Transl Med* **2009**, *1* (11), 11ra22 DOI: 10.1126/scitranslmed.3000397.
5. Shoffstall, A. J.; Atkins, K. T.; Groynom, R. E.; Varley, M. E.; Everhart, L. M.; Lashof-Sullivan, M. M.; Martyn-Dow, B.; Butler, R. S.; Ustin, J. S.; Lavik, E. B., Intravenous Hemostatic Nanoparticles Increase Survival Following Blunt Trauma Injury. *Biomacromolecules* **2012**, *13* (11), 3850-3857 DOI: 10.1021/bm3013023.
6. Hubbard, W. B.; Lashof-Sullivan, M. M.; Lavik, E. B.; VandeVord, P. J., Steroid-Loaded Hemostatic Nanoparticles Combat Lung Injury after Blast Trauma. *ACS Macro Letters* **2015**, *4* (4), 387-391 DOI: 10.1021/acsmacrolett.5b00061.
7. Onwukwe, C.; Maisha, N.; Holland, M.; Varley, M.; Groynom, R.; Hickman, D.; Uppal, N.; Shoffstall, A.; Ustin, J.; Lavik, E., Engineering Intravenously

Administered Nanoparticles to Reduce Infusion Reaction and Stop Bleeding in a Large Animal Model of Trauma. *Bioconjugate chemistry* **2018**, 29 (7), 2436-2447 DOI: 10.1021/acs.bioconjchem.8b00335.

8. Ricklin, D.; Lambris, J. D., Complement in immune and inflammatory disorders: pathophysiological mechanisms. *J Immunol* **2013**, 190 (8), 3831-8 DOI: 10.4049/jimmunol.1203487.

9. Benjamini, E., *Immunology: a short course*. Vol. 77.

10. Moghimi, S. M.; Simberg, D., Complement activation turnover on surfaces of nanoparticles. *Nano Today* **2017**, 15, 8-10 DOI: 10.1016/j.nantod.2017.03.001.

11. Szebeni, J., Hemocompatibility testing for nanomedicines and biologicals: predictive assays for complement mediated infusion reactions. *European Journal of Nanomedicine* **2012**, 4 (1), DOI: 10.1515/ejnm-2012-0002.

12. Chanan-Khan, A.; Szebeni, J.; Savay, S.; Liebes, L.; Rafique, N. M.; Alving, C. R.; Muggia, F. M., Complement activation following first exposure to pegylated liposomal doxorubicin (Doxil): possible role in hypersensitivity reactions. *Ann Oncol* **2003**, 14 (9), 1430-7 DOI: 10.1093/annonc/mdg374.

13. Banda, N. K.; Mehta, G.; Chao, Y.; Wang, G.; Inturi, S.; Fossati-Jimack, L.; Botto, M.; Wu, L.; Moghimi, S. M.; Simberg, D., Mechanisms of complement activation by dextran-coated superparamagnetic iron oxide (SPIO) nanoworms in mouse versus human serum. *Particle and fibre toxicology* **2014**, 11 (1), 64 DOI: 10.1186/s12989-014-0064-2.

14. Szeto, G. L.; Lavik, E. B., Materials design at the interface of nanoparticles and innate immunity. *J Mater Chem B* **2016**, *4* (9), 1610-1618 DOI: 10.1039/C5TB01825K.
15. Ouyang, X.; Huang, X.; Pan, Q.; Zuo, C.; Huang, C.; Yang, X.; Zhao, Y., Synthesis and characterization of triethylene glycol dimethacrylate nanocapsules used in a self-healing bonding resin. *J Dent* **2011**, *39* (12), 825-33 DOI: 10.1016/j.jdent.2011.09.001.
16. Pramanik, S. K.; Sreedharan, S.; Singh, H.; Khan, M.; Tiwari, K.; Shiras, A.; Smythe, C.; Thomas, J. A.; Das, A., Mitochondria Targeting Non-Isocyanate-Based Polyurethane Nanocapsules for Enzyme-Triggered Drug Release. *Bioconjug Chem* **2018**, *29* (11), 3532-3543 DOI: 10.1021/acs.bioconjchem.8b00460.
17. Boffito, M.; Torchio, A.; Tonda-Turo, C.; Laurano, R.; Gisbert-Garzaran, M.; Berkmann, J. C.; Cassino, C.; Manzano, M.; Duda, G. N.; Vallet-Regi, M.; Schmidt-Bleek, K.; Ciardelli, G., Hybrid Injectable Sol-Gel Systems Based on Thermo-Sensitive Polyurethane Hydrogels Carrying pH-Sensitive Mesoporous Silica Nanoparticles for the Controlled and Triggered Release of Therapeutic Agents. *Front Bioeng Biotechnol* **2020**, *8*, 384 DOI: 10.3389/fbioe.2020.00384.
18. Niu, Y.; Stadler, F. J.; Song, J.; Chen, S.; Chen, S., Facile fabrication of polyurethane microcapsules carriers for tracing cellular internalization and intracellular pH-triggered drug release. *Colloids Surf B Biointerfaces* **2017**, *153*, 160-167 DOI: 10.1016/j.colsurfb.2017.02.018.

19. Menikheim, S.; Leckron, J.; Bernstein, S.; Lavik, E. B., On-Demand and Long-Term Drug Delivery from Degradable Nanocapsules. *ACS Applied Bio Materials* **2020**, *3* (11), 7369-7375 DOI: 10.1021/acsabm.0c01130.
20. Zhou, L.; Liang, D.; He, X.; Li, J.; Tan, H.; Li, J.; Fu, Q.; Gu, Q., The degradation and biocompatibility of pH-sensitive biodegradable polyurethanes for intracellular multifunctional antitumor drug delivery. *Biomaterials* **2012**, *33* (9), 2734-45 DOI: 10.1016/j.biomaterials.2011.11.009.
21. Bernacca, G.; Gulbransen, M.; Wilkinson, R.; Wheatley, D., In vitro blood compatibility of surface-modified polyurethanes. *Biomaterials* **1998**, *19* (13), 1151-1165.
22. Maisha, N.; Coombs, T.; Lavik, E., Development of a Sensitive Assay to Screen Nanoparticles in Vitro for Complement Activation. *ACS Biomaterials Science & Engineering* **2020**, *6* (9), 4903-4915 DOI: 10.1021/acsbmaterials.0c00722.
23. Lategan, K.; Alghadi, H.; Bayati, M.; de Cortalezzi, M. F.; Pool, E., Effects of Graphene Oxide Nanoparticles on the Immune System Biomarkers Produced by RAW 264.7 and Human Whole Blood Cell Cultures. *Nanomaterials (Basel)* **2018**, *8* (2), DOI: 10.3390/nano8020125.
24. Guo, J.; Pan, Q.; Huang, C.; Zhao, Y.; Ouyang, X.; Huo, Y.; Duan, S., The role of surfactant and costabilizer in controlling size of nanocapsules containing TEGDMA in miniemulsion. *Journal of Wuhan University of Technology-Mater. Sci. Ed.* **2009**, *24* (6), 1004-1006 DOI: 10.1007/s11595-009-7004-2.

25. Fearon, D. T.; Austen, K. F., Activation of the alternative complement pathway due to resistance of zymosan-bound. *Proceedings of the National Academy of Sciences* **1977**, 74 (4), 1683-1687.
26. Wibroe, P. P.; Anselmo, A. C.; Nilsson, P. H.; Sarode, A.; Gupta, V.; Urbanics, R.; Szebeni, J.; Hunter, A. C.; Mitragotri, S.; Mollnes, T. E.; Moghimi, S. M., Bypassing adverse injection reactions to nanoparticles through shape modification and attachment to erythrocytes. *Nat Nanotechnol* **2017**, 12 (6), 589-594 DOI: 10.1038/nnano.2017.47.
27. Szebeni, J.; Bedőcs, P.; Csukás, D.; Rosivall, L.; Bünger, R.; Urbanics, R., A porcine model of complement-mediated infusion reactions to drug carrier nanosystems and other medicines. *Advanced Drug Delivery Reviews* **2012**, 64 (15), 1706-1716 DOI: 10.1016/j.addr.2012.07.005.
28. Szebeni, J.; Bedőcs, P.; Rozsnyay, Z.; Weiszhar, Z.; Urbanics, R.; Rosivall, L.; Cohen, R.; Garbuzenko, O.; Báthori, G.; Tóth, M., Liposome-induced complement activation and related cardiopulmonary distress in pigs: factors promoting reactogenicity of Doxil and AmBisome. *Nanomedicine: Nanotechnology, Biology and Medicine* **2012**, 8 (2), 176-184 DOI: 10.1016/j.nano.2011.06.003.
29. Wang, G.; Chen, F.; Banda, N. K.; Holers, V. M.; Wu, L.; Moghimi, S. M.; Simberg, D., Activation of Human Complement System by Dextran-Coated Iron Oxide Nanoparticles Is Not Affected by Dextran/Fe Ratio, Hydroxyl Modifications, and Crosslinking. *Front Immunol* **2016**, 7, 418 DOI: 10.3389/fimmu.2016.00418.

30. De Sousa Delgado, A.; Léonard, M.; Dellacherie, E., Surface Properties of Polystyrene Nanoparticles Coated with Dextrans and Dextran–PEO Copolymers. Effect of Polymer Architecture on Protein Adsorption. *Langmuir* **2001**, *17* (14), 4386-4391 DOI: 10.1021/la001701c.
31. Fornaguera, C.; Caldero, G.; Mitjans, M.; Vinardell, M. P.; Solans, C.; Vauthier, C., Interactions of PLGA nanoparticles with blood components: protein adsorption, coagulation, activation of the complement system and hemolysis studies. *Nanoscale* **2015**, *7* (14), 6045-58 DOI: 10.1039/c5nr00733j.
32. Ruiz, A.; Alpízar, A.; Beola, L.; Rubio, C.; Gavilán, H.; Marciello, M.; Rodríguez-Ramiro, I.; Ciordia, S.; Morris, C. J.; Morales, M. d. P., Understanding the Influence of a Bifunctional Polyethylene Glycol Derivative in Protein Corona Formation around Iron Oxide Nanoparticles. *Materials* **2019**, *12* (14), 2218.
33. Hamad, I.; Christy Hunter, A.; Rutt, K. J.; Liu, Z.; Dai, H.; Moein Moghimi, S., Complement activation by PEGylated single-walled carbon nanotubes is independent of C1q and alternative pathway turnover. *Mol Immunol* **2008**, *45* (14), 3797-803 DOI: 10.1016/j.molimm.2008.05.020.
34. Hamad, I.; Al-Hanbali, O.; Hunter, A. C.; Rutt, K. J.; Andresen, T. L.; Moghimi, S. M., Distinct polymer architecture mediates switching of complement activation pathways at the nanosphere– serum interface: implications for stealth nanoparticle engineering. *ACS nano* **2010**, *4* (11), 6629-6638.
35. Szebeni, J.; Bedocs, P.; Urbanics, R.; Bunger, R.; Rosivall, L.; Toth, M.; Barenholz, Y., Prevention of infusion reactions to PEGylated liposomal doxorubicin

- via tachyphylaxis induction by placebo vesicles: a porcine model. *J Control Release* **2012**, *160* (2), 382-7 DOI: 10.1016/j.jconrel.2012.02.029.
36. Lashof-Sullivan, M.; Holland, M.; Groynom, R.; Campbell, D.; Shoffstall, A.; Lavik, E., Hemostatic Nanoparticles Improve Survival Following Blunt Trauma Even after 1 Week Incubation at 50 (°)C. *ACS biomaterials science & engineering* **2016**, *2* (3), 385-392 DOI: 10.1021/acsbiomaterials.5b00493.
37. Cherng, J. Y.; Hou, T. Y.; Shih, M. F.; Talsma, H.; Hennink, W. E., Polyurethane-based drug delivery systems. *Int J Pharm* **2013**, *450* (1-2), 145-62 DOI: 10.1016/j.ijpharm.2013.04.063.
38. Rojas, I. A.; Slunt, J. B.; Grainger, D. W., Polyurethane coatings release bioactive antibodies to reduce bacterial adhesion. *Journal of Controlled Release* **2000**, *63* (1-2), 175-189.
39. Peng, Q.; Li, K.; Sacks, S. H.; Zhou, W., The role of anaphylatoxins C3a and C5a in regulating innate and adaptive immune responses. *Inflammation & Allergy-Drug Targets (Formerly Current Drug Targets-Inflammation & Allergy)* **2009**, *8* (3), 236-246 DOI: 10.2174/187152809788681038.
40. Ember, J.; Jagels, M.; Hugli, T.; Volanakis, J.; Frank, M., The human complement system in health and disease. *Marcel Dekker* **1998**, 241-84.
41. Wojta, J.; Kaun, C.; Zorn, G.; Ghannadan, M.; Hauswirth, A. W.; Sperr, W. R.; Fritsch, G.; Printz, D.; Binder, B. R.; Schatzl, G., C5a stimulates production of plasminogen activator inhibitor-1 in human mast cells and basophils. *Blood, The Journal of the American Society of Hematology* **2002**, *100* (2), 517-523.

42. Verhoef, J. J.; de Groot, A. M.; van Moorsel, M.; Ritsema, J.; Beztsinna, N.; Maas, C.; Schellekens, H., Iron nanomedicines induce Toll-like receptor activation, cytokine production and complement activation. *Biomaterials* **2017**, *119*, 68-77.
43. Andersen, A. J.; Wibroe, P. P.; Moghimi, S. M., Perspectives on carbon nanotube-mediated adverse immune effects. *Adv Drug Deliv Rev* **2012**, *64* (15), 1700-5 DOI: 10.1016/j.addr.2012.05.005.
44. Murphy, F. A.; Schinwald, A.; Poland, C. A.; Donaldson, K., The mechanism of pleural inflammation by long carbon nanotubes: interaction of long fibres with macrophages stimulates them to amplify pro-inflammatory responses in mesothelial cells. *Part Fibre Toxicol* **2012**, *9*, 8 DOI: 10.1186/1743-8977-9-8.
45. Shoffstall, A. J.; Everhart, L. M.; Varley, M. E.; Soehnlen, E. S.; Shick, A. M.; Ustin, J. S.; Lavik, E. B., Tuning Ligand Density on Intravenous Hemostatic Nanoparticles Dramatically Increases Survival Following Blunt Trauma. *Biomacromolecules* **2013**, *14* (8), 2790-2797 DOI: 10.1021/bm400619v.

Chapter 6: Conclusions

Summary of findings

Complement-mediated infusion reactions are a significant hurdle to the translation of nanotechnology-based products. The infusion reactions can start within minutes to hours after the nanotherapeutic is received, and the consequences can be as severe as anaphylaxis, a fatal condition.¹ This may require the dosages to be administered in reduced amounts or treatment discontinuation.² Due to such complications, over the years, the number of regulatory board-approved nanotherapeutics is few.³⁻⁴ The activation of the complement pathways in parts is implicated for such infusion reactions.⁵⁻⁶ The complement pathways recognize the nanoparticles in the bloodstream as a foreign agent and work on clearing them off, leading to the uptake of nanoparticles through various macrophages generated due to the immune reactions.⁷ Because of the sheer surface area exposed to complement proteins, it is not unexpected that nanoparticles can evoke such an innate immune response. Hence, we worked on evaluating the surface properties that do not lead to complement-mediated initial infusion reactions.

Highly sensitive immunoassays for quantifying complement response are required for the development of safer nanomedicines. The possibility of screening nanomaterials before moving into experiments involving large animal models or, potentially, replacing large animal models with sensitive screening tools can

significantly increase the number of nanomaterials that can be translated to the clinic. We have developed an assay with high sensitivity for evaluating complement response *in vitro*, and the developed assay mimics the observations seen *in vivo*.

We then investigated the impact of PEGylation on complement activation *in vitro* utilizing the developed screening tool. We tracked the changes in anaphylatoxin C5a, produced upon complement activation, as a biomarker. The highest possible PEGylation of the nanomaterials led to the least amount of C5a detected in the blood *in vitro*. As we investigated the impact of PEG chain length, we found that the increasing PEG length from 3400Da to 5000Da leads to the least amount of C5a within the sample *in vitro*. The concept of PEG pairing is intriguing as we can leverage this to design stealth nanoparticles with better targeting capability. We also tracked whether pro-inflammatory cytokines are generated *in vitro* and found the levels remained close to the observations for the vehicle control for the critical pro-inflammatory cytokines.

As physiochemical properties are essential regulators of the interaction between the nanomaterials and blood proteins, we further extended this study to include the nanoparticle core's role. We developed a PEGylated polyurethane nanocapsule system that leads to the least amount of changes in the complement system. We utilized that to generate the new generation of hemostatic nanocapsules. The hemostatic nanocapsules lead to lower clot formation time *in vitro*; that is, the system can form a stable clot plug faster to vehicle control and control nanoparticles. Hence, the nanomaterials designed to impart stealth properties maintain the intended

activity as well. The outcomes of this study are significant as it would guide future studies for testing these *in vivo* in small and large animal models and for eventual clinical translation.

Validation of the stealth activity of hemostatic nanoparticles in vivo

While answering our research questions, we determined that a higher amount of PEGylation reduced the change in complement protein C5a in vitro in whole blood and serum. Hence based on the results, the PLA-PEG nanoparticles with the highest amount of PEG on the surface were chosen as hemostatic nanoparticles. The treatment batches had the GRGDS peptide motif covalently bound to the PEG, while control batches were devoid of any peptide motif. A summary of the characterization data for the nanoparticles are given below:

Table 2: Summary of hydrodynamic diameter and zeta-potential of the hemostatic PLA-PEG nanoparticles with peptide motif GRGDS and control PLA-PEG nanoparticles

Type of Nanoparticle	Z-Average (nm)	Zeta-potential (mV)
Hemostatic nanoparticles	367.5 \pm 28.8	-13.7 \pm 1.0
Control nanoparticles	334.1 \pm 18.9	-15.5 \pm 0.4

The nanoparticles were administered in a large animal (swine) pressure-targeted hemorrhagic shock polytrauma model for a controlled liver injury. The study was

conducted in collaboration with the Naval Medical Research Unit in San Antonio, Texas. Detailed protocols outlining the study are provided in the appendix section. In addition, the Survival rate in the injured and uninjured arms of the study are summarized in the table below:

Arm	Subgroup	Survival rate (%)
Injured Arm	Vehicle Control (n=6)	100
	Control Nanoparticles (n=6)	66.7
	Hemostatic Nanoparticles (n=7)	57.1

As a preliminary assessment of whether complement activation takes place, we tracked the changes in the cardiopulmonary vitals. The changes in respiration rate, heart rate and mean arterial pressure did not show drastic changes upon comparing the groups receiving either the Vehicle Control, the Control Nanoparticles, or the Hemostatic Nanoparticles. (Figure 28)

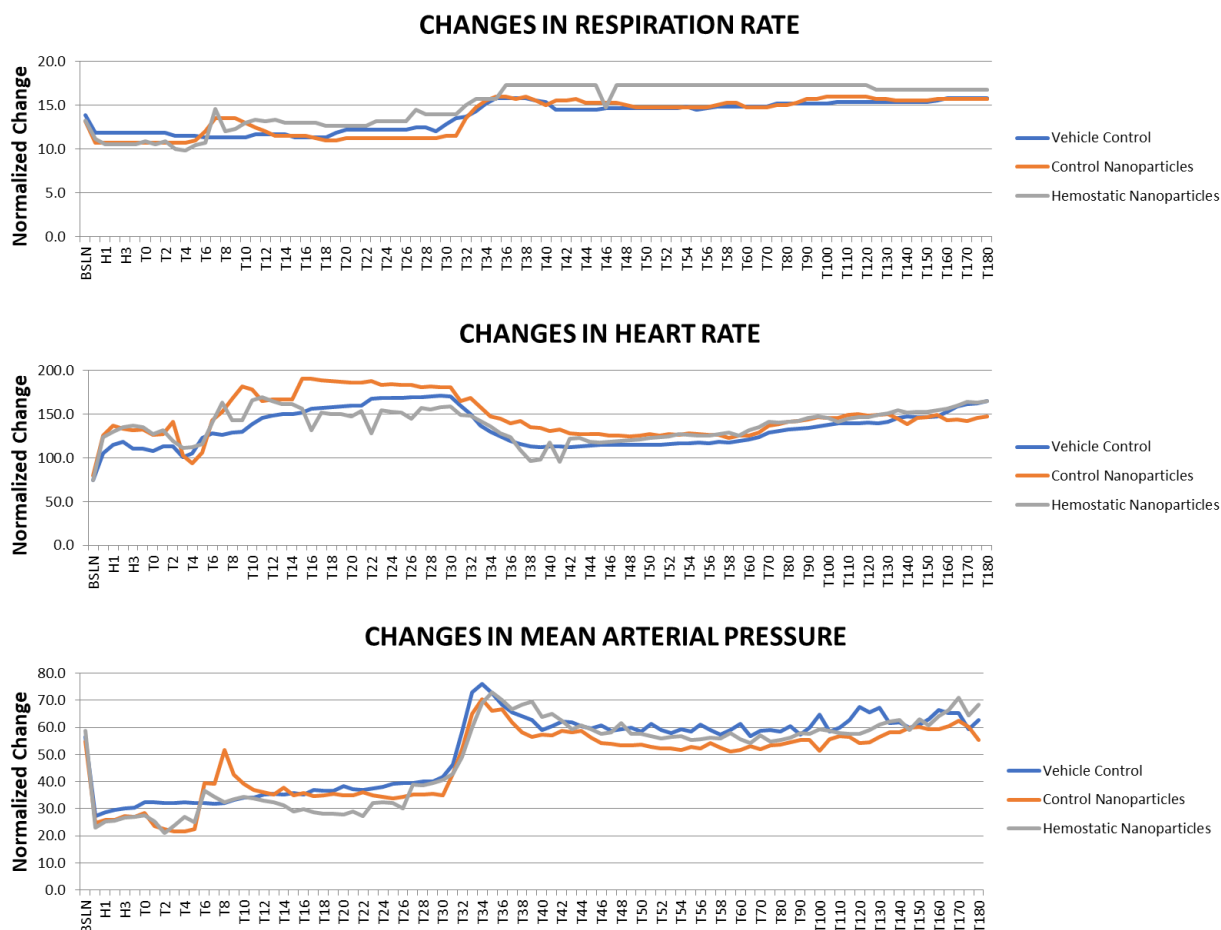


Figure 28: Changes in cardiopulmonary vitals in large animals receiving PLA-PEG nanoparticles

Further assessment of the coagulation parameters like prothrombin time also decreases in the group of animals receiving hemostatic nanoparticles. Hence, the nanoparticles do lead to a hemostatic activity as well. (Figure 29)

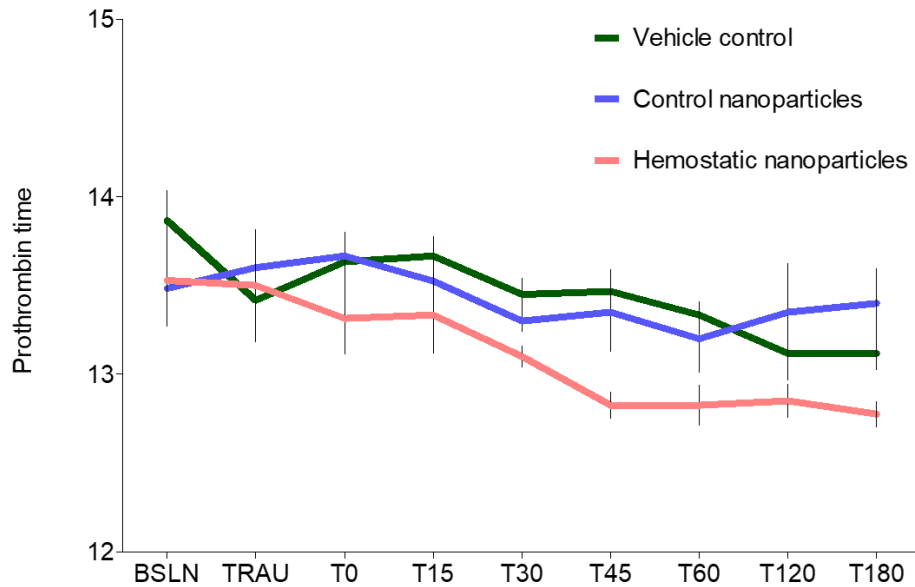


Figure 29: Changes in prothrombin time after infusion of PLA-PEG based hemostatic and control nanoparticles in the in vivo porcine trauma model

While we do not see complement activation immediately after infusion of the nanoparticles intravenously, further analysis is being carried out to understand whether nanoparticles may exacerbate the formation of microthrombi. This is mainly of concern, as some of the animals receiving nanoparticles show signs of clot formation based on the pathology outcomes. It should also be noted that trauma itself can lead to hypercoagulability states and lead to complications such as thromboembolism.⁸ We are incorporating data science techniques that could detect the changes in coagulation factors and critical blood components temporally to correlate with the clotting and survival outcomes.

Future Directions

We have developed an *in vitro* assay with high sensitivity for quantifying the complement proteins generated.⁹ While the infusion reactions are in parts complement-mediated, there is further scope to extend this study to evaluate how the pro-inflammatory cytokines are changing. We have performed initial studies to track the cytokines detected *in vitro* after incubating blood matrices with nanoparticles. We have initially investigated changes in pro-inflammatory cytokines like IL-6 in rat endothelial cells and citrated whole rat blood and not observed changes compared to baseline. However, as the macrophages mediate the uptake and clearance,⁷ using human macrophage cell lines for detecting and quantifying the pro-inflammatory cytokines can be critical in validating the safety of nanomedicine.

Moreover, Kupffer cells in humans can generate platelet-activating factors (PAF) and lead to toxicities after encountering nanoparticles.¹⁰ It could be beneficial to include PAF among the biomarkers to be screened to ensure the nanomaterials' stealth properties. Expanding the biomarkers to be screened for, especially *in vitro*, can be vital before moving into experiments involving large animal models and significantly increase the number of nanomaterials that can be translated to the clinic.

As the library grows, incorporating more biomarkers and how these change with changing materials and surface properties, it becomes critical to introduce data management techniques that can determine the similarities between different outcomes or determine the exact properties that are critical hemocompatibility and for avoiding infusion reactions. To find the similarities in outcomes, data analysis

techniques like Piecewise Aggregate Approximation(PAA),¹¹SMerg¹² algorithms can be helpful. SMerg (Similarity-based Merging) is an algorithm used to discover the temporal neighborhood in a dataset based on similarities. Unsupervised learning algorithms like the K-Means clustering algorithm can be of guidance, too, as it separates data points aggregated together because of similarities across nanoparticles.¹³ Moreover, to study predictive findings, class Association rule mining¹⁴ can be used to determine if certain nanoparticles are predictors of specific outcomes.

Polyurethane nanocapsules are synthesized as polyurethane linkages between aromatic isocyanate groups and aliphatic diols form.¹⁵ The ratio of the hard and soft segments present is critical in determining whether the material is soft and rubbery.¹⁶ The polyurethane nanomaterials developed in this work have a hard to soft segment ratio close to 30% based on the mass of the aromatic hard segment and aliphatic soft segment present. While the ratio still ensures that the material is a soft elastomer, the aliphatic diol can be switched to introduce polyols of higher molecular weight for making it softer and rubberier. As for the polyurethane hemostatic nanocapsule system, there is scope for further work on tuning the amounts of peptide density as it plays a critical role in modulating the hemostatic activity.¹⁷

Moreover, the applications of polyurethane nanocapsules can be extended to encapsulate therapeutics as well that are released upon triggers such as sonication.¹⁵ A potential route of leveraging on that property could be encapsulating anti-

inflammatory therapeutics to be delivered at the site of injury along with the hemostatic nanocapsules.

Broader impact

This dissertation focused on developing stealth nanomaterials that are clinically translatable in the long run. The optimum assay conditions and methods of sample preparation developed to generate *in vitro* complement response like *in vivo* provide means to quantify complement proteins. These screening tools, upon further expansion, could be critical to assess the safety and efficacy of the nanomedicines before moving to *in vivo* studies, especially in large animals. The sensitive assays developed and the library generated by investigating the impact of surface chemistry and the properties of the material of nanoparticles in complement activation would help identify the physiological and chemical properties that do not trigger the complement pathways. Overall, the findings of this study guide in designing stealth nanomaterials for therapeutic applications to overcome initial infusion reactions.

References

1. Szebeni, J.; Simberg, D.; Gonzalez-Fernandez, A.; Barenholz, Y.; Dobrovolskaia, M. A., Roadmap and strategy for overcoming infusion reactions to nanomedicines. *Nat Nanotechnol* **2018**, *13* (12), 1100-1108 DOI: 10.1038/s41565-018-0273-1.
2. Lenz, H. J., Management and preparedness for infusion and hypersensitivity reactions. *Oncologist* **2007**, *12* (5), 601-9 DOI: 10.1634/theoncologist.12-5-601.
3. Anselmo, A. C.; Mitragotri, S., Nanoparticles in the clinic: An update. *Bioengineering & Translational Medicine* **2019**, e10143 DOI: 10.1002/btm2.10143.
4. Anselmo, A. C.; Mitragotri, S., Nanoparticles in the clinic. *Bioengineering & translational medicine* **2016**, *1* (1), 10-29 DOI: 10.1002/btm2.10003.
5. Wibroe, P. P.; Anselmo, A. C.; Nilsson, P. H.; Sarode, A.; Gupta, V.; Urbanics, R.; Szebeni, J.; Hunter, A. C.; Mitragotri, S.; Mollnes, T. E.; Moghimi, S. M., Bypassing adverse injection reactions to nanoparticles through shape modification and attachment to erythrocytes. *Nat Nanotechnol* **2017**, *12* (6), 589-594 DOI: 10.1038/nnano.2017.47.
6. Szebeni, J.; Bedőcs, P.; Csukás, D.; Rosivall, L.; Bünger, R.; Urbanics, R., A porcine model of complement-mediated infusion reactions to drug carrier nanosystems and other medicines. *Advanced Drug Delivery Reviews* **2012**, *64* (15), 1706-1716 DOI: 10.1016/j.addr.2012.07.005.

7. Gustafson, H. H.; Holt-Casper, D.; Grainger, D. W.; Ghandehari, H., Nanoparticle uptake: the phagocyte problem. *Nano today* **2015**, *10* (4), 487-510 DOI: 10.1016/j.nantod.2015.06.006.
8. Selby, R.; Geerts, W.; Ofosu, F. A.; Craven, S.; Dewar, L.; Phillips, A.; Szalai, J. P., Hypercoagulability after trauma: hemostatic changes and relationship to venous thromboembolism. *Thromb Res* **2009**, *124* (3), 281-7 DOI: 10.1016/j.thromres.2008.10.002.
9. Maisha, N.; Coombs, T.; Lavik, E., Development of a Sensitive Assay to Screen Nanoparticles in Vitro for Complement Activation. *ACS Biomaterials Science & Engineering* **2020**, *6* (9), 4903-4915 DOI: 10.1021/acsbmaterials.0c00722.
10. Jackson, M. A.; Patel, S. S.; Yu, F.; Cottam, M. A.; Glass, E. B.; Hoogenboezem, E. N.; Fletcher, R. B.; Dollinger, B. R.; Patil, P.; Liu, D. D.; Kelly, I. B.; Bedingfield, S. K.; King, A. R.; Miles, R. E.; Hasty, A. M.; Giorgio, T. D.; Duvall, C. L., Kupffer cell release of platelet activating factor drives dose limiting toxicities of nucleic acid nanocarriers. *Biomaterials* **2021**, *268*, 120528 DOI: 10.1016/j.biomaterials.2020.120528.
11. Guo, C.; Li, H.; Pan, D. In *An improved piecewise aggregate approximation based on statistical features for time series mining*, International conference on knowledge science, engineering and management, Springer: 2010; pp 234-244.
12. Dey, S.; Janeja, V. P.; Gangopadhyay, A. In *Temporal neighborhood discovery using markov models*, 2009 Ninth IEEE International Conference on Data Mining, IEEE: 2009; pp 110-119.

13. Teknomo, K., K-means clustering tutorial. *Medicine* **2006**, *100* (4), 3.
14. Agrawal, R.; Srikant, R. In *Fast algorithms for mining association rules*, Proc. 20th int. conf. very large data bases, VLDB, 1994; pp 487-499.
15. Menikheim, S.; Leckron, J.; Bernstein, S.; Lavik, E. B., On-Demand and Long-Term Drug Delivery from Degradable Nanocapsules. *ACS Applied Bio Materials* **2020**, *3* (11), 7369-7375 DOI: 10.1021/acsabm.0c01130.
16. Cherng, J. Y.; Hou, T. Y.; Shih, M. F.; Talsma, H.; Hennink, W. E., Polyurethane-based drug delivery systems. *Int J Pharm* **2013**, *450* (1-2), 145-62 DOI: 10.1016/j.ijpharm.2013.04.063.
17. Shoffstall, A. J.; Everhart, L. M.; Varley, M. E.; Soehnlen, E. S.; Shick, A. M.; Ustin, J. S.; Lavik, E. B., Tuning Ligand Density on Intravenous Hemostatic Nanoparticles Dramatically Increases Survival Following Blunt Trauma. *Biomacromolecules* **2013**, *14* (8), 2790-2797 DOI: 10.1021/bm400619v.

Appendices

Supplementary materials for chapter 3

Impact of anticoagulant in blood and plasma on complement response

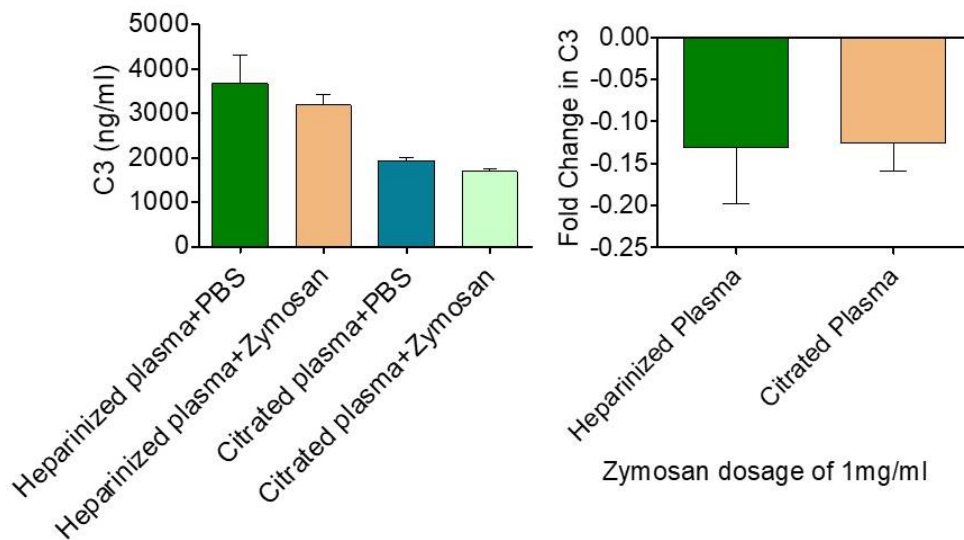


Figure 30. Comparison of fold change for complement protein C3 in heparinized and citrated human blood plasma. For similar experimental conditions and a zymosan dosage of 1mg/ml, heparinized human blood plasma showed higher complement response, indicating that anticoagulants like heparin preserved with the complement activity.

Impact of species of blood donor on quantifying complement response

Generating response with lower dosages of zymosan

C3 ELISA assay designed for guinea pigs, that has previously been validated for testing porcine *in vivo* samples,¹ was used for lower dosages of 0.15 and 0.3 mg/ml zymosan caused a slight decline in the number of quantified C3 (Figure 31). Generating a complement response *in vitro* for collected porcine blood samples required the usage of zymosan at dilute dosages as well as shorter incubation times. Moreover, the lack of immunoassays available for quantifying the response is also a hurdle. In comparison, heparinized human whole blood and plasma were able to generate a reproducible simulation of the complement response *in vitro*. Hence, complement response in whole heparinized blood, plasma, and serum was utilized to develop the complement assays to generate the response *in vitro*.

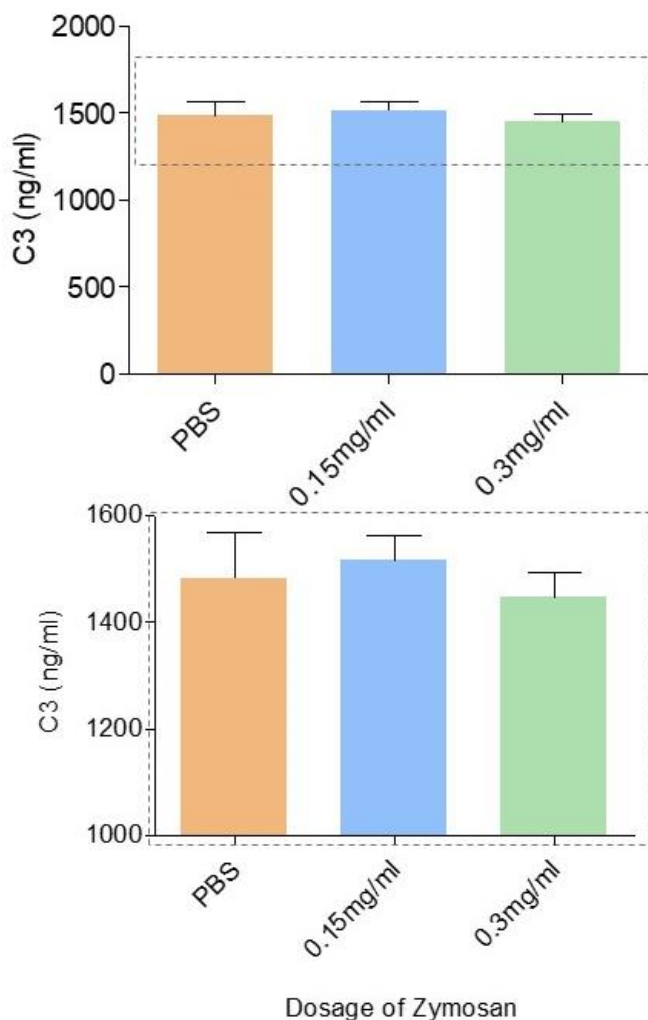


Figure 31. Change in complement protein C3 in heparinized porcine plasma. The data in the dashed box is expanded below for clarity.

Synthesis of Polymers

PLLA-PEG with amines or carboxyl groups and PDLA is prepared by ring-opening polymerization of lactide. For PLLA-PEG-NH₂ and PLLA-PEG-COOH, 5000Da heterobifunctional PEG containing hydroxyl and carboxyl groups, or hydroxyl and amine groups, were used.²⁻³ PDLA is prepared by ring-opening

polymerization of d-lactide using methanol as initiator. The polymerization reaction uses 1,3-Bis(2,4,6-trimethylphenyl)-1,3-dihydro-2H-imidazol-2-ylidene (IMes) as the catalyst, where dried lactide monomers and PEG are dissolved in dichloromethane (DCM) and the catalyst dissolved in DCM is added to start the reaction. The reaction is maintained in an inert atmosphere under argon. The reaction is halted by exposing to air and adding acetic acid. The polymer synthesized is precipitated in diethyl ether and separated through filtration. The synthesized polymer is stored at -20°C.

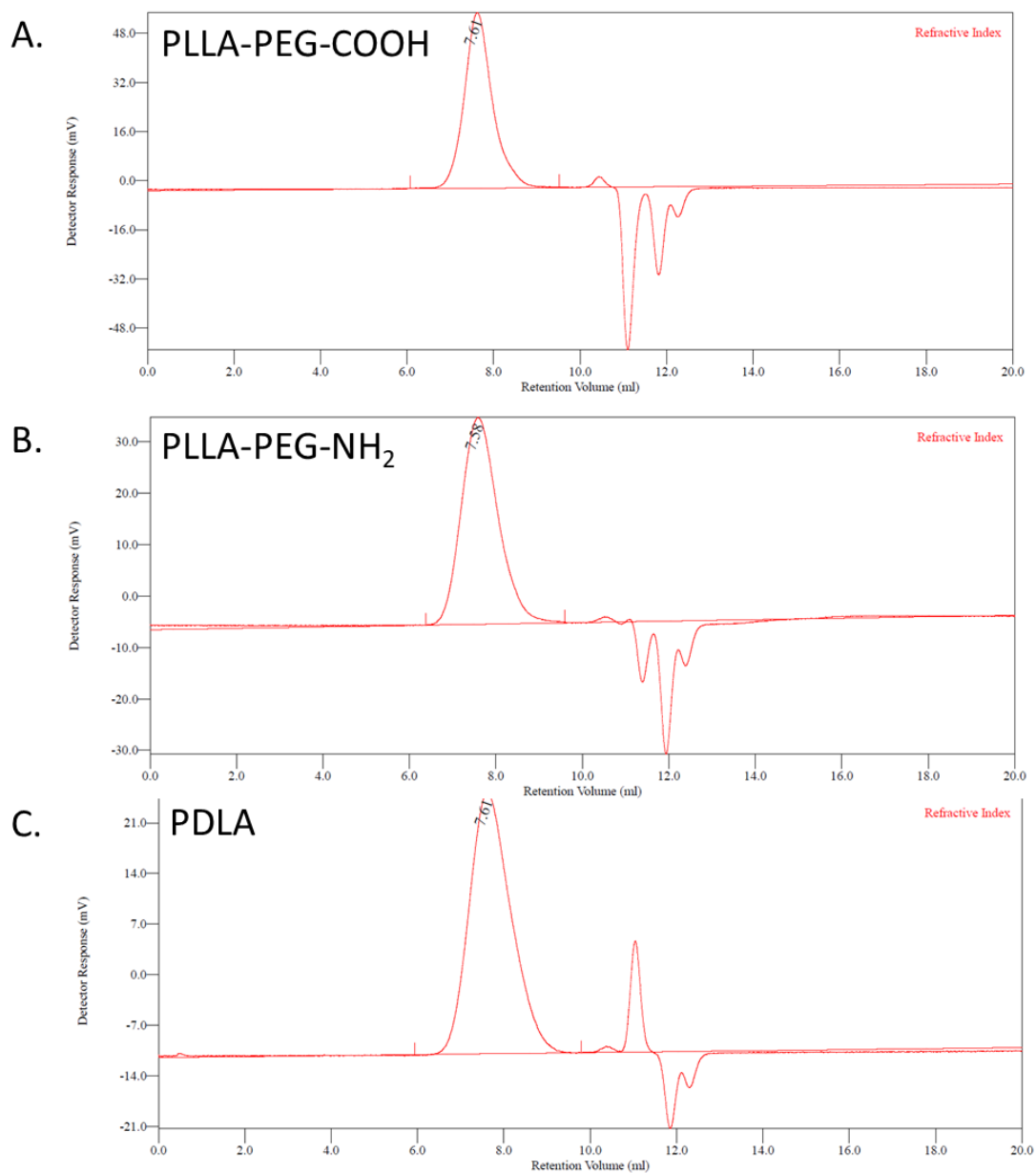


Figure 32. Poly(l-lactic acid)-b-poly(ethylene glycol) (PLLA-PEG) with terminal amine and carboxyl groups, and poly(d-lactic acid) (PDLA) were synthesized through ring-opening polymerization. The polymer is synthesized through ring-opening

polymerization based on Connor et al.² The gel permeation chromatography peaks were used to determine the molecular weights of the polymer

Supplementary Table 1. A summary of the numbered molecular weight for batches along with their polydispersity index

Synthesized Polymer	Molecular weight, Mn (kDa)	PDI
PLLA-PEG-NH ₂	26273±754	1.73±0.09
PLLA-PEG-COOH	26852±955	1.65±0.11
PDLA	23824±853	1.63±0.29

Fabrication of nanoparticles with different zeta-potentials

The nanoparticles are prepared through nanoprecipitation, where the polymers dissolved in tetrahydrofuran (THF) at a concentration of 20mg/ml was added dropwise to double the volumetric amount of phosphate-buffered saline and stir hardened to form the nanoparticles. Using excess air, residual THF is removed. The nanoparticles are stabilized with poloxamer added and further stirred for an hour. The amount of poloxamer added is optimized for the batches based on amount NH₂ present and surface charge of the nanoparticles. The nanoparticles were characterized by dynamic light scattering to determine

A. Change in Zeta potential with increasing amount of PLA-PEG-NH₂ in nanoparticles

Formulation	Zeta potential (mV)
PLA-PEG-COOH	-15.61
PLA-PEG-NH ₂ and PLA-PEG-COOH blend in 2:1 ratio	-9.93
PLA-PEG-NH ₂ and PLA-PEG-COOH blend in 5:1 ratio	-7.74
PLA-PEG-NH ₂ and PLA-PEG-COOH blend in 8:1 ratio	-5.74
PLA-PEG-NH ₂ and PLA-PEG-COOH blend in 17:1 ratio	-4.4
Nanoparticles with PLA-PEG-NH ₂	-1.8

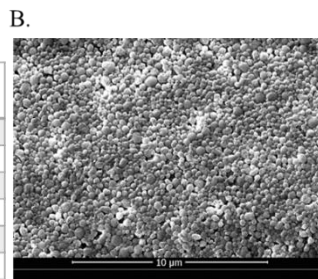


Figure 33. A. Impact of blending PLA-PEG-NH₂ and PLA-PEG-COOH in zeta-potential of nanoparticles. B. SEM image of synthesized nanoparticles

Fabrication and characterization of aggregated nanoparticles

The nanoparticles were prepared in the same way as mentioned above using PLLA-PEG-NH₂, PLLA-PEG block copolymers and PDLA. However, long term storage lead to aggregation and the particles were characterized using DLS before using in the assay.

Impact of the dosage of PLA-PEG nanoparticles on the complement response in porcine and human whole blood

The effect of dosages in complement response was evaluated for the porcine and human heparinized whole blood samples. We compared the concentrations of 0.25mg/ml and 0.6mg/ml of spherical poly(lactic acid)-*b*-poly(ethylene glycol) block copolymer (PLA-PEG) nanoparticles in human heparinized whole blood. Nanoparticles were incubated with the whole blood at mentioned concentrations and incubated at 37°C for 45 minutes. The blood samples were then centrifuged at 4000g for 5 minutes, and the plasma separated was diluted as required to quantify the

complement change for C5a. We did not see any statistically significant difference in the mean C5a level observed in the two groups. So, for the experiments comparing impact of PLA-PEG and PLGA-PLL-PEG nanoparticles on the complement changes, we used the concentration of 0.25mg/ml as well for the human heparinized blood samples.

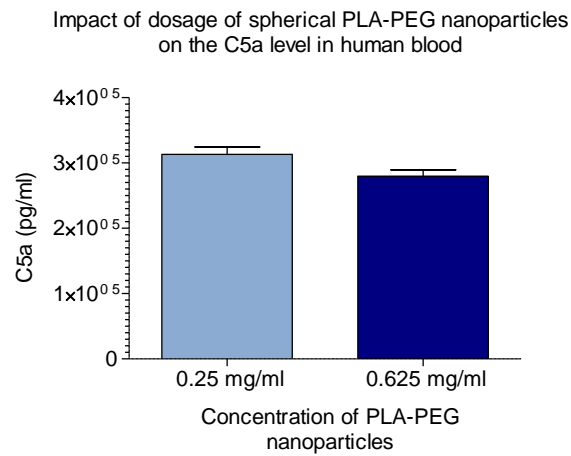


Figure 34. Change in complement protein C5a for different concentrations of PLA-PEG nanoparticles in human heparinized blood.

References

1. Onwukwe, C.; Maisha, N.; Holland, M.; Varley, M.; Groynom, R.; Hickman, D.; Uppal, N.; Shoffstall, A.; Ustin, J.; Lavik, E., Engineering Intravenously Administered Nanoparticles to Reduce Infusion Reaction and Stop Bleeding in a Large Animal Model of Trauma. *Bioconjugate chemistry* **2018**, 29 (7), 2436-2447 DOI: 10.1021/acs.bioconjchem.8b00335.
2. Connor, E. F.; Nyce, G. W.; Myers, M.; Möck, A.; Hedrick, J. L., First Example of N-Heterocyclic Carbenes as Catalysts for Living Polymerization: Organocatalytic Ring-Opening Polymerization of Cyclic Esters. *Journal of the American Chemical Society* **2002**, 124 (6), 914-915 DOI: 10.1021/ja0173324.
3. Lashof-Sullivan, M.; Holland, M.; Groynom, R.; Campbell, D.; Shoffstall, A.; Lavik, E., Hemostatic Nanoparticles Improve Survival Following Blunt Trauma Even after 1 Week Incubation at 50 (°)C. *ACS biomaterials science & engineering* **2016**, 2 (3), 385-392 DOI: 10.1021/acsbiomaterials.5b00493.

Supplementary materials for chapter 4

Calculating extent of PEGylation

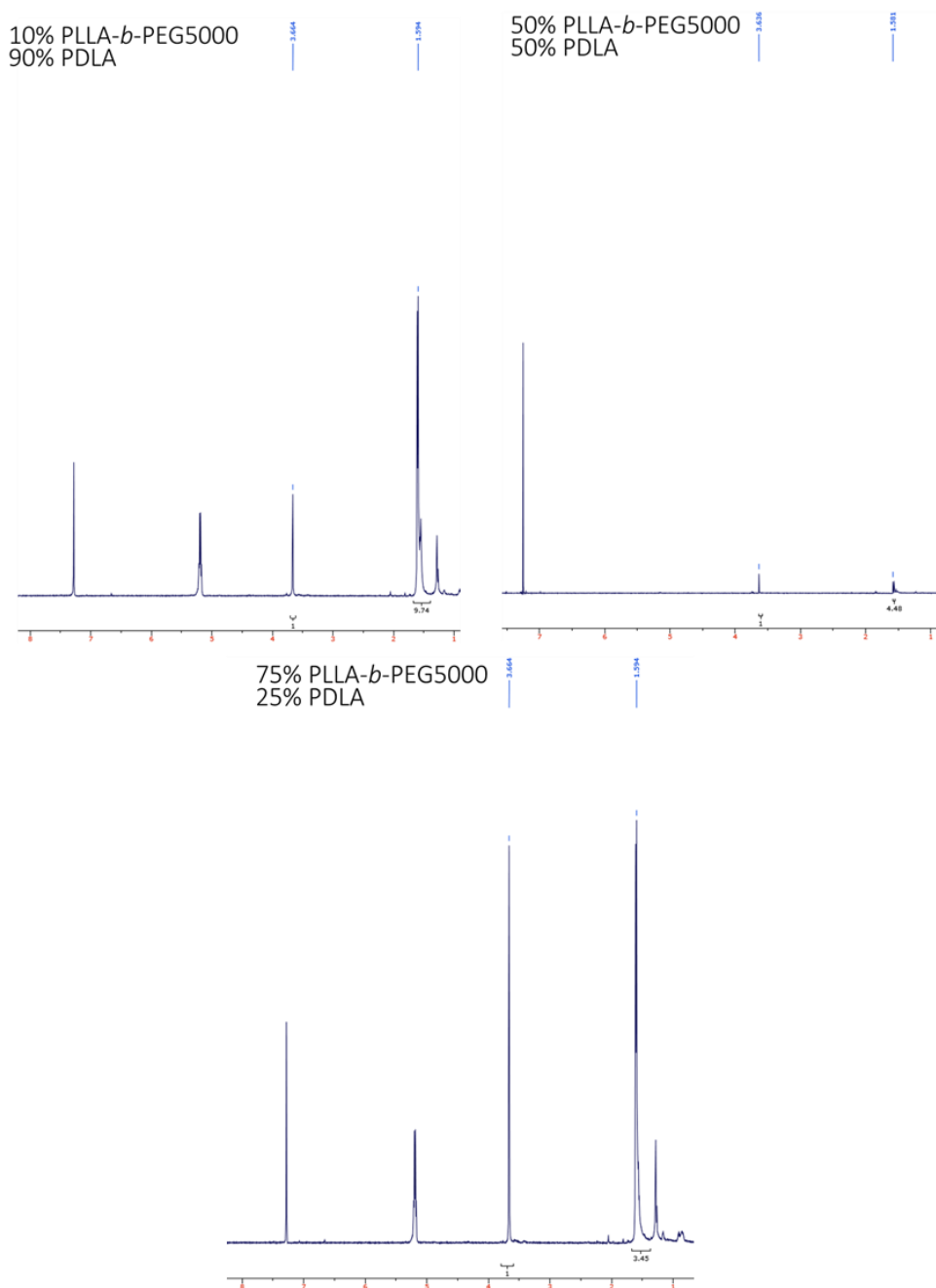


Figure 35. ¹H NMR peak in CDCl₃ for varying extents of PEGylation

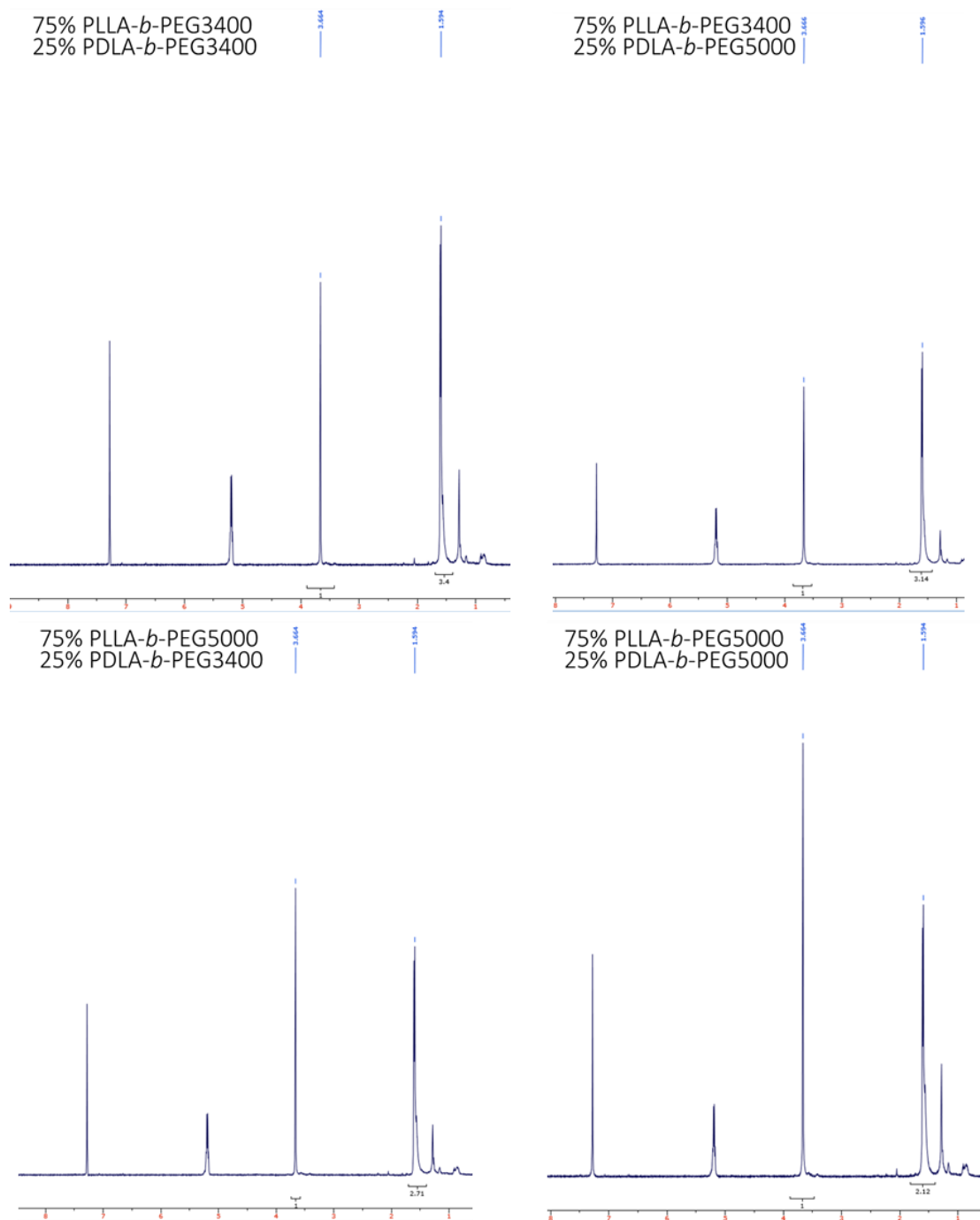


Figure 36. ^1H NMR peak in CDCl_3 for varying PEG chain lengths on the surface

Method of calculation

The PLA peak was observed at approximately 1.59 ppm

The PEG peak was observed at approximately 3.67 ppm

Based on using PLA of 25k g/mol and PEG of 5000 g/mol or 3400g/mol,

Moles of PEG

$$\frac{\frac{4H}{4H}}{1 \text{ monomer PEG}} = 0.25 \text{ monomer PEG} \times \frac{1 \text{ mol PEG}}{77.3 \text{ or } 113.6 \text{ monomers PEG}}$$
$$= \text{__moles of PEG}$$

Moles of PLA

$$\frac{\frac{\text{Ratio } 3H \text{ PLA}}{3H}}{1 \text{ monomer PLA}} = \text{__monomer PLA} \times \frac{1 \text{ mol PLA}}{347.2 \text{ monomer}} = \text{__moles of PLA}$$

Percent PEGylation is equal to Moles of PEG divided by Moles of PLA

$$\text{Percent PEGylation} = \frac{\text{moles of PEG}}{\text{moles of PLA}} \times 100$$

Change in complement protein C5a for medium and high-density PEG brush in complement protected human serum

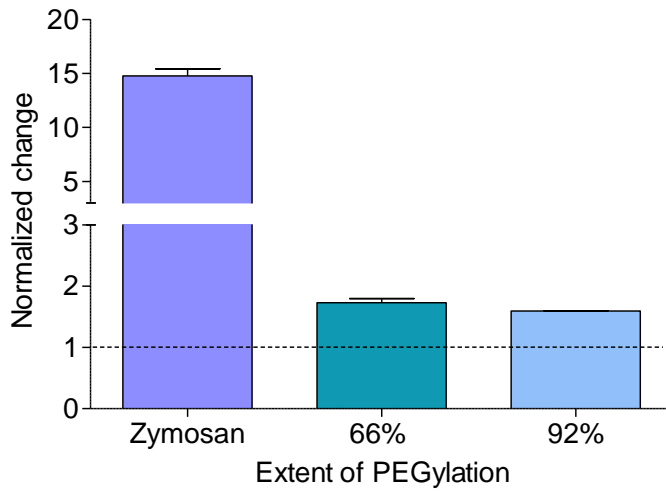


Figure 37. Change in complement protein C5a for changing amount of surface PEGylation in complement protected human serum

Impact of PEG length in dense PEG corona structures: Change in complement protein C5a in complement protected human serum

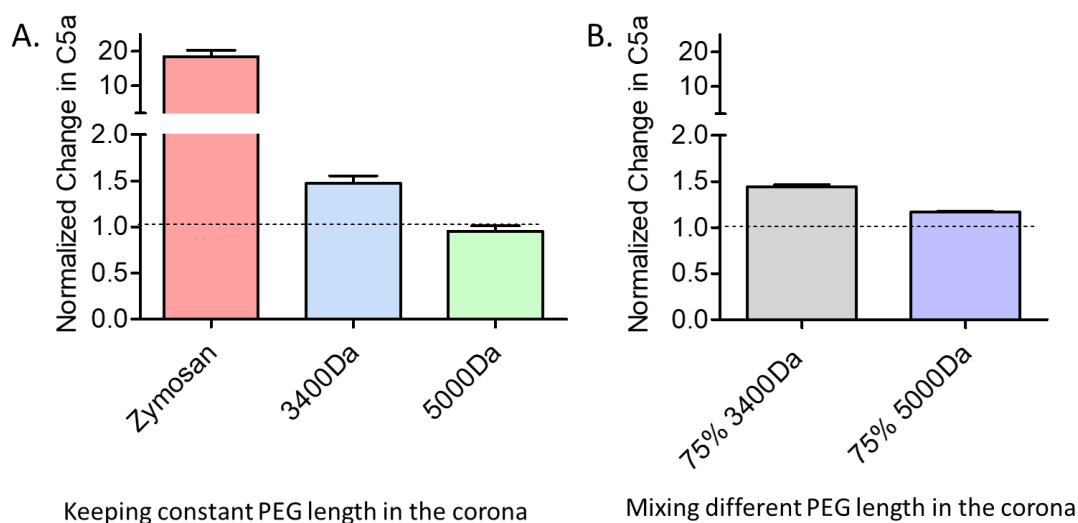


Figure 38. Impact of PEG length on change in complement protein C5a for dense PEG corona. A. The normalized change in C5a observed for PEG lengths of 3400Da and 5000Da in complement protected serum. B. The normalized change in C5a observed for mixing different PEG lengths in complement protected serum.

Supplementary materials for chapter 5

Calculating amount of PEG present

Samples were prepared by resuspending nanocapsules in deuterated water at a concentration of 5mg/ml. 800ul of sample was taken for the NMR spectrum generation. The integrated peaks are highlighted in figure 1 (Polyurethane nanocapsules) and 2(PEGylated polyurethane nanocapsules).

Supplementary Table 2. List of integrated peaks from NMR data for PEGylated and non-PEGylated polyurethane nanocapsules in deuterated water

Compound	Group	Peak @	Integrated area PU	Integrated area COOH- PEG-PU	Integrated area mPEG-PU
IPDI (methyl side groups)	CH3	0.75ppm ³	0.452	0.215	0.564
	CH3-C- CH3	1.158ppm ³	1.51	0.972	1.13
IPDI (cyclohexyl ring)	-CH2-	1.41ppm ³	1.13	0.947	0.99
1,6 HDOH	(-CH2-) ₄	1.223ppm ⁴	1.04	0.884	0.644

PEG	-CH2- CH2-O-	3.572ppm ⁵	-	0.172	0.147
-----	-----------------	-----------------------	---	-------	-------

Supplementary Table 3. Setting PEG deuterium ratio to 1

Compound	Group	Peak @	Integrated area mPEG-PU (setting PEG peak deuterium to 1)	Integrated area COOH-PEG-PU (setting PEG peak deuterium to 1)
IPDI (methyl side groups)	CH3	0.762ppm	1.25	3.84
	CH3-C- CH3	1.158ppm	5.65	7.69
IPDI (cyclohexyl ring)	-CH2-	1.42ppm	5.51	6.73
1,6 HDOH	(-CH2-) ₄	1.223ppm	5.14	4.38
PEG	-CH2- CH2-O-	3.572ppm	1	1

Calculating moles of PEG on in sample

The molecular weight of PEG monomer=44 g/mol

Each PEG monomer has 4 hydrogens per peak (-CH2-CH2-O-)

Mn of PEG=5000g/mol i.e. repeat units per chain is 113.6 (~114 monomers)

$$\frac{\frac{1^2H}{4H}}{1 \text{ monomer PEG}} = 0.25 \text{ monomer PEG} \times \frac{1 \text{ mole PEG}}{114 \text{ monomer units}} = 2.2 \text{ mmol PEG}$$

Calculating moles of IPDI in sample (Using peak area for -CH₂- within the cyclohexyl ring)

$$\frac{\text{Ratio } ^2H}{\frac{6H}{1 \text{ mole IPDI}}}$$

For mPEG-PU, moles of IPDI=918 mmoles

Moles of PEG per Moles of IPDI = 1mole PEG/419 moles of IPDI

For COOH-PEG-PU, moles of IPDI=1123 mmoles

Moles of PEG per Moles of IPDI = 1mole PEG/512 moles of IPDI

From previous NMR data,

For PEG-PU (2X), moles of IPDI=327mmoles

Moles of PEG per Moles of IPDI = 1mole PEG/149 moles of IPDI

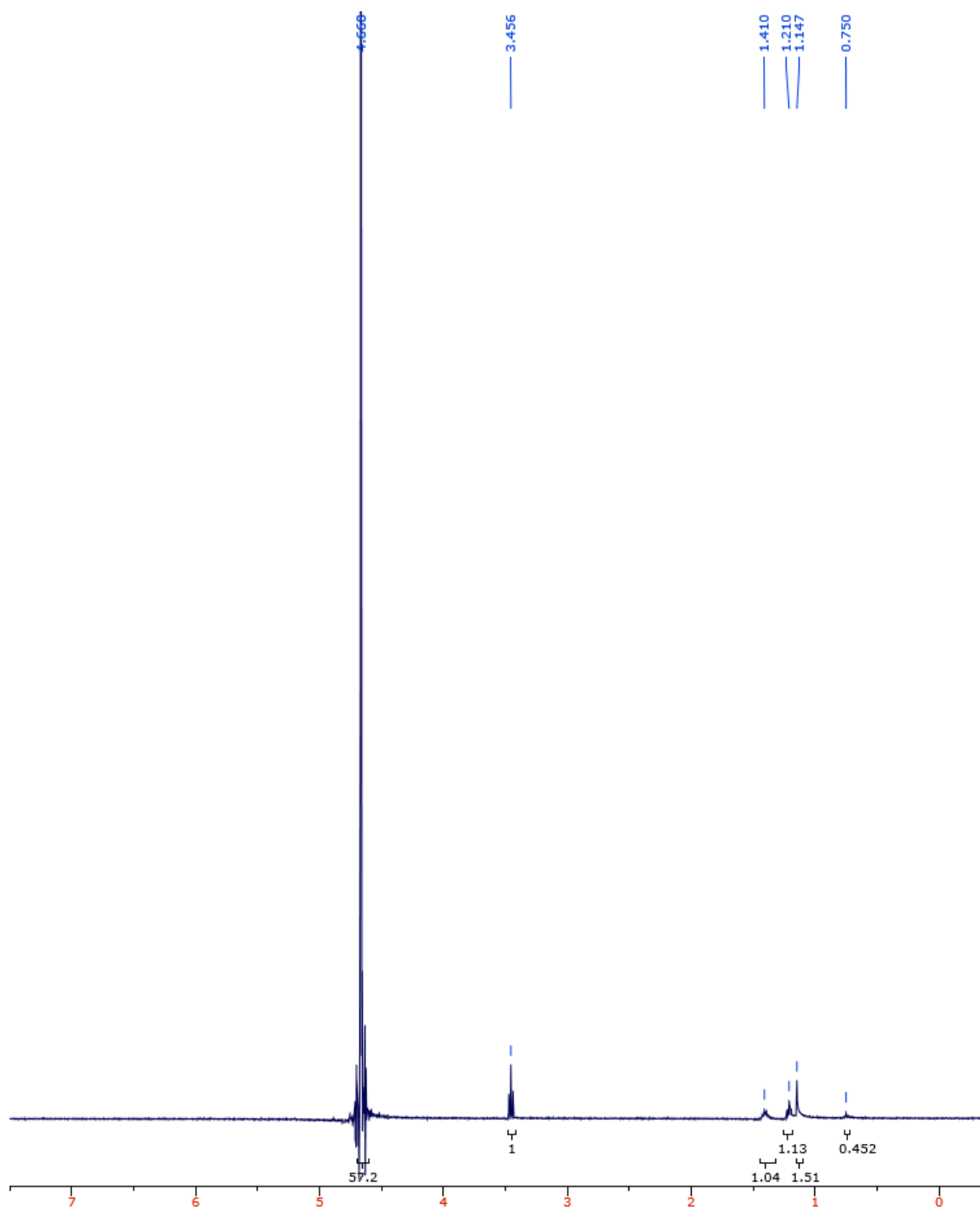


Figure 39. 1H-NMR peak for Polyurethane nanocapsules in deuterated water

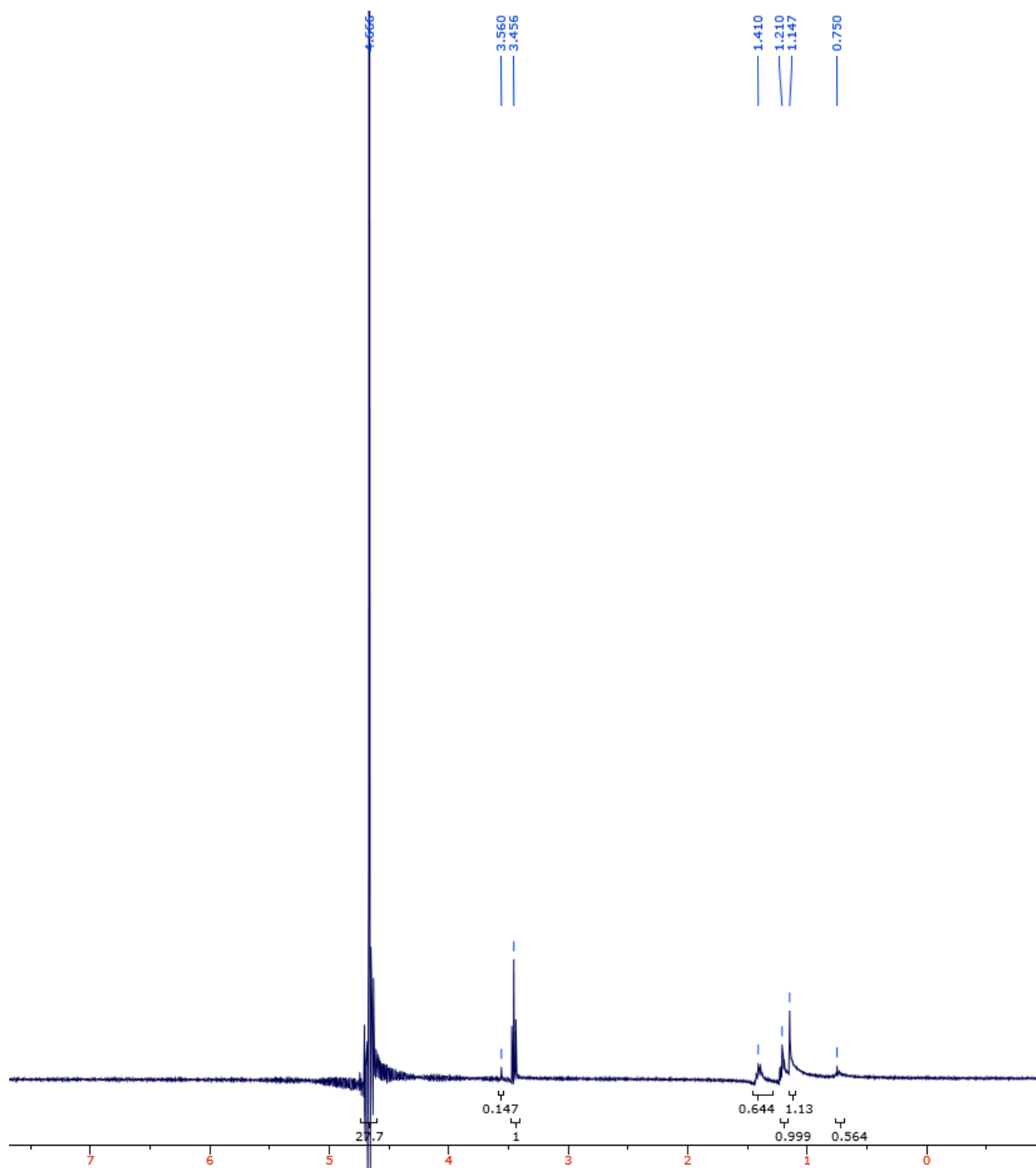


Figure 40. ^1H NMR Peak for PEGylated Polyurethane (PEGm) nanocapsules in deuterated water

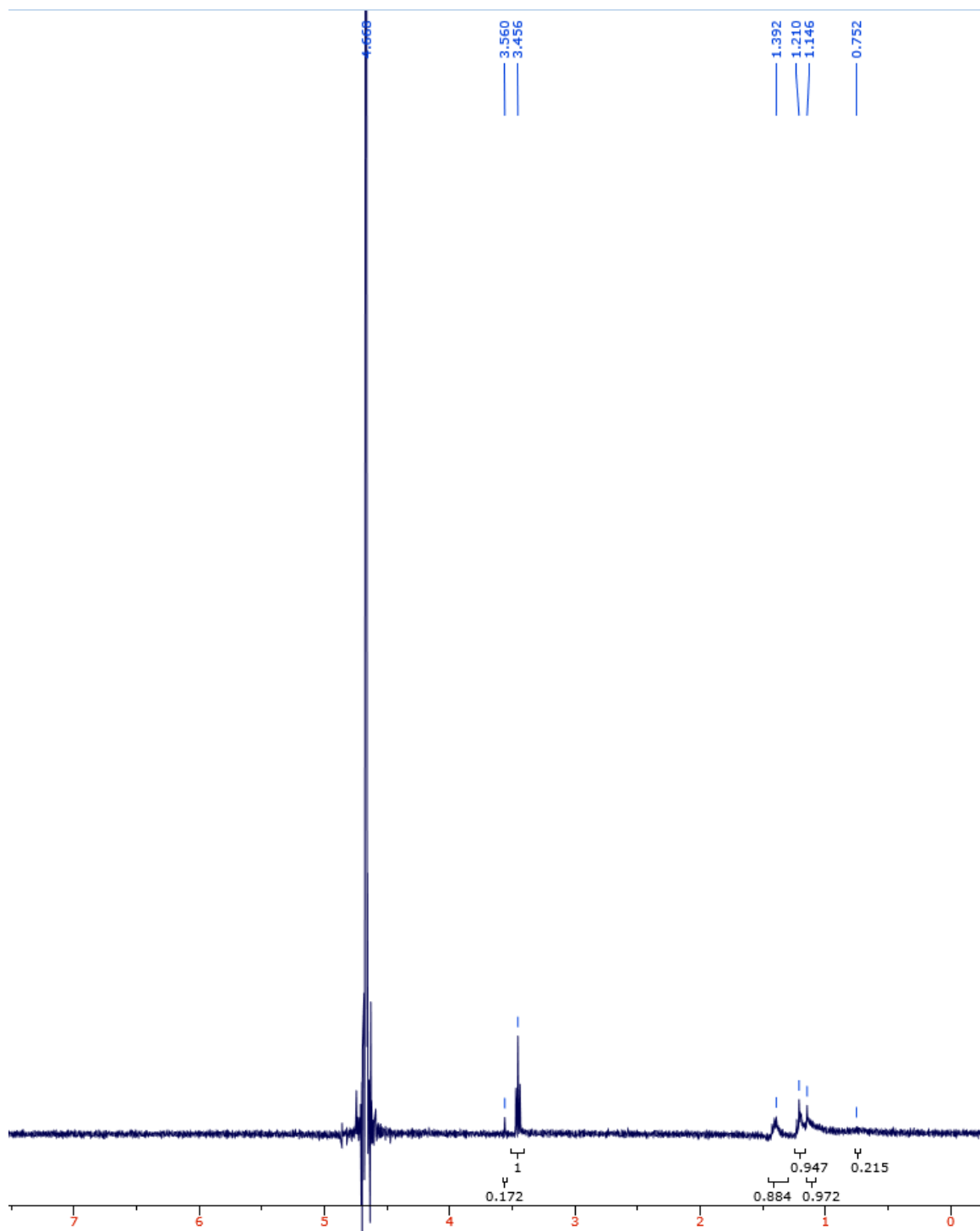


Figure 41. ^1H NMR peak for PEGylated Polyurethane (PEG-COOH) nanocapsules in deuterated water

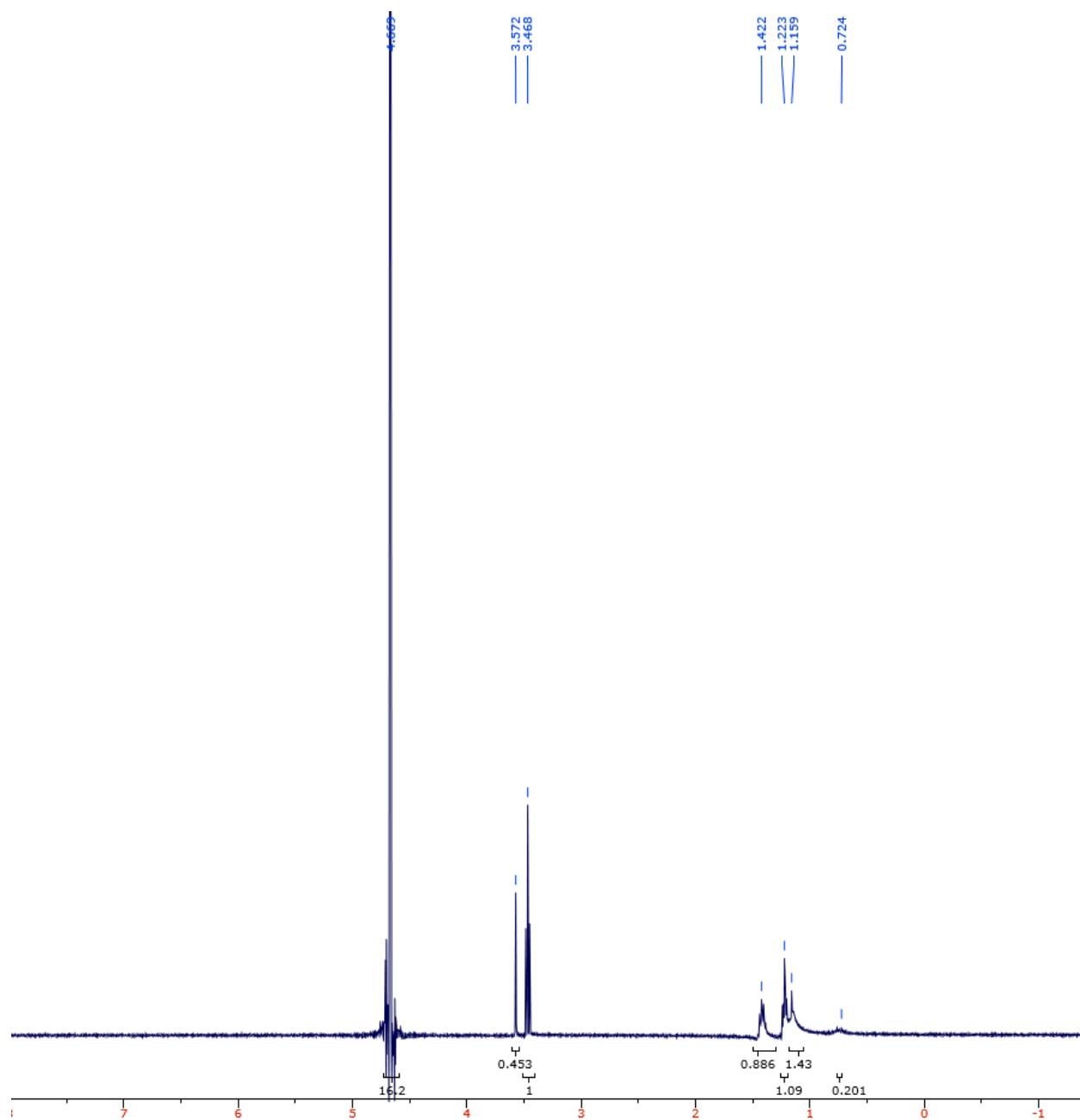


Figure 42. ^1H NMR peak for NMR Peak for PEGylated Polyurethane nanocapsule in deuterated water

References

1. Menikheim, S.; Leckron, J.; Bernstein, S.; Lavik, E. B., On-Demand and Long-Term Drug Delivery from Degradable Nanocapsules. *ACS Applied Bio Materials* **2020**, *3* (11), 7369-7375 DOI: 10.1021/acsabm.0c01130.
2. Maisha, N.; Coombs, T.; Lavik, E., Development of a Sensitive Assay to Screen Nanoparticles in Vitro for Complement Activation. *ACS Biomaterials Science & Engineering* **2020**, *6* (9), 4903-4915 DOI: 10.1021/acsbiomaterials.0c00722.
3. Mendoza-Novelo, B.; Mata-Mata, J. L.; Vega-González, A.; Cauich-Rodríguez, J. V.; Marcos-Fernández, Á., Synthesis and characterization of protected oligourethanes as crosslinkers of collagen-based scaffolds. *Journal of Materials Chemistry B* **2014**, *2* (19), 2874-2882.
4. Boyer, C.; Granville, A.; Davis, T. P.; Bulmus, V., Modification of RAFT-polymers via thiol-ene reactions: A general route to functional polymers and new architectures. *Journal of Polymer Science Part A: Polymer Chemistry* **2009**, *47* (15), 3773-3794 DOI: 10.1002/pola.23433.
5. Zhang, Y.; Zhao, Q.; Shao, H.; Zhang, S.; Han, X., Synthesis and Characterization of Star-Shaped Block Copolymer sPCL-b-PEG-GA. *Advances in Materials Science and Engineering* **2014**, *2014*, 1-6 DOI: 10.1155/2014/107375.

Supplementary Materials: Injury model used for the porcine trauma

*The summarized materials and methods section is provided by the Naval Medical Research Unit at San Antonio, and also a part of the technical report ‘Intravenously Infusible Nanoparticles to Stop Bleeding and Increase Survival Following Trauma’¹

Ethical Approval and Accreditation

The study protocol was reviewed and approved by the 711th HPW/RHD JBSA-Fort Sam Houston Institutional Animal Care and Use Committee (IACUC) in compliance with all applicable Federal regulations governing the protection of animals in research. All procedures were performed in facilities accredited by the AAALAC international.

Injury model and in vivo study

A standardized grade III liver injury model based on Gurney et al. was used. The injury model would result in ~25% lobectomy, and 5 minutes post-injury, the treatment or control infusion will be administered. The objective of this study was to investigate whether the nanoparticles with stealth properties in vitro cause any adverse reaction in vivo. The animal study consisted of two arms: Injured and uninjured arm. The injured arm had three subgroups: Vehicle control arm receiving 0.9% NaCl normal saline (n=6), control arm receiving control nanoparticles at a dosage of 2mg/kg (n=6), and treatment arm receiving the hemostatic nanoparticles at a dosage of 2mg/kg (n=7). The uninjured arm had three subgroups: Vehicle control arm receiving 0.9% NaCl normal saline (n=3), control arm receiving control nanoparticles at a dosage of 2mg/kg (n=3), and treatment arm receiving the hemostatic nanoparticles at a dosage of 2mg/kg (n=3).

The timeline of the study begins with baseline measurements of vitals as well as blood sample collection. With anticoagulant citrate phosphate dextrose adenine, 30% of total blood was also collected before the injury was made for infusion post-injury. Catheters were placed for administration of resuscitation fluids and treatment infusions, and pressure monitoring. Once injury was made, after 5 minutes of spontaneous bleeding, 30 mL bolus of either 1) 0.9% NaCl, 2) 2 mg/kg control nanoparticles, or 3) 2 mg/kg hemostatic nanoparticles were administered. At the end of the treatment phase, after 60 minutes of administration of the infusion fluids, the swine were under observation for 120 minutes. At the end of the timeline, swine were humanely euthanized at T=180 min with pentobarbital sodium and phenytoin sodium (Euthasol®, 390 mg/mL, Virbac Corporation, Fort Worth, TX, USA) During the study; whole blood was drawn for arterial blood gas, complete blood count, serum chemistries, rotational thromboelastometry (ROTEM), and STAGO at BSLN, TRAU, T=0min, 15min, 30min, 45min, 60min, 120min, 180min.

References

1. Lavik, E. Intravenously Infusible Nanoparticles to Stop Bleeding and Increase Survival Following Trauma; MARYLAND UNIV BALTIMORE COUNTY
BALTIMORE MD: 2020.

